

ENTANGLEMENT AND OTHER MEASURES OF NON-CLASSICALITY

by
Göktuğ Karpat

Submitted to the Graduate School of Engineering and Natural Sciences
in partial fulfillment of
the requirements for the degree of
Doctor of Philosophy

Sabancı University
Spring 2013

ENTANGLEMENT AND OTHER MEASURES OF NON-CLASSICALITY

APPROVED BY

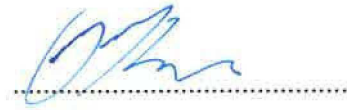
Assoc. Prof. Dr. Zafer Gedik
(Thesis Supervisor)



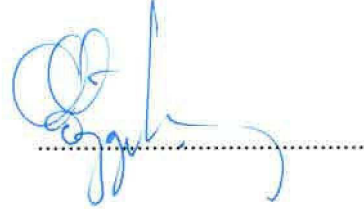
Prof. Dr. Cihan Saçlıođlu



Assoc. Prof. Dr. İsmet İnönü Kaya



Assoc. Prof. Dr. Özgür Erçetin



Assoc. Prof. Dr. Özgür Esat Müstecaplıođlu



DATE OF APPROVAL

25.02.2013

© Göktuğ Karpat 2013

All Rights Reserved

ENTANGLEMENT AND OTHER MEASURES OF NON-CLASSICALITY

Göktuğ Karpat

Physics, Doctor of Philosophy Thesis, 2013

Thesis Supervisor: Assoc. Prof. Dr. Zafer Gedik

Abstract

Quantum information theory (QIT) is an emerging field of physics which aims to develop new methods of dealing with information by harnessing the power of quantum mechanics. Besides its potential to revolutionize the techniques of information processing and communication, it also provides novel approaches to better comprehend the foundations of quantum mechanics. Among many important problems in QIT, manipulation and dynamical characterization of correlations present in quantum systems stand out due to their relevance for the practical applications of the theory. This thesis intends to explore such correlations of quantum and classical nature from various perspectives. In particular, our discussions involve the investigation of local transformations among a class of entangled states and the examination of correlation measures in some physical models.

We first examine the classification of the flip (0-1) and exchange symmetric (FES) states under local quantum operations. We study the optimal local one-shot conversions of FES states to determine the entanglement transformations that relate multiqubit FES states with the maximum possible probability of success. Next, we investigate the exchange symmetry properties of certain symmetric states when the qubits evolve according to a dephasing model which is also invariant under swap operation. We find that there exist states which do not preserve the exchange symmetry with unit probability during the time evolution, leading to the spontaneous breaking of exchange symmetry. Later, we turn our attention to the dynamics of quantum and classical correlations for qubit-qutrit systems in independent and global dephasing environments. In these cases, we demonstrate several interesting phenomena such as the transition from classical to quantum decoherence. Lastly, we investigate the thermal quantum and total correlations in the one-dimensional anisotropic XY model in transverse field. We discuss the ability of different measures to estimate the critical point of the quantum phase transition at finite temperature. We also consider the relation between correlations and the factorized ground state in this model. Furthermore, we study the effect of temperature on long-range correlations.

DOLAŞIKLIK VE KLASİK DIŞILIĞIN DİĞER ÖLÇÜTLERİ

Göktuğ Karpat

Fizik, Doktora Tezi, 2013

Tez Danışmanı: Doç. Dr. Zafer Gedik

Özet

Kuantum enformasyon kuramı son yıllarda fizikte yoğun olarak ilgi gören konulardan biri haline gelmiştir. Kuramın temel amacı, enformasyon kavramını kuantum mekaniksel olarak ele alarak klasik bilgi işleme ve haberleşme protokollerini kuantum mekaniğinin yasaları çerçevesinde daha verimli bir şekilde çalışacak hale getirmektir. Bunun yanı sıra, kuramın kuantum mekaniğinin bazı temel sorunlarının incelenmesi konusunda da faydaları olmaktadır. Kuantum enformasyon kuramındaki bir çok önemli problem arasından belki de en öne çıkanlardan bir tanesi, kuantum mekaniksel sistemlerin sahip olduğu bir takım ilintilerin çeşitli bakış açılarıyla tanımlanmasıdır. Bu çalışmanın amacı klasik ya da kuantum mekaniksel temellere sahip olabilen bu ilintilerin farklı açılardan incelenmesidir.

Tez içerisinde ilk olarak takas ve 0-1 simetrisine sahip hallerin oluşturduğu altuzayın yapısı incelenmiş ve bahsi geçen simetriye sahip çok parçacıklı hallerin yerel işlemler altında kendi aralarındaki azami dolaşma olasılıkları tespit edilmiştir. Ardından takas simetrisine sahip bir eşevresizlik modeli altında zaman evrimi geçiren bir takım simetrik hallerin simetri özellikleri incelenmiştir. Hem model hem de başlangıç hali takas simetrisine sahip olduğu halde, bazı hallerin zaman evrimi sonrasında kendiliğinden simetri kırılmasına uğrayıp bu simetriyi kaybettikleri gözlenmiştir. Tez kapsamında çalışılan bir diğer konu da çeşitli klasik ve kuantum mekaniksel ilinti ölçütlerinin farklı eşevresizlik modelleri altında evrilen kübit-kütrit sistemleri için incelenmesidir. Bu durumda ilinti ölçütlerinin klasik eşevresizlikten kuantum mekaniksel eşevresizliğe geçiş gibi bir çok ilginç davranış gösterdiği tespit edilmiştir. Son olarak, bir boyutlu XY modelindeki ilintiler araştırılmış ve bu ilintilerin sistemde oluşan kuantum faz geçişi ile ilişkileri tartışılmıştır.

ACKNOWLEDGEMENTS

Although obtaining a doctoral degree in physics at Sabancı University has been a fairly long and an occasionally disappointing journey for me, I still want to acknowledge the assistance of few individuals. I would like to first thank my thesis advisor for introducing me to the exciting field of quantum information science and also for encouraging me to work on my own problems independently. It is also a pleasure to thank my collaborators, friends and family for their contributions and support. Lastly, I appreciate the financial support received from the Scientific and Technological Research Council of Turkey (TUBITAK) under grants 111T232 and 107T530 during my doctoral studies.

Contents

ABSTRACT	iv
ÖZET	v
ACKNOWLEDGEMENTS	vi
1 INTRODUCTION	1
1.1 Motivation	1
1.2 Overview	2
2 FUNDAMENTAL CONCEPTS	3
2.1 Postulates of quantum mechanics	3
2.1.1 State space of quantum systems	4
2.1.2 Evolution of quantum states	5
2.1.3 Quantum measurements	6
2.2 Density matrix formalism	8
2.2.1 Qubits and qudits	10
2.2.2 Geometric representation of qubits	11
2.2.3 The reduced density matrix	13
2.3 Quantum operations	14
2.3.1 Completely positive transformations	14
2.3.2 Realization of quantum operations	15
3 ENTANGLEMENT	18
3.1 Separability of quantum states	18
3.1.1 Peres criterion for separability of bipartite states	19
3.1.2 Schmidt decomposition	21
3.2 Quantification of entanglement	21
3.2.1 Entropy of entanglement	23
3.2.2 Concurrence	24
3.2.3 Negativity	24

3.3	Classification of entangled states	25
3.3.1	Stochastic local operations and classical communication	27
3.3.2	Equivalence classes of flip and exchange symmetric states	30
3.3.3	Optimal local conversion of flip and exchange symmetric states	32
4	DECOHERENCE	37
4.1	Basics of the decoherence program	37
4.1.1	Dynamics of quantum measurements	39
4.1.2	A simple model of one-qubit decoherence	41
4.2	Decoherence induced symmetry breaking	43
4.2.1	Classical dephasing noise	43
4.2.2	Exchange symmetry of the Bell states	45
4.2.3	Quantum mechanical dephasing	47
4.2.4	Experimental demonstration of symmetry breaking	49
5	BEYOND ENTANGLEMENT	50
5.1	Measures of quantum correlations	50
5.1.1	Quantum discord	51
5.1.2	Geometric quantum discord	52
5.2	Measures of total correlations	54
5.2.1	Measurement-induced non-locality	54
5.2.2	Wigner-Yanase information based measure	54
5.3	Correlations of qubit-qutrit states under dephasing	55
5.3.1	Correlations under multilocal dephasing	58
5.3.2	Correlations under global dephasing	59
5.3.3	Time invariant quantum discord	62
5.4	Thermal correlations in the anisotropic XY chain	63
5.4.1	Estimation of the critical points	68
5.4.2	Long-range behavior of the correlations	70
6	CONCLUSION	71
	BIBLIOGRAPHY	88

List of Figures

2.1	Geometric representation of a qubit state on Bloch sphere	12
2.2	Unitary realization of quantum operations	17
3.1	Graphical representation of three, four and five-qubit flip and exchange symmetric states under invertible local operations	31
3.2	Optimal transformations of three-qubit flip and exchange symmetric states under invertible local operations	34
3.3	Optimal transformations of four-qubit flip and exchange symmetric states under invertible local operations	35
3.4	Optimal transformations of five-qubit flip and exchange symmetric states under invertible local operations	36
5.1	Dynamics of quantum and classical correlation measures under multilocal classical dephasing noise	59
5.2	Dynamics of quantum and classical correlation measures under global classical dephasing noise	60
5.3	Dynamics of quantum and classical correlation measures under local classical dephasing noise	63
5.4	The thermal total correlations of the one-dimensional anisotropic XY model for first nearest neighbors	66
5.5	The first derivatives of the thermal total correlations of the one-dimensional anisotropic XY model for first nearest neighbors	66
5.6	The thermal quantum correlations of the one-dimensional anisotropic XY model for first nearest neighbors	67
5.7	The first derivatives of the thermal quantum correlations of the one-dimensional anisotropic XY model for first nearest neighbors	67
5.8	The estimated values of critical points in the one-dimensional anisotropic XY model at finite temperature	69
5.9	Long-range behavior of the thermal total and quantum correlations in the one-dimensional anisotropic XY model	70

Chapter 1

INTRODUCTION

1.1 Motivation

The concept of entanglement has been known since the birth of quantum mechanics. It was Schrödinger himself who first realised that the linearity of quantum mechanics might have strange consequences when a composite system is considered [1]. Entanglement, having no classical analogue, can be defined as a purely quantum mechanical correlation among the subsystems of a composite quantum system. Although, after the work of Einstein, Podolsky and Rosen [2], it has been seen as a foundational problem of quantum theory for many years, entanglement is no longer a mere philosophical issue but instead is recognized as a fundamental resource to be exploited in many useful tasks [3]. The study of entanglement has become a very active field of research due to its possible applications such as teleportation of an unknown state, superdense coding of classical information and secure distribution of keys for encoding purposes [4]. Thus, it is of great importance to comprehend the properties of entanglement from as many angles as possible.

Until recent years, entanglement has been the defining subject of the quantum information theory. However, various investigations have demonstrated that it is not the only kind of useful correlation in quantum states and some separable states might also perform better than their classical counterparts [5]. These advances have started a new era of defining correlation measures to detect the nonclassical correlations that cannot be captured by entanglement. In fact, the study of correlations in quantum systems is not only limited to relating them with practical applications. The methods of quantum information theory have been also proved to be useful for the investigation of condensed matter systems [6].

On the other hand, as most quantum traits, nonclassical correlations in a quantum system tend to be very fragile when the system is exposed to environmental disturbances, which is inevitably the case in real world situations [7]. Therefore, gaining an understanding of the effect of environment on the dynamics of such correlations is crucial for the practical applications that aim to utilize these correlations as a resource.

1.2 Overview

The second chapter of this thesis serves as a brief review of some important mathematical tools which are to be used for the description of quantum systems. We introduce the postulates of quantum mechanics and review the density matrix formalism. We discuss the mathematical formulation and physical realization of quantum operations.

In the third chapter, we consider the separability problem of quantum states. We discuss the properties of some well known entanglement measures. The manipulation and classification of certain entangled states under local operations and classical communication are examined. In particular, we study the one-shot flip (0-1) and exchange symmetric (FES) entanglement transformations of FES states. We determine the optimal transformations that relate multiqubit FES states with the maximum possible probability of success. We also demonstrate that certain entangled states are more robust than others, in the sense that the optimum probability of converting these robust states to the states lying in the close neighborhood of separable ones vanishes under local FES operations.

The fourth chapter provides an introduction to the fundamentals of the decoherence program. We study the exchange symmetry properties of Bell states when two qubits interact with local baths having identical parameters. We consider a decoherence Hamiltonian which is invariant under swapping the first and second qubits. We find that as the system evolves in time, two of the three symmetric Bell states preserve their qubit exchange symmetry with unit probability, whereas the symmetry of the remaining state survives with a maximum probability of 0.5 at the asymptotic limit. We identify decoherence as the main mechanism leading to breaking of qubit exchange symmetry.

In the fifth chapter, we review several recently introduced measures of quantum and total correlations. First, we study the dynamics of classical and quantum correlations for qubit-qutrit systems in dephasing environments. Our discussion involves a comparative analysis of the Markovian dynamics of negativity, quantum discord, geometric measure of quantum discord and classical correlation. Second, we investigate the thermal correlations in the anisotropic XY spin chain in transverse field. While we adopt concurrence and geometric quantum discord to measure quantum correlations, we use measurement-induced nonlocality and an alternative quantity defined in terms of Wigner-Yanase information to quantify total correlations. We show that the ability of these measures to estimate the critical point at finite temperature strongly depends on the anisotropy parameter of the Hamiltonian. We also identify a correlation measure which detects the factorized ground state. Lastly, we study the effect of temperature on long-range correlations.

The last chapter includes a short summary of the main results obtained in this thesis.

Chapter 2

FUNDAMENTAL CONCEPTS

This preliminary chapter is meant to be a brief review of some important mathematical tools utilized for the description of quantum systems. We will commence by introducing the fundamental postulates of quantum mechanics regarding the time evolution of quantum systems and the measurements performed on them. We will then be interested in the density matrix formalism of quantum mechanics, which will play an important role in our later discussions. Composite quantum systems will also be shortly mentioned although a more detailed discussion of them will be provided in the next chapter. Lastly, we will study how general quantum operations are mathematically formulated, as well as how they can be physically realized. For a comprehensive overview of the subjects covered in this chapter, interested reader may refer to [4, 8–10]. The present chapter will also set the notation to be used throughout this thesis.

2.1 Postulates of quantum mechanics

At the end of nineteenth century it became evident that predictions of classical physics were in contradiction with experiments. This inconsistency gave rise to a need for a profoundly new way of understanding the nature. Quantum mechanics, developed in the early twentieth century, has given us a completely novel mathematical framework for the development of physical theories. There are now many excellent textbooks on quantum mechanics which study the mathematical aspects of the subject in detail on various levels [11–16]. However, in this section, we will limit ourselves to the mere basics of the theory that have been crucial for the establishment of the foundations of quantum information science. In classical mechanics, the state of a physical system at a given time is determined by the position and velocity of the system at this time. If these initial conditions are known, various different approaches of classical mechanics might be used to deduce the state of the system at any time. As will be discussed in the following section, when it comes to quantum theory, even the state of a system is defined in a quite different way.

2.1.1 State space of quantum systems

In quantum mechanics, any isolated physical system has an associated d -dimensional complex vector space with inner product (a Hilbert space \mathcal{H}^d) known as the state space of the system. The system is completely described by its state vector $|\psi\rangle$, which is a unit vector in the system's state space. This unit vector (also known as the ket vector) contains all the information that we can possibly acquire about the state of the system. In addition, associated to every ket vector $|\psi\rangle$ in Hilbert space \mathcal{H} , there also exists another kind of vector that resides in the dual vector space \mathcal{H}^* . Elements of this dual vector space are called bra vectors and are denoted by $\langle\psi|$. In Dirac notation, ket and bra vectors read as

$$|\psi\rangle = (c_1, c_2, \dots, c_d)^T, \quad \langle\psi| = (c_1^*, c_2^*, \dots, c_d^*), \quad (2.1)$$

where c_i 's are complex numbers satisfying $\sum_i |c_i|^2 = 1$, and the superscript T denotes the transposition operation. The inner product between two state vectors $|\alpha\rangle = (\alpha_1, \alpha_2, \dots, \alpha_d)^T$ and $|\beta\rangle = (\beta_1, \beta_2, \dots, \beta_d)^T$ in Hilbert space \mathcal{H}^d is defined by

$$\langle\alpha|\beta\rangle = \sum_{i=1}^d \alpha_i^* \beta_i = \alpha_1^* \beta_1 + \alpha_2^* \beta_2 + \dots + \alpha_d^* \beta_d. \quad (2.2)$$

A family of state vectors $\{|x_1\rangle, |x_2\rangle, \dots, |x_n\rangle\}$ is said to be orthonormal if

$$\langle x_i | x_j \rangle = \delta_{ij}, \quad (i, j = 1, 2, \dots, n), \quad (2.3)$$

where δ_{ij} is the Kronecker delta symbol, defined as $\delta_{ij} = 1$ for $i = j$ and $\delta_{ij} = 0$ for $i \neq j$. The same collection of state vectors is also said to be linearly independent if the relation $c_1|x_1\rangle + c_2|x_2\rangle + \dots + c_n|x_n\rangle = 0$ with c_1, c_2, \dots, c_n complex numbers, holds if and only if $c_1 = c_2 = \dots = c_n = 0$. Furthermore, a set of d linearly independent vectors in a d -dimensional vector space is called a basis for that vector space. For a given orthonormal basis $\{|k_1\rangle, |k_2\rangle, \dots, |k_d\rangle\}$ of the Hilbert space \mathcal{H}^d , any state vector can be expanded as a linear combination of the basis vectors as

$$|\psi\rangle = \sum_{i=1}^d u_i |k_i\rangle, \quad (2.4)$$

where the complex coefficients u_i satisfy the normalization condition $\langle\psi|\psi\rangle = \sum_i |u_i|^2 = 1$. From this section on, we will refer to state vectors as states for the sake of simplicity.

There are many situations in quantum mechanics where one needs to deal with quantum systems made up of two or more distinct physical systems. In these instances, the state space of a composite system is constructed from the state spaces of the individual

subsystems. Given that we have two independent quantum states $|u\rangle = (u_1, u_2, \dots, u_m)^T \in \mathcal{H}_A$ and $|v\rangle = (v_1, v_2, \dots, v_n)^T \in \mathcal{H}_B$, we can describe the state of the both systems together as a tensor product of these two states, written as $|w\rangle = |u\rangle \otimes |v\rangle \in \mathcal{H}_A \otimes \mathcal{H}_B$ (We will mostly use the short hand notation of denoting $|u\rangle \otimes |v\rangle$ simply by $|u\rangle|v\rangle$ or $|uv\rangle$). The resulting $m * n$ dimensional state $|w\rangle$ can be obtained as

$$\begin{aligned} |w\rangle &= |u\rangle \otimes |v\rangle = (u_1|v\rangle, u_1|v\rangle, \dots, u_m|v\rangle)^T \\ &= (u_1v_1, u_1v_2, \dots, u_1v_n, u_2v_1, \dots, u_mv_n)^T. \end{aligned} \quad (2.5)$$

If we have many independent quantum systems numbered as $1, 2, \dots, n$ in quantum states $|\psi_1\rangle, |\psi_2\rangle, \dots, |\psi_n\rangle$, then the state of the joint system is given by $|\psi_1\rangle \otimes |\psi_2\rangle \otimes \dots \otimes |\psi_n\rangle$.

2.1.2 Evolution of quantum states

Having set up the stage where quantum mechanics takes place, we are now in a position to describe how a quantum state propagates in time. Quantum theory postulates that dynamical evolution of a closed quantum system is realized by a unitary transformation

$$|\psi(t)\rangle = U(t, t_0)|\psi(t_0)\rangle. \quad (2.6)$$

The unitary operator $U(t, t_0)$ satisfies $U^\dagger = U^{-1}$, where U^\dagger denotes the adjoint of U . An important property of unitary operators is that they preserve the inner products between the vectors, leaving the norm of quantum states invariant. In particular, the time evolution of the state $|\psi\rangle$ is determined by the Schrödinger equation

$$i\hbar \frac{d}{dt} |\psi(t)\rangle = H|\psi(t)\rangle, \quad (2.7)$$

where H is a Hermitian (self-adjoint) operator known as the Hamiltonian of the closed system. Given an initial state $|\psi(t_0)\rangle$, the time evolved state $|\psi(t)\rangle$ is uniquely and deterministically obtained by solving (2.7). Moreover, the Schrödinger equation is linear, that is, if $|\alpha(t)\rangle$ and $|\beta(t)\rangle$ are solutions to (2.7), then $|\psi(t)\rangle = a|\alpha(t)\rangle + b|\beta(t)\rangle$, where a and b are complex numbers, is also a valid solution. This additive property of solutions in linear systems is known as the superposition principle. If the Hamiltonian H is time-independent, the solution to the Schrödinger equation can be verified to be

$$|\psi(t)\rangle = \exp \left[-\frac{i}{\hbar} H(t - t_0) \right] |\psi(t_0)\rangle. \quad (2.8)$$

Then, the time evolution operator $U(t, t_0)$ (also known as the propagator) is given by $U(t, t_0) = \exp \left[-\frac{i}{\hbar} H(t - t_0) \right]$, where the exponential of the operator $-iH(t - t_0)/\hbar$ is

defined as

$$\exp\left[-\frac{i}{\hbar}H(t-t_0)\right] \equiv \sum_{n=0}^{\infty} \frac{1}{n!} \left[-\frac{i}{\hbar}(t-t_0)\right]^n H^n. \quad (2.9)$$

Using (2.9), it is not difficult to see that $U(t, t_0)$ is unitary and, furthermore, any unitary operator U can be written in the form $U = \exp(iH)$ for some Hermitian operator H .

2.1.3 Quantum measurements

The process of measurement in quantum mechanics is a very delicate concept. Although the evolution of closed quantum systems, which do not interact with their environments, are determined according to the Schrödinger equation, measurements on these systems cannot be described in terms of unitary evolution and exhibits an unavoidable probabilistic nature. When an experimentalist observes a system, there occurs an interaction between the system and the experimental equipment. Thus, the system can no longer be treated as closed, causing its evolution to be non-unitary. The measurement postulate provides a means for explaining what happens when a quantum system is measured.

Generalized quantum measurements are described by a collection of operators $\{M_n\}$ which satisfy the completeness relation

$$\sum_n M_n^\dagger M_n = I, \quad (2.10)$$

where I denotes the identity operator. The labels n on the operators represent the different possible outcomes. If the state of the system is represented by $|\psi\rangle$ immediately before the measurement, then the n th outcome occurs with probability

$$p(n) = \langle\psi|M_n^\dagger M_n|\psi\rangle, \quad (2.11)$$

and the state of the system after the measurement becomes

$$\frac{M_n|\psi\rangle}{\sqrt{\langle\psi|M_n^\dagger M_n|\psi\rangle}}. \quad (2.12)$$

The completeness relation makes sure that the probabilities of different measurement outcomes sum to unity. This measurement scheme is called a selective quantum measurement, since the pre-measurement state $|\psi\rangle$ is selected into a set of conditional post-measurement states according to the obtained measurement outcomes.

For some of the applications in quantum information theory, the state of the system after the measurement is not of interest, and only the probabilities of possible measure-

ment outcomes matter. For instance, when a photon is detected by a photomultiplier, it is destroyed in the measurement process, and hence doing repeated measurements on the system is not possible. In such cases, it is convenient to define a new set of measurement operators $\{E_n\}$ where $E_n \equiv M_n^\dagger M_n$. With this definition, we can obtain the probabilities of different measurement outcomes as

$$p(n) = \langle \psi | E_n | \psi \rangle, \quad \sum_n E_n = I. \quad (2.13)$$

The positive (and thus automatically Hermitian) operators E_n are said to be the positive operator valued measure (POVM) elements associated with the measurement. The complete set of operators $\{E_n\}$ is said to be a POVM.

A particularly important subclass of generalized quantum measurements is projective (von Neumann) measurements. Projective measurements can be described by an observable K , represented by means of an Hermitian operator (whose eigenvalues n are the possible values of that observable)

$$K = \sum_n n P_n, \quad (2.14)$$

where the family of operators $\{P_n\}$, satisfying $P_n P_{n'} = \delta_{nn'} P_n$ and $\sum_n P_n = I$, is called a complete set of orthonormal projectors. It is evident that projective measurements are a very special instance of POVMs, where all the POVM elements are the same as the measurement operators themselves, since $E_n \equiv P_n^\dagger P_n = P_n$. In case of projective measurements, the probability of getting result n upon measuring the state $|\psi\rangle$ is given by $p(n) = \langle \psi | P_n | \psi \rangle$. If the result n occurs, then the post-measurement state of the system becomes

$$\frac{P_n |\psi\rangle}{\sqrt{\langle \psi | P_n | \psi \rangle}}. \quad (2.15)$$

Another aspect of projective measurements is that they have a special property called repeatability, that is, if we perform a projective measurement once and obtain the outcome n , repeating the measurement doesn't affect the state and gives the same outcome n again. We note that non-orthogonal measurements do not have this property. Despite the fact that a projective measurement is a restricted version of the general measurement postulate, there is no loss of generality in allowing only projective measurements. Neumark's theorem guarantees that an arbitrary measurement of a given quantum system can always be realized by only performing a projective measurement and unitary transformations on a larger quantum system [16]. In other words, generalized measurements are equivalent to projective measurements on a larger Hilbert space.

2.2 Density matrix formalism

We have so far introduced the fundamental postulates of quantum mechanics using the language of state vectors. Consequently, we have limited ourselves to the study of the quantum systems that can be represented by a single state vector. However, in reality, a quantum system often cannot be specified by a single state vector since it is not always possible to have complete knowledge of the considered system. We therefore need a new approach to deal with quantum systems about which we only have partial information. The density matrix formalism of quantum mechanics provides the required tools for describing such quantum systems.

Imagine a procedure in which a quantum system is prepared in one of a number of normalized (but not necessarily orthogonal) states from the ensemble $\{|\psi_1\rangle, |\psi_2\rangle, \dots, |\psi_i\rangle\}$, with respective probabilities $\{p_1, p_2, \dots, p_i\}$, satisfying the condition of total unit probability $\sum_i p_i = 1$. The density matrix for the system is then given by the equation

$$\rho = \sum_i p_i |\psi_i\rangle\langle\psi_i|. \quad (2.16)$$

Here, the terms $|\psi_i\rangle\langle\psi_i|$ are matrices constructed from the outer products of the states $|\psi_i\rangle$. If the state of a quantum system is known and described by a state vector $|\psi\rangle$, it is said to be in a pure state. The density matrix of a pure state, which is simply defined by a projector $\rho = |\psi\rangle\langle\psi|$, corresponds to the case where one of the probabilities p_i is equal to one while all others are zero. On the other hand, a quantum system whose state is constructed from a statistical ensemble of different pure states is called a mixed state. It should be emphasized that a mixed state is not a quantum superposition of pure states since a superposition of pure states is just another pure state. Using the definition of the density matrix given by (2.16), we can obtain the following general properties that must be satisfied by all density matrices:

- ρ is Hermitian since it is constructed from a sum of Hermitian outer products,

$$\rho = \sum_i p_i |\psi_i\rangle\langle\psi_i| = \rho^\dagger. \quad (2.17)$$

- The diagonal elements of ρ sum to one, that is, ρ has trace equal to one,

$$\text{Tr}(\rho) = \sum_i p_i \text{Tr}(|\psi_i\rangle\langle\psi_i|) \quad (2.18)$$

$$= \sum_i p_i = 1. \quad (2.19)$$

- ρ is a positive operator, which implies that the eigenvalues ρ of are non-negative,

$$\langle \phi | \rho | \phi \rangle = \sum_i p_i \langle \phi | \psi_i \rangle \langle \psi_i | \phi \rangle \quad (2.20)$$

$$= \sum_i p_i |\langle \phi | \psi_i \rangle|^2 \geq 0 \quad (2.21)$$

- The pure state ρ satisfies the equation $\rho^2 = \rho$,

$$\rho^2 = |\psi\rangle\langle\psi| |\psi\rangle\langle\psi| = |\psi\rangle\langle\psi| = \rho. \quad (2.22)$$

- The inequality $\text{Tr}(\rho^2) \leq 1$ holds, with equality if and only if ρ is a pure state. The proof of this last property, which we omit here, can be straightforwardly done, for example, by making use of the decomposition of the Hermitian matrix ρ into a set of orthonormal projectors.

The postulates of quantum mechanics can be reformulated using the density operator approach. For instance, we can describe the dynamical evolution of a mixed quantum system in the language of density matrices. Starting from

$$\begin{aligned} \frac{d}{dt}\rho(t) &= \frac{d}{dt} \sum_i p_i |\psi_i(t)\rangle\langle\psi_i(t)| \\ &= \sum_i p_i \left[\left(\frac{d}{dt} |\psi_i(t)\rangle \right) \langle\psi_i(t)| + |\psi_i(t)\rangle \left(\frac{d}{dt} \langle\psi_i(t)| \right) \right], \end{aligned} \quad (2.23)$$

and using the Schrödinger equation given by (2.7) along with its conjugate, we obtain

$$\frac{d}{dt}\rho(t) = \frac{1}{i\hbar} (H\rho(t) - \rho(t)H) = \frac{1}{i\hbar} [H, \rho(t)]. \quad (2.24)$$

Since the time evolution is unitary for closed systems, the density matrix $\rho(t_0)$ is related to the density matrix $\rho(t)$ by the equation

$$\begin{aligned} \rho(t) &= \sum_i p_i |\psi_i(t)\rangle\langle\psi_i(t)| = \sum_i p_i U(t, t_0) |\psi_i(t_0)\rangle\langle\psi_i(t_0)| U^\dagger(t, t_0) \\ &= U(t, t_0) \rho(t_0) U^\dagger(t, t_0). \end{aligned} \quad (2.25)$$

Moreover, we can also express the measurement postulate in the density operator picture. Provided that the state of a quantum system is described by ρ immediately before the measurement, the probability of obtaining the outcome n is given by $p(n) = \text{Tr}(M_n \rho M_n^\dagger)$, and the state of the system after the measurement becomes

$$\frac{M_n \rho M_n^\dagger}{\text{Tr}(M_n \rho M_n^\dagger)}, \quad (2.26)$$

where the measurement operators satisfy the completeness relation $\sum_n M_n^\dagger M_n = I$. Considering the above discussion, it is clear that describing a pure system in terms of either the state vector $|\psi(t)\rangle$ or the density matrix $\rho = |\psi(t)\rangle\langle\psi(t)|$ is completely equivalent. Besides, since multiplying the state vector by a global complex phase yields the same density matrix, such global phases have no observable effects on quantum systems. We note that this is no longer correct for the relative phase factors between state vectors.

We should lastly mention that a given density matrix ρ does not represent a unique ensemble of pure quantum states. For example, looking at the density matrix

$$\rho = \frac{1}{5}|0\rangle\langle 0| + \frac{4}{5}|1\rangle\langle 1|, \quad (2.27)$$

one might conclude that the system would be in the state $|0\rangle$ with probability $1/5$ and in the state $|1\rangle$ with probability $4/5$. However, this is not the only statistical ensemble of pure states giving the density matrix (2.27). Suppose we define

$$\begin{aligned} |a\rangle &\equiv \sqrt{\frac{1}{5}}|0\rangle + \sqrt{\frac{4}{5}}|1\rangle \\ |b\rangle &\equiv \sqrt{\frac{1}{5}}|0\rangle - \sqrt{\frac{4}{5}}|1\rangle, \end{aligned} \quad (2.28)$$

and the quantum system is prepared in such a way that we have equal probabilities of finding the system either in the state $|a\rangle$ or in the state $|b\rangle$. In this case, we obtain the density matrix

$$\rho = \frac{1}{2}|a\rangle\langle a| + \frac{1}{2}|b\rangle\langle b| = \frac{1}{5}|0\rangle\langle 0| + \frac{4}{5}|1\rangle\langle 1|. \quad (2.29)$$

As a consequence, we see that two completely different ensembles of quantum states give rise to the exact same density matrix. In fact, there are infinitely many ensembles that would yield the same density matrix.

2.2.1 Qubits and qudits

Central to quantum information science is the concept of a quantum bit, also known as qubit. Unlike the usual bits of data used in classical information theory, which are either a zero or a one, qubits can store a superposition of the bits zero and one. In other words, qubits can hold both zero and one at the same time. Mathematically, a qubit is a unit vector in a 2-dimensional complex Hilbert space. As the states $|0\rangle \equiv (1, 0)^T$ and $|1\rangle \equiv (0, 1)^T$ form an orthonormal basis for this vector space, state of a qubit can be written as

$$|\psi\rangle = \alpha|0\rangle + \beta|1\rangle, \quad (2.30)$$

where the complex numbers α and β satisfy the normalization condition $|\alpha|^2 + |\beta|^2 = 1$. This particular basis, denoted by the vectors $|0\rangle$ and $|1\rangle$, is known as the computational basis. Although we can inspect a classical bit to find out whether it is in the state one or zero, it is not possible to directly examine a qubit to deduce its quantum state. Postulates of quantum mechanics allow us to only talk about probabilities instead of certainties, that is, when we measure a qubit we get either the outcome $|0\rangle$ with probability $|\alpha|^2$, or the outcome $|1\rangle$ with probability $|\beta|^2$. Qubits can be physically realized in many different ways. In fact, any two-level quantum system is a potential candidate for a qubit, such as, the two spin states of an electron or the two states of the polarization of a photon. On the other hand, as an obvious extension of qubits to multilevel quantum systems, we can define d -dimensional states called qudits. Qubits and qudits have many surprising properties absent in classical systems, including the no-cloning theorem [17], which forbids the creation of identical copies of an arbitrary unknown quantum state.

2.2.2 Geometric representation of qubits

We can represent all one-qubit density matrices by the points of a 3-dimensional unit sphere. As previously discussed, a qubit is a two-level quantum system whose state can be expressed in computational basis as

$$|\psi\rangle = \alpha|0\rangle + \beta|1\rangle, \quad |\alpha|^2 + |\beta|^2 = 1. \quad (2.31)$$

With a natural parametrization that automatically takes the normalization condition into account, the state of a qubit becomes

$$|\psi\rangle = e^{i\gamma} \left(\cos \frac{\theta}{2} |0\rangle + e^{i\varphi} \sin \frac{\theta}{2} |1\rangle \right), \quad (2.32)$$

where $\theta \in [0, \pi]$ and $\varphi \in [0, 2\pi]$. Knowing that a global phase in front has no observable effects in quantum mechanics, we can ignore the factor $e^{i\gamma}$ without any loss of generality, and effectively represent the state of a qubit by

$$|\psi\rangle = \cos \frac{\theta}{2} |0\rangle + e^{i\varphi} \sin \frac{\theta}{2} |1\rangle. \quad (2.33)$$

In this angular notation, the density matrix of a pure qubit can be easily calculated to be

$$\rho = |\psi\rangle\langle\psi| = \begin{pmatrix} \cos^2 \frac{\theta}{2} & e^{-i\varphi} \sin \frac{\theta}{2} \cos \frac{\theta}{2} \\ e^{i\varphi} \sin \frac{\theta}{2} \cos \frac{\theta}{2} & \sin^2 \frac{\theta}{2} \end{pmatrix}, \quad (2.34)$$

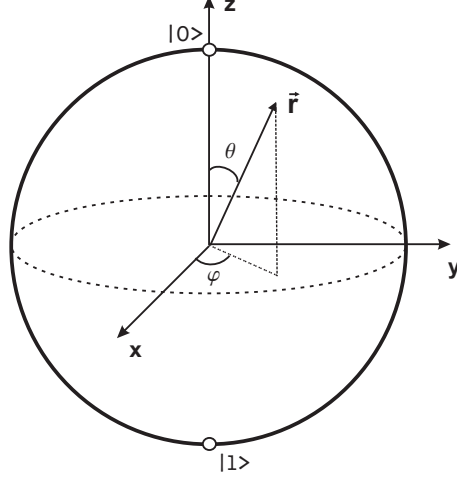


Figure 2.1: The set of all one-qubit density matrices can be represented by the points of a 3-dimensional unit sphere of Bloch vectors \vec{r} . While the surface points of the sphere, $|\vec{r}| = 1$, represent the pure states, the interior points of the sphere, $|\vec{r}| \leq 1$, correspond to mixed states. The maximally mixed state $I/2$ is described by the Bloch vector $|\vec{r}| = 0$. The closer the Bloch vector to the origin the more mixed is the corresponding state.

and using the elementary trigonometric identities, it reads

$$\rho = \frac{1}{2} \begin{pmatrix} 1 + \cos \theta & \cos \varphi \sin \theta - i \sin \varphi \sin \theta \\ \cos \varphi \sin \theta + i \sin \varphi \sin \theta & 1 - \cos \theta \end{pmatrix}. \quad (2.35)$$

On the other hand, any 2×2 Hermitian matrix can be expanded over the basis of matrices $\{I, \sigma_x, \sigma_y, \sigma_z\}$ with real expansion coefficients, where I is the usual 2×2 identity matrix, and the other three matrices are known as Pauli matrices

$$\sigma_x = \begin{pmatrix} 0 & 1 \\ 1 & 0 \end{pmatrix}, \quad \sigma_y = \begin{pmatrix} 0 & -i \\ i & 0 \end{pmatrix}, \quad \sigma_z = \begin{pmatrix} 1 & 0 \\ 0 & -1 \end{pmatrix}. \quad (2.36)$$

Decomposing the density matrix (2.35) in this basis, we observe that

$$\begin{aligned} \rho &= \frac{1}{2} (I + \sigma_x \cos \varphi \sin \theta + \sigma_y \sin \varphi \sin \theta + \sigma_z \cos \theta) \\ &= \frac{1}{2} (I + \hat{n} \cdot \vec{\sigma}), \end{aligned} \quad (2.37)$$

where $\hat{n} = (n_x, n_y, n_z) = (\cos \varphi \sin \theta, \sin \varphi \sin \theta, \cos \theta)$ is the 3-dimensional unit vector in spherical coordinates, and $\vec{\sigma}$ is a three element vector of Pauli matrices $\{\sigma_x, \sigma_y, \sigma_z\}$. Consequently, there is a one-to-one correspondence between the set of all pure qubit states and the surface points of the 3-dimensional unit sphere known as the Bloch sphere. The natural metric on the Bloch sphere is given by the Fubini-Study metric, under which the distance between two pure qubits is defined as $\cos^{-1} |\langle \psi_1 | \psi_2 \rangle|$. We can also visualize the mixed qubit states with the points inside the Bloch sphere. Defining a new vector \vec{r} , which

might have a length shorter than one, we can represent any mixed state in the form

$$\rho = \frac{1}{2} (I + \vec{r} \cdot \vec{\sigma}), \quad (2.38)$$

where \vec{r} is called the Bloch vector. This matrix clearly satisfies the unit trace condition, since the Pauli matrices are traceless. Besides, a density matrix is required to be positive, meaning it must have a non-negative eigenvalue spectrum. Considering that the eigenvalues of (2.38) are given by $\frac{1}{2}(1 \pm |\vec{r}|)$, we must have $|\vec{r}| \leq 1$. In accordance with the previous results, pure states correspond to the case of having unit Bloch vectors $|\vec{r}| = 1$.

2.2.3 The reduced density matrix

The density matrix formalism of quantum mechanics is particularly effective when we want to describe the subsystems of a composite quantum system. The reduced density operator provides the required mathematical tool for the representation of such subsystems. Given that we have two quantum systems A and B , whose composite state can be described by a density matrix ρ^{AB} acting on $\mathcal{H}_A \otimes \mathcal{H}_B$. We can define the reduced density matrix for the subsystem A as

$$\rho^A \equiv \text{Tr}_B (\rho^{AB}), \quad (2.39)$$

where Tr_B denotes the partial trace operation over the subsystem B . The partial trace over the second subsystem (B) of a composite system AB is defined by

$$\begin{aligned} \text{Tr}_B (|x_1\rangle\langle x_2| \otimes |y_1\rangle\langle y_2|) &= \sum_i \langle e_i | (|x_1\rangle\langle x_2| \otimes |y_1\rangle\langle y_2|) |e_i\rangle \\ &= \sum_i |x_1\rangle\langle x_2| \langle e_i | y_1\rangle\langle y_2 | e_i\rangle \\ &= |x_1\rangle\langle x_2| \text{Tr} (|y_1\rangle\langle y_2|) \\ &= |x_1\rangle\langle x_2| \langle y_1 | y_2\rangle, \end{aligned} \quad (2.40)$$

where $\{|e_i\rangle\}$ is an orthonormal basis of \mathcal{H}_B . While the state vectors $|x_1\rangle$ and $|x_2\rangle$ are any two vectors in \mathcal{H}_A , the state vectors $|y_1\rangle$ and $|y_2\rangle$ are any two vectors in \mathcal{H}_B . The partial trace operation over the subsystem B is the unique operation which gives the correct measurement statistics for measurements made on the subsystem A [4, 18].

If we have a composite quantum system in product form such as $\rho^{AB} = \rho^A \otimes \rho^B$, where ρ^A and ρ^B are the density matrices corresponding to the subsystems A and B respectively, then the reduced density matrix for the subsystem A is simply given by the density matrix representing the system A itself, that is $\rho^A = \text{Tr}_B(\rho^A \otimes \rho^B) = \rho^A \text{Tr}(\rho^B) =$

ρ^A . Interestingly, almost all of the applications of quantum information theory involve quantum systems that cannot be written in product form. These remarkable systems, properties of which we study in the next section, are called entangled. Supposing that a given two-qubit composite quantum system is described by the entangled state

$$|\psi\rangle_{AB} = \frac{1}{\sqrt{2}} (|0\rangle_A|0\rangle_B + |1\rangle_A|1\rangle_B), \quad (2.41)$$

the corresponding density matrix can be written as

$$\rho^{AB} = \frac{1}{2} (|00\rangle\langle 00| + |00\rangle\langle 11| + |11\rangle\langle 00| + |11\rangle\langle 11|), \quad (2.42)$$

where the indices denoting the subsystems are dropped for simplicity. We obtain the reduced density operator of the subsystem A by tracing over the second qubit,

$$\begin{aligned} \rho^A &= \frac{1}{2} (|0\rangle\langle 0|\langle 0|0\rangle + |0\rangle\langle 1|\langle 0|1\rangle + |1\rangle\langle 0|\langle 1|0\rangle + |1\rangle\langle 1|\langle 1|1\rangle) \\ &= \frac{1}{2} (|0\rangle\langle 0| + |1\rangle\langle 1|), \end{aligned} \quad (2.43)$$

which is the maximally mixed state of one qubit.

2.3 Quantum operations

In this section, we introduce a rigorous formalism for describing the general transformations of quantum mechanical systems. A quantum operation, for instance, can be used to represent the dynamical evolution experienced by a quantum system as a result of some physical interaction between the system and its surroundings. Mathematically, it is a completely positive trace non-increasing linear map which transforms density matrices into density matrices, $\rho' = \Phi(\rho)$, up to a possible normalization factor. The previously discussed subjects of unitary evolution and quantum measurements can be understood using the framework of quantum operations.

2.3.1 Completely positive transformations

Since quantum mechanics is a linear theory, transformations describing the dynamics of quantum systems need to be linear, that is $\Phi(p_1\rho_1 + p_2\rho_2) = p_1\Phi(\rho_1) + p_2\Phi(\rho_2)$. As required by the conditions on density matrices, the transformations should also preserve the cone of positive elements and self-adjointness. In particular, Φ must be a linear positive map, transforming a density matrix ρ into a non-negative Hermitian matrix having trace less than or equal to one. An important subset of positive maps are called completely

positive maps. A positive map is said to be completely positive if the operator $\Phi \otimes I_e$ is positive for any extension of the Hilbert space \mathcal{H} to $\mathcal{H} \otimes \mathcal{H}_e$. Complete positivity is a physically motivated requirement for quantum operations. It implies that provided an ancillary system of arbitrary dimensionality, having a trivial dynamics, is coupled to the primary system, the corresponding operator $\Phi \otimes I_e$ must still be positive. All completely positive maps can be brought to a so-called Kraus (operator-sum) form [19, 20]

$$\Phi(\rho) = \sum_i M_k \rho M_k^\dagger, \quad \sum_k M_k^\dagger M_k \leq I. \quad (2.44)$$

It is also true that all the maps that can be written in Kraus form are completely positive. We note that this decomposition is not unique, meaning there exist infinitely many different sets of Kraus matrices $\{M_k\}$ that give rise to the same transformation. There is a unitary freedom in the operator-sum representation, that is, the collective action of a set of Kraus operators $\{M_1, M_2, \dots, M_m\}$ on the density matrix representing a quantum system ρ is equivalent to the collective action of another set of Kraus operators $\{E_1, E_2, \dots, E_n\}$ if and only if there exist complex numbers u_{ij} such that $E_i = \sum_j u_{ij} M_j$ where u_{ij} are the elements of a $m \times n$ unitary matrix [4]. If the dimensions of m and n do not match, we can add zero operators to the smaller set. Although completely positive maps can be physically realized in many different ways, it is not possible to realize non-completely positive maps such as the transposition map.

2.3.2 Realization of quantum operations

Imagine that we couple an additional ancillary system E (modeling the environment) to the principal system S . While the composite system of E and S is considered as being closed, the principal system S can no longer be considered as closed due to its interaction with the environment. We want to investigate the dynamics of this (open) principal system alone while the combined (closed) system undergoes a unitary evolution. There is no loss of generality by assuming that the environment is initially in a pure state, since we can always enlarge the Hilbert space of the environment to purify it. We also assume that the initial state of the combined system is in a product state, that is, $\rho_{se} = \rho_s \otimes |e_0\rangle\langle e_0|$, where $\{|e_0\rangle, |e_1\rangle, \dots, |e_k\rangle\}$ forms an orthonormal basis for the environment. Although this assumption cannot be fulfilled in all situations, experimental preparation of a system in a certain state typically destroys all correlations between the system and the environment. The non-unitary evolution of the principal system S can be obtained by tracing over the environmental degrees of freedom as $\Phi(\rho_s) = \text{Tr}_e [U(\rho_s \otimes \rho_e)U^\dagger]$. It is straightforward to see that this quantum operation can be expressed in Kraus form. We

first observe that U can be decomposed as $U = \sum_i a_i X_i \otimes Y_i$, where X_i and Y_i are linear operators acting on the system S and the environment E , respectively. Then, we have

$$\begin{aligned}
\Phi(\rho_s) &= \sum_k \langle e_k | \sum_i (a_i X_i \otimes Y_i) (\rho_s \otimes \rho_e) \sum_j (a_j X_j \otimes Y_j)^\dagger | e_k \rangle \\
&= \sum_k \sum_{ij} a_i a_j^* \langle e_k | \left(X_i \rho_s X_j^\dagger \otimes Y_i \rho_e Y_j^\dagger \right) | e_k \rangle \\
&= \sum_k \sum_{ij} a_i a_j^* X_i \rho_s X_j^\dagger \langle e_k | Y_i | e_0 \rangle \langle e_0 | Y_j^\dagger | e_k \rangle \\
&= \sum_k \left(\sum_i a_i X_i \langle e_k | Y_i | e_0 \rangle \right) \rho_s \left(\sum_j a_j X_j \langle e_k | Y_j | e_0 \rangle \right)^\dagger \\
&= \sum_k \left(\langle e_k | \sum_i a_i X_i \otimes Y_i | e_0 \rangle \right) \rho_s \left(\langle e_k | \sum_j a_j X_j \otimes Y_j | e_0 \rangle \right)^\dagger \\
&= \sum_k \langle e_k | U | e_0 \rangle \rho_s \langle e_k | U | e_0 \rangle^\dagger.
\end{aligned} \tag{2.45}$$

Defining the operators $M_k \equiv \langle e_k | U | e_0 \rangle$, we arrive at the operator-sum representation

$$\Phi(\rho_s) = \sum_k M_k \rho_s M_k^\dagger. \tag{2.46}$$

Since the resulting density matrix $\Phi(\rho_s)$ must have unit trace, the Kraus operators $\{M_k\}$ satisfy the completeness relation

$$\begin{aligned}
1 &= \text{Tr} \left(\sum_k M_k \rho_s M_k^\dagger \right) \\
&= \text{Tr} \left(\sum_k M_k^\dagger M_k \rho_s \right)
\end{aligned} \tag{2.47}$$

For the above relation to hold for all density matrices, we must have

$$\sum_k M_k^\dagger M_k = I. \tag{2.48}$$

Since different environmental interactions may result in the same dynamics on the system, the same quantum operation Φ can be obtained by choosing a different environmental basis or by considering a different unitary interaction. We have thus far shown that the unitary evolution of the combined state of the system S and the environment E gives rise to a Kraus representation for the quantum operation Φ describing the dynamics of the system S . The inverse relationship is also true, that is, given the Kraus operators of a quantum operation, one can always construct an environmental basis along with some unitary dynamics that corresponds to the desired Kraus representation [4, 9].

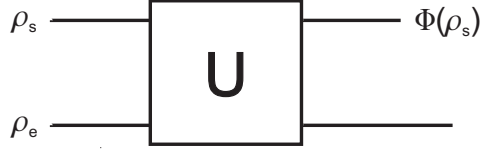


Figure 2.2: We first let an ancillary system (modeling the environment) interact with the principle system via a unitary interaction. Reduced non-unitary dynamics of the principal system can then be obtained by discarding the state of the environment.

We can interpret each of the terms in operator-sum representation individually. Suppose that, after the unitary evolution of the combined system of S and E , we perform a projective measurement on the environment in the orthonormal basis $\{|e_k\rangle\}$. The measurement operators are given by

$$\Pi_k = I_s \otimes |e_k\rangle\langle e_k|. \quad (2.49)$$

Provided that the projective measurement is performed in a non-selective way (by considering the statistical ensemble of conditional post-measurement states), the reduced dynamics of the principal system remains unchanged. However, if the projective measurement is performed in a selective way (by transforming the pre-measurement state into a set of conditional post-measurement states according to the possible measurement outcomes), then we can obtain the individual terms appearing in the operator-sum representation [10]. Assuming that the initial state of the composite system is $\rho_{se} = \rho_s \otimes |e_0\rangle\langle e_0|$, the state of the combined system after the measurement changes into

$$\frac{\Pi_k U(\rho_s \otimes |e_0\rangle\langle e_0|) U^\dagger \Pi_k}{\text{Tr}[\Pi_k U(\rho_s \otimes |e_0\rangle\langle e_0|) U^\dagger \Pi_k]}, \quad (2.50)$$

with probability $p_n = \text{Tr}[\Pi_k U(\rho_s \otimes |e_0\rangle\langle e_0|) U^\dagger \Pi_k]$. Tracing over the environmental degrees of freedom, the post-measurement state of the principle system reads

$$\frac{M_k \rho_s M_k^\dagger}{\text{Tr}(M_k \rho_s M_k^\dagger)}, \quad (2.51)$$

with probability $p_n = \text{Tr}(M_k \rho_s M_k^\dagger)$. Here, the matrices M_k are nothing but the Kraus operators defined as $M_k \equiv \langle e_k | U | e_0 \rangle$. Thus, we see that each of the terms appearing in the operator sum representation corresponds to the possible outcomes of a selective projective measurement performed on the environment.

Chapter 3

ENTANGLEMENT

In this chapter we will first consider the separability problem of quantum states to introduce the concept of quantum entanglement, which is one of the most central subjects to be investigated in this thesis. We will then discuss the quantification of entanglement and review the properties of some well known entanglement measures such as concurrence and negativity. The manipulation and classification of certain entangled states under local operations and classical communication will also be examined. For a detailed review of quantum entanglement and related concepts, interested reader may refer to [3]. Finally, we will conclude the chapter by presenting our results related to the optimal transformations of flip and exchange symmetric entangled states via local operations [21].

3.1 Separability of quantum states

We start by considering the simple case of a pure bipartite quantum system. Assuming that the finite dimensional Hilbert spaces \mathcal{H}_A and \mathcal{H}_B of individual parts have orthonormal basis states $\{|a_i\rangle\}$ and $\{|b_j\rangle\}$, respectively, the Hilbert space of the composite system can be described by basis states $\{|a_i b_j\rangle\}$, according to the postulates of quantum theory. Consequently, an arbitrary pure state living in $\mathcal{H}_A \otimes \mathcal{H}_B$ can be written as the superpositions of the basis states,

$$|\psi\rangle = \sum_{ij} c_{ij} |a_i b_j\rangle. \quad (3.1)$$

If a quantum state $|\phi\rangle \in \mathcal{H}_A \otimes \mathcal{H}_B$ can be expressed in the form

$$|\phi\rangle = |\alpha\rangle \otimes |\beta\rangle, \quad (3.2)$$

where $|\alpha\rangle \in \mathcal{H}_A$ and $|\beta\rangle \in \mathcal{H}_B$, then $|\phi\rangle$ is said to be a separable state, otherwise it is said to be an entangled state. In other words, an entangled state cannot be written as a tensor product of individual states representing each subsystem. At this point, we want

to emphasize that the remarkable phenomenon of entanglement is not only essential for almost all of the applications of quantum information science but also for the foundations of quantum mechanics [1, 2]. Schrödinger himself stressed its importance, saying that "I would not call (entanglement) one but rather the characteristic trait in quantum mechanics, the one that enforces an entire departure from all our classical lines of thought." Let us now give a simple example of an entangled and a separable state of two-qubits. It is easy to see that while the entangled quantum state

$$|\psi\rangle = \frac{1}{\sqrt{2}}(|01\rangle + |10\rangle), \quad (3.3)$$

cannot be written as a tensor product of its individual states, the quantum state

$$|\phi\rangle = \frac{1}{\sqrt{2}}(|10\rangle + |00\rangle), \quad (3.4)$$

is separable since it can be written as

$$|\phi\rangle = \frac{1}{\sqrt{2}}(|1\rangle + |0\rangle) \otimes |0\rangle. \quad (3.5)$$

Next, we turn our attention to the case of quantum states that cannot be represented by a single state vector. A mixed bipartite system described by a density matrix ρ^{AB} is said to be separable if and only if it can be decomposed as [22]

$$\rho^{AB} = \sum_k p_k \rho_k^A \otimes \rho_k^B, \quad (3.6)$$

where ρ_k^A and ρ_k^B are the density matrices of the individual subsystems, and the positive weights p_k satisfy $\sum_k p_k = 1$. This requirement implies that a separable mixed state can be prepared by two parties, that have access to a form of classical communication, using local operations while an entangled mixed state cannot. It is not difficult to imagine that the above discussion of separability for both pure and mixed quantum states can be straightforwardly extended to multipartite states.

3.1.1 Peres criterion for separability of bipartite states

Despite the fact that some simple pure quantum states might be easily determined to be entangled or separable, it is no trivial task to find out whether a given arbitrary mixed quantum state can be written as a convex sum of product states as in (3.6). A necessary condition, which is based on the partial transpose operation, for the existence of such decomposition has been given by Peres [23]. This condition, also known as the Peres criterion or positive partial transpose (PPT) criterion, is violated by all entangled states.

Let us now consider the following form of the density matrix ρ^{AB} describing the state of two subsystems A and B ,

$$\rho^{AB} = \sum_{ijkl} p_{kl}^{ij} |i\rangle\langle j| \otimes |k\rangle\langle l|. \quad (3.7)$$

The partial transpose of this density matrix with respect to the subsystem B is given by

$$(\rho^{AB})^{T_B} = \sum_{ijkl} p_{kl}^{ij} |i\rangle\langle j| \otimes (|k\rangle\langle l|)^T = \sum_{ijkl} p_{kl}^{ij} |i\rangle\langle j| \otimes |l\rangle\langle k|, \quad (3.8)$$

where the identity operator acts on the subsystem A . The statement of the criterion is simple: If ρ^{AB} is separable, then $(\rho^{AB})^{T_B}$ is a PPT state, that is, it has a non-negative eigenvalue spectrum. On the other hand, even a single negative eigenvalue of $(\rho^{AB})^{T_B}$ is sufficient to conclude that ρ^{AB} is entangled. We note that the outcome of the test does not depend on the subsystem with respect to which transposition is performed. Even though there exists no general method to decide whether a given PPT state is separable or not in general, Horodecki et al. has proved that all PPT states of $2 \otimes 2$ (qubit-qubit) and $2 \otimes 3$ (qubit-qutrit) systems are separable [24]. Thus, the Peres criterion gives a necessary and sufficient condition for the entanglement of quantum states in these dimensions. In order to see the usefulness of the Peres criterion in an illustrative example, consider the simple two-qubit class of Werner states,

$$\rho^{AB} = \frac{(1-p)}{4} I_4 + \frac{p}{2} (|01\rangle - |10\rangle)(\langle 01| - \langle 10|), \quad (3.9)$$

where $0 \leq p \leq 1$ and I_4 is the 4×4 identity operator. The density matrix ρ^{AB} can be represented in the product basis $\{|00\rangle, |01\rangle, |10\rangle, |11\rangle\}$ as

$$\rho^{AB} = \frac{1}{4} \begin{pmatrix} 1-p & 0 & 0 & 0 \\ 0 & 1+p & -2p & 0 \\ 0 & -2p & 1+p & 0 \\ 0 & 0 & 0 & 1-p \end{pmatrix}. \quad (3.10)$$

Evaluating the partial transpose with respect to the subsystem B , we end up with

$$(\rho^{AB})^{T_B} = \frac{1}{4} \begin{pmatrix} 1-p & 0 & 0 & -2p \\ 0 & 1+p & 0 & 0 \\ 0 & 0 & 1+p & 0 \\ -2p & 0 & 0 & 1-p \end{pmatrix}, \quad (3.11)$$

whose only potential negative eigenvalue is $\lambda = (1-3p)/4$. Therefore, we conclude that the considered Werner state is separable for $0 \leq p \leq 1/3$ and entangled for $1/3 < p \leq 1$.

3.1.2 Schmidt decomposition

We now introduce a fundamental theorem for pure bipartite quantum states, known as the Schmidt decomposition theorem. The statement of the theorem is as follows: Supposing that $|\psi_{AB}\rangle$ is a pure state of a bipartite quantum system AB , there always exists a decomposition of the form

$$|\psi_{AB}\rangle = \sum_i \lambda_i |i_A\rangle |i_B\rangle, \quad (3.12)$$

where $|i_A\rangle$ and $|i_B\rangle$ define an orthonormal basis (Schmidt basis) for the subsystems A and B , respectively, and the non-negative real Schmidt coefficients λ_i satisfy $\sum_i \lambda_i^2 = 1$. The proof of this theorem can be done with the help of the singular value decomposition theorem [4]. It is worth to emphasize that there is no direct analogue of the Schmidt decomposition for multipartite or mixed states. Due to the simple structure of (3.12), we can immediately obtain the reduced density matrices ρ^A and ρ^B by tracing out each subsystem separately:

$$\rho^A = \sum_i \lambda_i^2 |i_A\rangle \langle i_A|, \quad \rho^B = \sum_i \lambda_i^2 |i_B\rangle \langle i_B|. \quad (3.13)$$

Since the eigenvalues of the reduced density matrices ρ^A and ρ^B turns out to be identical, various important properties of the composite quantum state $|\psi_{AB}\rangle$ can be determined by either of the reduced density matrices. Moreover, it can be shown that a bipartite system is separable if and only if it has a single non-zero eigenvalue in its decomposition.

3.2 Quantification of entanglement

Considering that the concept of entanglement plays a crucial role in quantum information science, it is very important to characterize it from various different perspectives. One of the most important aspects of the characterization of entanglement is the determination of the amount of entanglement in a given arbitrary quantum state. Although the quantification of entanglement is relatively well understood for the case of two-qubits [25–27], little is known about its generalization to multipartite or higher dimensional mixed systems. There is a zoo of entanglement measures available in literature [3], each having their own advantages for specific purposes. However, we will limit ourselves to the measures of entanglement that we intend to utilize in the following chapters.

Before starting to discuss the properties of entanglement measures, we introduce the concept of local operations and classical communication (LOCC) [28–31]. This proto-

col implies that, provided two spatially separated parties share a quantum state, they can classically communicate to coordinate the quantum operations they apply on their own subsystems. LOCC is an essential ingredient for the execution of many quantum information processing protocols such as quantum teleportation [32]. Besides, LOCC operations are also deeply connected with the characterization of entanglement. In fact, while classically correlated quantum states can be prepared by LOCC operations, entangled states can never be created using such operations alone. All LOCC operations can be naturally expressed in the form of a separable operation as (in case of a bipartite system)

$$\mathcal{E}(\cdot) = \sum_k A_k \otimes B_k(\cdot) A_k^\dagger \otimes B_k^\dagger, \quad (3.14)$$

where A_k and B_k are generalized measurement operators locally acting on the first and second subsystems, respectively. However, it is remarkable that not there exist separable operations that cannot be implemented by means of LOCC [33–38].

In the theory of entanglement measures, there are two main approaches to the quantification of entanglement, namely, operational and axiomatic approaches. The goal of the operational one is to adopt a protocol whose performance of success is directly connected with the amount of entanglement contained in the quantum state. On the other hand, in the axiomatic (or abstract) approach, one typically tries to define a real valued function with certain reasonable properties. A list of these desirable features, which are expected to be satisfied by good entanglement measures, is as follows:

- An entanglement measure $E(\rho)$ of a bipartite system ρ is a mapping that takes density matrices as inputs and produces positive real numbers as outputs.
- $E(\rho)$ vanishes provided that the input state ρ is separable.
- $E(\rho)$ is invariant under local unitaries, meaning $E(\rho) = E(U_A \otimes U_B \rho U_A^\dagger \otimes U_B^\dagger)$.
- E is an entanglement monotone, i.e., it does not increase under LOCC on average:

$$E(\rho) \geq \sum_i p_i E(\rho_i), \quad (3.15)$$

where the outcome ρ_i is obtained with probability p_i after the LOCC protocol.

Although there is no general agreement on the properties that an entanglement measure must satisfy, the above requirements are commonly considered sufficient to define a good measure [39–44]. We emphasize that the last condition related to the behavior of entanglement measures under LOCC transformations is more restrictive than the requirement that $E(\rho) \geq E(\sum_i p_i \rho_i)$. Nonetheless, this simplified version might be considered

as more fundamental as it gives direct information about the entanglement of the transformed state, while (3.15) only tells about the average entanglement of an ensemble. As a result, some experts also recognize the functions that satisfy $E(\rho) \geq E(\sum_i p_i \rho_i)$ as entanglement monotones [3]. We lastly note that some optional conditions can be imposed on entanglement measures depending on the context, such as convexity and additivity. Detailed reviews of the theory of entanglement measures can be found in [3, 43, 44].

3.2.1 Entropy of entanglement

Let us start by giving a brief overview of the von Neumann entropy. In classical information theory, Shannon entropy [45] is used to measure the amount of information we have gained after learning the value of a random variable X . In particular, it quantifies the amount of randomness in a classical system. Given a probability distribution p_1, \dots, p_n , its Shannon entropy is defined by

$$H(p_1, \dots, p_n) = - \sum_i p_i \log p_i, \quad (3.16)$$

where the logarithm is taken in base two and it is assumed that $0 \log 0 \equiv 0$. This definition can be extended to quantum mechanical systems by replacing probability distributions with density matrices. Therefore, the von Neumann entropy of a quantum system described by the density matrix ρ can be straightforwardly calculated as

$$S(\rho) = - \sum_i \lambda_i \log \lambda_i, \quad (3.17)$$

with λ_i being the eigenvalues of the density matrix ρ .

Having discussed the von Neumann entropy, we are now ready to define the entropy of entanglement, which is considered to be a reliable measure of entanglement for pure bipartite systems in all dimensions [29, 46]. Entropy of entanglement of a pure bipartite system represented by the density matrix ρ^{AB} is given by

$$E(\rho^{AB}) = S(\rho^A) = S(\rho^B), \quad (3.18)$$

where the reduced density matrices ρ^A and ρ^B are calculated by evaluating the partial trace over the subsystems B and A , respectively. Despite the fact that a composite system is in a pure state, individual subsystems might be mixed. Indeed, only separable systems have their subsystems in a pure state as the only non-zero eigenvalue for each of the pure subsystems is one. On the other hand, d -dimensional states of the form $|\psi\rangle = (|00\rangle + |11\rangle + \dots + |(d-1)(d-1)\rangle)/\sqrt{d}$ attain the maximum value of E , which is $\log d$.

3.2.2 Concurrence

A concrete measure of entanglement for two qubit states is provided by concurrence [25]. In order to evaluate the concurrence of a two-qubit system described by the density matrix ρ , one first needs to calculate the spin-flipped density matrix $\tilde{\rho}$, which is given by

$$\tilde{\rho} = (\sigma^y \otimes \sigma^y) \rho^* (\sigma^y \otimes \sigma^y). \quad (3.19)$$

Here σ^y is the usual Pauli spin operator in y-direction, and ρ^* is obtained from ρ via complex conjugation in the standard two qubit basis $\{|00\rangle, |01\rangle, |10\rangle, |11\rangle\}$. Then, the amount of entanglement contained in the state ρ is given by the concurrence function:

$$C(\rho) = \max \left\{ 0, \sqrt{\lambda_1} - \sqrt{\lambda_2} - \sqrt{\lambda_3} - \sqrt{\lambda_4}, \right\}, \quad (3.20)$$

where $\{\lambda_i\}$ are the eigenvalues of the product matrix $\rho\tilde{\rho}$ in decreasing order. For the two-qubit pure states given in the standard basis as

$$|\psi\rangle = a|00\rangle + b|01\rangle + c|10\rangle + d|11\rangle, \quad (3.21)$$

concurrence is given by $C(|\psi\rangle) = 2|ad - bc|$. This observation clearly shows the significance of concurrence as a non-separability measure since a state of the form (3.21) is separable if and only if $ad = bc$.

The concurrence of a two-qubit system can also be used for the calculation of another entanglement measure known as entanglement of formation [26]:

$$\mathcal{E}(\rho) = h \left(\frac{1 + \sqrt{1 - C^2(\rho)}}{2} \right); \quad (3.22)$$

$$h(x) = -x \log x - (1 - x) \log (1 - x), \quad (3.23)$$

where the logarithm is taken in base two and $C(\rho)$ is the concurrence given by (3.20). We note that, while concurrence is an abstract quantity, entanglement of formation is a resource based measure, that is, it quantifies the required amount of maximally entangled states to be able to construct a given mixed state.

3.2.3 Negativity

Negativity enjoys the advantage that it can be computed easily for an arbitrary bipartite state regardless of its dimension, provided that the considered state has a negative partial transpose (NPT) [27]. As discussed in Section 3.1.1, it is in general not possible to conclude whether a positive partial transpose state is separable or not, yet, all PPT states

of qubit-qubit and qubit-qutrit systems are separable. Hence, negativity completely characterizes the qubit-qubit and qubit-qutrit entanglement. For a given bipartite state ρ^{AB} , negativity is calculated as the absolute sum of the negative eigenvalues of partial transpose of ρ^{AB} with respect to the smaller dimensional system,

$$N(\rho^{AB}) = \frac{1}{2} \sum_i |\eta_i| - \eta_i, \quad (3.24)$$

where η_i are all of the eigenvalues of the partially transposed density matrix $(\rho^{AB})^{T_A}$. The relation of the above expression to Peres separability criterion is evident as (3.24) measures the degree to which $(\rho^{AB})^{T_A}$ fails to become positive.

3.3 Classification of entangled states

In quantum information science, the characterization of entanglement is not limited to the investigation of entanglement measures and their properties. It is also desirable to have means for grouping entangled states into operational equivalence classes, in the sense that if two states can be used to accomplish same tasks, then they should be considered equivalent. For this purpose, various different classification schemes have been proposed. One of the most obvious ideas is to make use of local unitary (LU) operations, which are both reversible and deterministic. This scheme is motivated by a quite reasonable physical requirement: Recognizing the fact that LU operations just correspond to a local change of basis for a given quantum state, LU equivalent states possess the same amount of entanglement. Mathematically, an n-partite quantum state $|\psi\rangle$ is said to be LU equivalent to $|\phi\rangle$ if there exist local unitary operators U_1, U_2, \dots, U_n such that

$$|\psi\rangle = U_1 \otimes U_2 \otimes \dots \otimes U_n |\phi\rangle. \quad (3.25)$$

Recently, Kraus has obtained a necessary and sufficient condition for the LU equivalence of two n-partite qubit states [47, 48]. Furthermore, Liu has proposed a classification scheme for general multipartite pure states in arbitrary dimensions under LU [49].

Although LU operations have a significant operational meaning, more general local transformations are required for the realization of quantum communication schemes. In addition to the unitary operations, such transformations may also include introduction of ancillary systems, measurements, removing parts of systems, and in general can be described by completely positive linear maps (as discussed in Section 2.3). When augmented with the possibility of classical communication, multi-local application of these operations correspond to what we have defined as LOCC transformations. More precisely,

LOCC transformations are completely positive linear trace non-increasing maps that can be locally implemented with classical coordination among the parties. As contrary to LU operations, LOCC transformations are not generally reversible. All the same, for the special case of pure states, it has been shown that two states are deterministically interconvertible by LOCC (equivalent under LOCC) if and only if they are equivalent under LU operations [31, 39]. Accordingly, if two states are equivalent under LOCC, they have the same amount of entanglement. At this point, we want to emphasize that the possibility of one-way conversion of a quantum state to another under LOCC operations does not necessarily imply the two-way LOCC conversion of the considered states. Moreover, there are certain quantum states, namely, maximally entangled states from which all others can be generated by means of LOCC. As an example, suppose that two spatially separated parties A and B share a maximally entangled two-qubit state

$$|\psi\rangle_{AB} = \frac{1}{\sqrt{2}}(|00\rangle + |11\rangle). \quad (3.26)$$

It is not difficult to see that any pure state having a Schmidt decomposition

$$|\psi\rangle = \alpha|00\rangle + \beta|11\rangle, \quad (3.27)$$

can be generated from (3.26) by LOCC transformations. Imagine that we first introduce an ancillary qubit to subsystem A , resulting in the state

$$\frac{|00\rangle_A|0\rangle_B + |01\rangle_A|1\rangle_B}{\sqrt{2}}. \quad (3.28)$$

Then, when the unitary transformation

$$|00\rangle_A \rightarrow \alpha|00\rangle_A + \beta|11\rangle_A, \quad |01\rangle_A \rightarrow \beta|01\rangle_A + \alpha|10\rangle_A, \quad (3.29)$$

is applied on the first two qubits, we end up with the state

$$\frac{|0\rangle_A(\alpha|00\rangle_{AB} + \beta|11\rangle_{AB}) + |1\rangle_A(\beta|10\rangle_{AB} + \alpha|01\rangle_{AB})}{\sqrt{2}}. \quad (3.30)$$

As a last step, a local measurement is performed on the ancillary qubit. If the result of the measurement turns out to be $|0\rangle$, then no operation is required on the subsystem B . On the other hand, if the ancilla is measured to be $|1\rangle$, then the Pauli σ_x is applied on the subsystem B to obtain (3.27). This example demonstrates how the coordination of local operations can make otherwise not multi-locally implementable transformations possible.

Finally, we turn our attention back to the states which are not interconvertible under LOCC operations. Nielsen has investigated this subject and revealed an important connection between the problem of state conversion under LOCC and the algebraic theory of ma-

majorization [50]. Supposing that we have two real d -dimensional vectors $x = (x_1, \dots, x_d)$ and $y = (y_1, \dots, y_d)$, x is said to be majorized by y (written as $x \prec y$), if for each j ,

$$\sum_{i=1}^j x_i^\downarrow \leq \sum_{i=1}^j y_i^\downarrow, \quad (3.31)$$

with equality holding when $j = d$, and where the \downarrow indicates that the elements are taken in decreasing order. With this definition in mind, Nielsen's theorem can be summarized as follows: Consider two parties A and B sharing a bipartite quantum state $|\psi\rangle$. The reduced density matrix ρ_ψ , whose eigenvalues are denoted by λ_ψ , can be obtained by taking partial trace with respect to the subsystem A . Then, the theorem states that $|\psi\rangle$ can be deterministically transformed to $|\phi\rangle$ under LOCC if and only if $\lambda_\psi \prec \lambda_\phi$. This result automatically implies that two pure states are LOCC equivalent if and only if they have the same Schmidt coefficients, since λ_ψ and λ_ϕ are nothing but the Schmidt coefficients of the states $|\psi\rangle$ and $|\phi\rangle$, respectively. We also note that the condition (3.31) gives rise to states which are incomparable under LOCC to each other.

3.3.1 Stochastic local operations and classical communication

Classification of quantum states under LOCC transformations (LU operations) is not the only method of partitioning the Hilbert space into subspaces. In fact, the LU equivalence based scheme has its disadvantages: Since LU operations do not change the amount of entanglement contained in a quantum state, representatives of entanglement classes are labeled by continuous parameters, which means that there are infinitely many types of entangled states even in the case of two-qubit states. In order to simplify the classification problem, the condition of determinism can be removed from LOCC operations to allow for probabilistic conversion of states through stochastic local operations and classical communication (SLOCC) [31]. This coarse-graining not only simplifies the structure of equivalence classes but also has a direct operational meaning. Provided that two states can be obtained from each other with some non-vanishing probability, then they might still be used as a resource for the same tasks of quantum information processing, although this time the success chance of the task may differ from $|\phi\rangle$ to $|\psi\rangle$. With the consideration of SLOCC, two states are said to have same kind of entanglement if an invertible local operation (ILO) relating them exists [51]. Mathematically, n -partite states $|\psi\rangle$ and $|\phi\rangle$ are considered to be in the same equivalence class under SLOCC transformations if there exist 2×2 matrices A_1, A_2, \dots, A_n , with non-zero determinants, such that

$$|\phi\rangle = A_1 \otimes A_2 \otimes \dots \otimes A_n |\psi\rangle. \quad (3.32)$$

While SLOCC transformations cannot increase entanglement on average, they can still increase or decrease the amount entanglement of entanglement contained in a quantum state with a certain non-zero probability. However, they can never create entanglement out of nowhere due to their local nature. We also note that LU equivalent states are also equivalent under SLOCC operations but not vice versa.

In case of pure two-qubit states, there are two equivalence classes [51, 52]: the separable one consisting of all product states, and the entangled one, members of which are all equivalent to the maximally entangled state

$$|\psi\rangle_{AB} = \frac{1}{\sqrt{2}}(|00\rangle + |11\rangle). \quad (3.33)$$

For pure three qubit states, the classification problem has been solved by making use of the local ranks of the reduced density matrices, which are invariant under SLOCC transformations [51]. It has been shown that there exist six non-equivalent SLOCC classes: the separable class, three biseparable classes $AB - C$, $AC - B$, $BC - A$, and two fully entangled classes GHZ and W that are represented by

$$|GHZ\rangle = \frac{1}{\sqrt{2}}(|000\rangle + |111\rangle), \quad (3.34)$$

$$|W\rangle = \frac{1}{\sqrt{3}}(|001\rangle + |010\rangle + |100\rangle). \quad (3.35)$$

While the separable class corresponds to the states with local ranks $r(\rho_a) = r(\rho_b) = r(\rho_c) = 1$, biseparable classes have only one of their reduced density matrices with rank 1. For instance, the states in the class $AB - C$ have entanglement only between the subsystems B and C , thus they have $r(\rho_a) = r(\rho_b) = 2$ and $r(\rho_c) = 1$. In spite of the fact that there exist two inequivalent kinds of true tripartite entanglement, only the members of the GHZ class have non-vanishing 3-tangle [53] (a measure of entanglement for pure tripartite states). In this regard, quantum states with GHZ-type of entanglement are said to have genuine tripartite entanglement. Indeed, almost all three qubit entangled states belong to the GHZ class, i.e., the W-type states are of zero measure in this Hilbert space.

Starting from the case of four qubits, the number of the equivalence classes become infinite. However, it is still desirable to partition these infinitely many classes into a finite number of groups or families sharing certain properties. In recent literature, two main (complementary) strategies have been used to solve the problem of SLOCC classification for four qubits. Whereas the first method aims to exploit the vanishing or not of certain covariants or invariants to distinguish different equivalence classes [54–58], the second method uses the normal forms to construct families of quantum states [59–61]. For example, Verstrate et al. have used the latter approach to classify the pure four qubit states into

eight inequivalent families under SLOCC operations [59]. In particular, given an arbitrary pure state of four qubit, it can always be transformed into one of the following states by using determinant one ILOs:

$$G_{abcd} = \frac{a+d}{2}(|0000\rangle + |1111\rangle) + \frac{a-d}{2}(|0011\rangle + |1100\rangle) \\ + \frac{b+c}{2}(|0101\rangle + |1010\rangle) + \frac{b-c}{2}(|0110\rangle + |1001\rangle), \quad (3.36)$$

$$L_{abc_2} = \frac{a+b}{2}(|0000\rangle + |1111\rangle) + \frac{a-b}{2}(|0011\rangle + |1100\rangle) \\ + c(|0101\rangle + |1010\rangle + |0110\rangle), \quad (3.37)$$

$$L_{a_2b_2} = a(|0000\rangle + |1111\rangle) + b(|0101\rangle + |1010\rangle) + c(|0101\rangle \\ + |1010\rangle + |0110\rangle), \quad (3.38)$$

$$L_{ab_3} = a(|0000\rangle + |1111\rangle) + \frac{a+b}{2}(|0101\rangle + |1010\rangle) + \frac{a-b}{2} \times \\ (|0110\rangle + |1011\rangle) + \frac{i}{\sqrt{2}}(|0001\rangle + |0010\rangle + |0111\rangle + |1011\rangle), \quad (3.39)$$

$$L_{a_4} = a(|0000\rangle + |0101\rangle + |1010\rangle + |1111\rangle) + (i|0110\rangle \\ + |0110\rangle - i|0110\rangle), \quad (3.40)$$

$$L_{a_2 0_{3\oplus\bar{1}}} = a(|0000\rangle + |111\rangle) + (|0011\rangle|0101\rangle|0110\rangle), \quad (3.41)$$

$$L_{0_{7\oplus\bar{1}}} = |0000\rangle + |1011\rangle + |1101\rangle + |1110\rangle, \quad (3.42)$$

$$L_{0_{3\oplus\bar{1}} 0_{3\oplus\bar{1}}} = |0000\rangle + |0111\rangle \quad (3.43)$$

Notice that the states, which are equivalent under SLOCC, belong to the same family but the inverse statement is not true. Moreover, while the completely separable state $|0000\rangle$ forms its own class in the former approach, it belongs to the family L_{abc_2} in the latter one, which also contains fully entangled states [60].

When it comes to classifying pure many qubit states under SLOCC, considerable efforts have been directed towards the solution of the problem. As multipartite entanglement has a much richer structure than the few particle scenario, the problem becomes particularly complicated in this case. Some partial results include the classification of $2 \times 2 \times n$ dimensional multipartite states [62], even n-qubit states [63], odd n-qubit states [64] and symmetric n-qubit states [65, 66]. In particular, exploiting the fact that all symmetric states can be related via symmetric ILOs [67], Bastin et al. have determined the equivalence classes of all symmetric states of n-qubits with the help of Majorana representation of symmetric states [66]. More recently, Li et al. have presented a scheme for classifying the general n-qubit states, which makes use of a relation between coefficient matrices associated with the states [68].

3.3.2 Equivalence classes of flip and exchange symmetric states

In this section, we review the classification of flip and exchange symmetric (FES) states, which are invariant when two qubits are interchanged or when all 0s (1s) are changed to 1s (0s), under ILOs. It has been recently shown that multiqubit FES states constitute a set of curves in the Hilbert space and equivalence classes of these states under ILOs can be determined in a systematic way for an arbitrary number of qubits [69]. In addition to the relative simplicity of the form of their entanglement classes under SLOCC, FES states are also important if one considers, for example, bosonic qubits where exchange symmetry is essential. Moreover, since these symmetric states are by definition invariant under spin flip errors (acting on all qubits simultaneously), they will not be altered by such global effects. In other words, FES states form a decoherence-free subspace under global spin flip type decoherence.

An n -qubit state $|\psi\rangle$ is said to have flip and exchange symmetry if it satisfies $\sigma_x|\psi\rangle = |\psi\rangle$ with σ_x being the Pauli spin matrix in x -direction, and $P_{ij}|\psi\rangle = |\psi\rangle$ where P_{ij} is the exchange operator for the i^{th} and j^{th} qubits. It has been noted that imposing these symmetries on the system drastically simplifies the form of the invertible operators. Thus, FES ILOs can be written as

$$M(t) = f(t) \begin{pmatrix} 1 & t \\ t & 1 \end{pmatrix}, \quad (3.44)$$

where $t \neq \pm 1$. Assuming that $|\psi(0)\rangle$ is a normalized n qubit FES state, all equivalent normalized FES states can then be obtained as

$$|\psi(t)\rangle = \frac{M^{\otimes n}|\psi(0)\rangle}{\sqrt{\langle\psi(0)|M^{\dagger}M)^{\otimes n}|\psi(0)\rangle}}. \quad (3.45)$$

They lie on a curve parameterized by t provided that t is real. As t changes from $-\infty$ to ∞ , excluding $t = \pm 1$, $|\psi(t)\rangle$ traces the curve. However, if $|\psi(0)\rangle$ turns out to be an eigenstate of $M^{\otimes n}(t)$, no FES ILO will alter it or by definition $|\psi(0)\rangle$ will form an equivalence class by itself. Eigenstates of $M^{\otimes n}$ are of the form $\otimes_{k=1}^n |\pm\rangle_k$ where $|\pm\rangle = (1/\sqrt{2})(|0\rangle \pm |1\rangle)$, and number of $|+\rangle$ and $|-\rangle$ states in the product are p and $q = n - p$, respectively. Flip symmetric ones are those with even q . Eigenvalues are given by

$$\lambda_{pq} = f^n(t)(1+t)^p(1-t)^q, \quad (3.46)$$

and they are $n!/p!q!$ fold degenerate. The eigenstate $|\psi_{pq}\rangle$ denotes the FES state obtained by evaluating the symmetric linear combination of degenerate eigenstates corresponding to eigenvalue λ_{pq} given by (3.46).

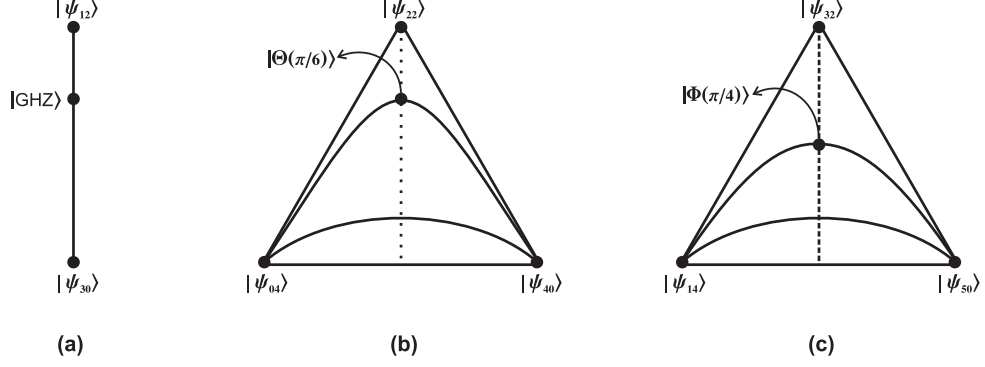


Figure 3.1: Graphical representation of 3, 4 and 5-qubit FES states under ILOs. (a) Almost all states are equivalent to $|GHZ\rangle$ under ILOs while $|W\rangle$ ($|\psi_{12}\rangle$) and $|S\rangle$ ($|\psi_{30}\rangle$) are the neighbors of this equivalence class. (b) $|\psi_{40}\rangle$ and $|\psi_{04}\rangle$ are the end points of the curves. The dotted line denotes a portion of the great circle $G_{a,a-d,0,d}$ and $|\psi_{22}\rangle$ corresponds to $G_{1,-1,0,2}$. The states lying inside the envelope can be generated using $|\Theta(\theta)\rangle = (\sin \theta/\sqrt{2})(|\psi_{40}\rangle + |\psi_{04}\rangle) + \cos \theta|\psi_{22}\rangle$ with $0 < \theta \leq \pi/2$ as a representative subset. (c) All curves extend between $|\psi_{14}\rangle$ and $|\psi_{50}\rangle$. The states lying inside the envelope can be generated using the representative subset $|\Phi(\theta)\rangle = (\sin \theta/\sqrt{2})(|\psi_{50}\rangle + |\psi_{14}\rangle) + \cos \theta|\psi_{32}\rangle$ with $0 < \theta \leq \pi/2$, which is denoted by the dashed line.

In case of three qubits, possible even q values are 0 and 2. While the former corresponds to the separable state $|\psi_{30}\rangle = |++\rangle$, the latter corresponds to the entangled state $|\psi_{12}\rangle = \frac{1}{\sqrt{3}}(|+-\rangle + |-+-\rangle + |--\rangle)$, which is equivalent to the $|W\rangle$ state. Since $|GHZ\rangle$ can be written as $|GHZ\rangle = \cos \theta|\psi_{12}\rangle + \sin \theta|\psi_{30}\rangle$ with $\theta = \pi/6$, it lies on the geodesic connecting the separable $|S\rangle$ state and the entangled FES $|W\rangle$ state.

Allowed q values for four qubits are 0, 2 and 4. The first and the third are separable $|\psi_{40}\rangle$ and $|\psi_{04}\rangle$ states, respectively. The only entangled one is $|\psi_{22}\rangle$ which is nothing but $G_{1,-1,0,2}$ as given by (3.36). Since there are three distinct eigenvalues, the FES subspace is a sphere. All curves start and end on $|\psi_{40}\rangle$ and $|\psi_{04}\rangle$. Expectedly, there exists infinitely many curves corresponding to infinitely many different SLOCC classes. Among the nine classes of four-qubit states, the only FES one is G_{abcd} with $b = d - a$ and $c = 0$, and it represents a great circle on the sphere passing through $|\psi_{22}\rangle$ and making equal angles with $|\psi_{40}\rangle$ and $|\psi_{04}\rangle$. Hence, all four-qubit FES states can be generated, by the application of FES ILOs, using $G_{a,a-d,0,d}$ as a representative subset. If one specifically wants to deal with the curves lying inside the envelope, then considering $|\Theta(\theta)\rangle = (\sin \theta/\sqrt{2})(|\psi_{40}\rangle + |\psi_{04}\rangle) + \cos \theta|\psi_{22}\rangle$ with $0 < \theta \leq \pi/2$ as a representative is sufficient.

When it comes to five qubits, the only separable eigenstate is $|\psi_{50}\rangle$. The remaining two are entangled states represented by $|\psi_{32}\rangle$ and $|\psi_{14}\rangle$. The FES subspace is again three dimensional and the curves join $|\psi_{50}\rangle$ and $|\psi_{14}\rangle$. Since all three distinct eigenstates are perpendicular to each other by construction, all curves lying inside the envelope can be generated by the application of FES ILOs to the representative subset $|\Phi(\theta)\rangle = (\sin \theta/\sqrt{2})(|\psi_{50}\rangle + |\psi_{14}\rangle) + \cos \theta|\psi_{32}\rangle$ with $0 < \theta \leq \pi/2$.

3.3.3 Optimal local conversion of flip and exchange symmetric states

Despite the fact that finding an ILO which relates two states with some non-zero probability is sufficient to show the equivalence of these two states under SLOCC, the success probabilities of transformations have fundamental operational importance in quantum information processes. For pure bipartite states, the transformations relating two states of the same class with the greatest probability of success have been found both in the cases of allowing and forbidding classical communication between the parties [70, 71]. For instance, when the parties sharing the state have access to classical communication, Vidal has obtained the following result: Suppose that we have two bipartite systems whose Schmidt decompositions are given as

$$|\psi\rangle = \sum_{i=1}^n \sqrt{\alpha_i} |i_A i_B\rangle, \quad \alpha_i \geq \alpha_{i+1} \geq 0, \quad \sum_{i=1}^n \alpha_i = 1, \quad (3.47)$$

$$|\phi\rangle = \sum_{i=1}^n \sqrt{\beta_i} |i_A i_B\rangle, \quad \beta_i \geq \beta_{i+1} \geq 0, \quad \sum_{i=1}^n \beta_i = 1. \quad (3.48)$$

Then, the maximal probability of obtaining the state $|\phi\rangle$ from the state $|\psi\rangle$ by means of SLOCC transformations is given by [71]

$$P(\psi \rightarrow \phi) = \min_{l \in [1, n]} \frac{\sum_{i=l}^n \alpha_i}{\sum_{i=l}^n \beta_i}. \quad (3.49)$$

While the complete solution of the optimal state conversion problem is not known for the states involving three or more qubits, there are several works in the literature providing partial solutions [72–76]. For example, Cui et al. have given some lower and upper bounds for the optimal probability of transformation from a GHZ state to other states of the GHZ class [74]. Moreover, using the results obtained by Kintaş and Turgut [76], they have determined the optimal SLOCC transformations among n-qubit W-class states [75].

In the remainder of this section, we intend to investigate the optimal local FES transformations relating two multiqubit FES states assuming that spatially separated parties are only allowed to apply one-shot local operations on their subsystems, i.e., they are not allowed to make use of classical communication [21]. Although the coordination of local operations by classical communication has been shown to enhance the power of transformations in certain cases [29], it has also been noted that classical communication is expensive in some situations [77].

Before starting our analysis, we first give an overview of the requirements that needs to be satisfied by elements of quantum channels. Necessary and sufficient conditions for the entries of a two by two matrix in order for the matrix to be an element of a single

qubit quantum operation can be obtained directly from the probability-sum condition of quantum measurements. Consider two operation elements M_1 and M_2 , which are 2×2 matrices, and the quantum operation $\rho \rightarrow \Phi(\rho) = M_1\rho M_1^\dagger + M_2\rho M_2^\dagger$ performed on a single qubit. The only constraint on the operation elements is the normalization condition that $M_1^\dagger M_1 + M_2^\dagger M_2 = I$, where I denotes the 2×2 identity matrix and M_1 and M_2 are defined as

$$M_1 = \begin{pmatrix} a_1 & a_2 \\ a_3 & a_4 \end{pmatrix}, \quad M_2 = \begin{pmatrix} a_5 & a_6 \\ a_7 & a_8 \end{pmatrix}. \quad (3.50)$$

For diagonal elements, the normalization condition requires that

$$|a_1|^2 + |a_3|^2 \leq 1, \quad |a_2|^2 + |a_4|^2 \leq 1. \quad (3.51)$$

Let us introduce the four dimensional state vectors

$$|v_o\rangle = \begin{pmatrix} |v_{ou}\rangle \\ |v_{od}\rangle \end{pmatrix} = \begin{pmatrix} a_1 \\ a_3 \\ a_5 \\ a_7 \end{pmatrix}, \quad |v_e\rangle = \begin{pmatrix} |v_{eu}\rangle \\ |v_{ed}\rangle \end{pmatrix} = \begin{pmatrix} a_2 \\ a_4 \\ a_6 \\ a_8 \end{pmatrix} \quad (3.52)$$

with

$$\begin{aligned} |v_{ou}\rangle &= (a_1, a_3)^T, & |v_{od}\rangle &= (a_5, a_7)^T, \\ |v_{eu}\rangle &= (a_2, a_4)^T, & |v_{ed}\rangle &= (a_6, a_8)^T. \end{aligned} \quad (3.53)$$

So that one have

$$M_1^\dagger M_1 + M_2^\dagger M_2 = \begin{pmatrix} \langle v_o|v_o\rangle & \langle v_o|v_e\rangle \\ \langle v_e|v_o\rangle & \langle v_e|v_e\rangle \end{pmatrix} = I. \quad (3.54)$$

Therefore, we have $\langle v_{ou}|v_{ou}\rangle + \langle v_{od}|v_{od}\rangle = \langle v_{eu}|v_{eu}\rangle + \langle v_{ed}|v_{ed}\rangle = 1$ and $\langle v_{eu}|v_{ou}\rangle = -\langle v_{ed}|v_{od}\rangle$. The Schwarz inequality $|\langle v_{ed}|v_{od}\rangle|^2 \leq \langle v_{od}|v_{od}\rangle \langle v_{ed}|v_{ed}\rangle$ implies that

$$|\langle v_{eu}|v_{ou}\rangle|^2 \leq (1 - \langle v_{ou}|v_{ou}\rangle)(1 - \langle v_{eu}|v_{eu}\rangle). \quad (3.55)$$

Writing the vectors in terms of a_i 's we obtain

$$|a_1|^2 + |a_2|^2 + |a_3|^2 + |a_4|^2 \leq 1 + |\Delta|^2 \quad (3.56)$$

where $\Delta = a_1 a_4 - a_2 a_3$ denotes the determinant of the operation element M_1 . On the other hand, if a_1, a_2, a_3, a_4 are given with $|a_5|^2 + |a_7|^2 = 1 - |a_1|^2 + |a_3|^2$ and $|a_6|^2 + |a_8|^2 = 1 - |a_2|^2 + |a_4|^2$, (3.56) will ensure that $\langle v_{eu}|v_{ou}\rangle = -\langle v_{ed}|v_{od}\rangle$. Hence, (3.51) together

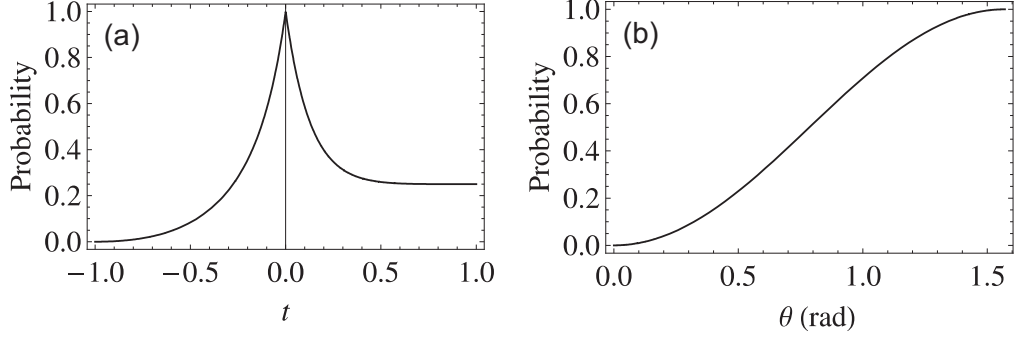


Figure 3.2: (a) Optimal probabilities of obtaining $|GHZ\rangle$ class FES states starting from the $|GHZ\rangle$ state. (b) Maximum probability of obtaining a final state in the vicinity of $|\psi_{30}\rangle$ assuming that the initial state is $|\Gamma(\theta)\rangle = \cos\theta|\psi_{12}\rangle + \sin\theta|\psi_{30}\rangle$ with $0 < \theta < \pi/2$.

with (3.56) give the necessary and sufficient conditions for a 2×2 matrix to be a valid operation element. Moreover, one can show that the inequalities given by (3.51) are guaranteed to be satisfied provided that (3.56) holds and $|a_1|^2 + |a_2|^2 + |a_3|^2 + |a_4|^2 \leq 2$. Thus, the constraints can be simplified as

$$|a_1|^2 + |a_2|^2 + |a_3|^2 + |a_4|^2 \leq 1 + |\Delta|^2 \leq 2. \quad (3.57)$$

Given an operation element M_1 with its corresponding probability of success p , the entries of M_1 can be multiplied by a complex number c to increase the success probability of the transformation by a factor of $|c|^2$. In this case, one has

$$|c|^2 \leq \frac{|a_1|^2 + |a_2|^2 + |a_3|^2 + |a_4|^2 - \sqrt{(|a_1|^2 + |a_2|^2 + |a_3|^2 + |a_4|^2)^2 - 4|\Delta|^2}}{2|\Delta|^2}. \quad (3.58)$$

It is obvious from the above expression that the greatest value of $|c|^2$, and consequently, of $p|c|^2$ will be obtained when $|c|^2$ is equal to the right hand side of (3.58). As a result, for the transformations having the maximum probability of success, (3.57) becomes

$$|a_1|^2 + |a_2|^2 + |a_3|^2 + |a_4|^2 = 1 + |\Delta|^2 \leq 2. \quad (3.59)$$

If (3.59) is not satisfied for a given operation element, one can easily scale it to give the optimal probability by multiplying with the maximum allowed value of $|c|^2$ given by (3.58). A special class of transformation schemes called one successful branch protocols (OSBP) have been considered for the distillation of entangled states in the literature [72, 73]. This scenario involves n parties performing a unique two outcome POVM, whose operation elements are constructed in a way that after each POVM, one of the two possible resulting states contains no n -partite entanglement. For each party, this restriction mathematically implies that $\det[I - M_1^\dagger M_1] = 0$, assuming the successful branch is realized by the application of M_1 . The fact that this condition is nothing but the equality part of (3.59)

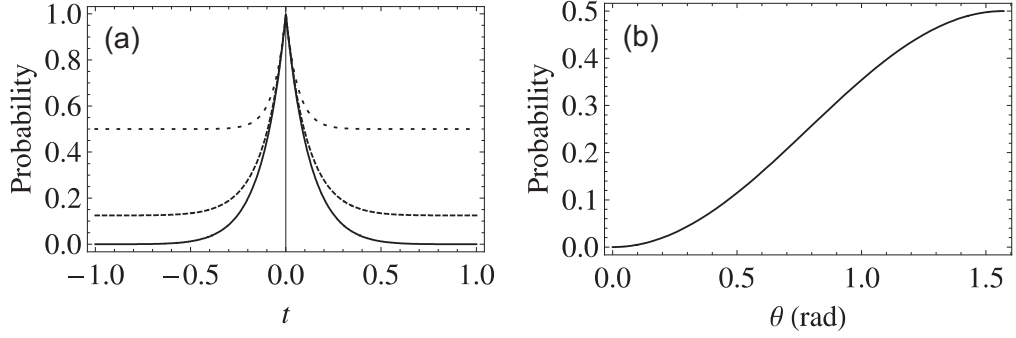


Figure 3.3: (a) Maximum probabilities of obtaining four-qubit FES states, under the assumption that the three initial states are $|\Theta(\pi/100)\rangle$ (solid line), $|\Theta(\pi/6)\rangle = |GHZ_4\rangle$ (dashed line) and $|\Theta(\pi/2)\rangle$ (dotted line). (b) Maximum probability of obtaining a final state in the close neighborhood of one of the separable states when the initial state is $|\Theta(\theta)\rangle = (\sin \theta/\sqrt{2})(|\psi_{40}\rangle + |\psi_{04}\rangle) + \cos \theta|\psi_{22}\rangle$ with $0 < \theta < \pi/2$.

guarantees the optimality of OSBP in the case of one-shot quantum operations. Finally, it is also possible to show that the necessary and sufficient conditions given by (3.57) are equivalent to the constraint on POVM elements that the eigenvalues of $M_1^\dagger M_1$ should be less than or equal to one. Since FES ILOs given by (3.44) have a fixed form, one can scale the operators to obtain the optimal local transformations of multiqubit FES states by multiplying the matrices with the greatest allowed value of the scaling factor $f^2(t)$, which is $1/(1 + |t|)^2$ with $t \in (-1, 1)$.

For three qubits, if one assumes that the initial state is $|GHZ\rangle$, then $|\psi(t)\rangle$ tends to the entangled state $|\psi_{12}\rangle$ as $t \rightarrow -1$. However, Fig. 3.2(a) shows that the maximum probability of obtaining a final state in the close neighborhood of the entangled state $|\psi_{12}\rangle$ decays to zero. On the other hand, $|\psi(t)\rangle$ tends to the separable state $|\psi_{30}\rangle$ as $t \rightarrow 1$. It can also be seen from Fig. 3.2(a) that the probability of obtaining a final state in the vicinity of the separable state $|\psi_{30}\rangle$ is at most $1/4$. Furthermore, the maximum probability of success for transforming an arbitrary initial state $|\Gamma(\theta)\rangle = \cos \theta|\psi_{12}\rangle + \sin \theta|\psi_{30}\rangle$ with $0 < \theta < \pi/2$ to a final state, which is in the vicinity of the separable state $|\psi_{30}\rangle$, is examined. Fig. 3.2(b) displays that the closer the initial state to the entangled state $|\psi_{12}\rangle$, the more robust it becomes against a possible FES noise source.

For four qubits, among the infinitely many curves joining $|\psi_{40}\rangle$ and $|\psi_{04}\rangle$, three of them are chosen for the investigation of the optimal FES transformations. As $t \rightarrow 1$ ($t \rightarrow -1$), all three initial states get closer and closer to the separable state $|\psi_{40}\rangle$ ($|\psi_{04}\rangle$). Fig. 3.3(a) shows the probability of success of optimal FES transformations, assuming that the initial states are $|\Theta(\pi/100)\rangle$ (solid line), $|\Theta(\pi/6)\rangle = |GHZ_4\rangle$ (dashed line) and $|\Theta(\pi/2)\rangle$ (dotted line). It should be noted that this discussion is fundamentally different from the three-qubit case since the initial states chosen here belong to different FES SLOCC classes. Fig. 3.3(b) displays the maximum probability of obtaining a final

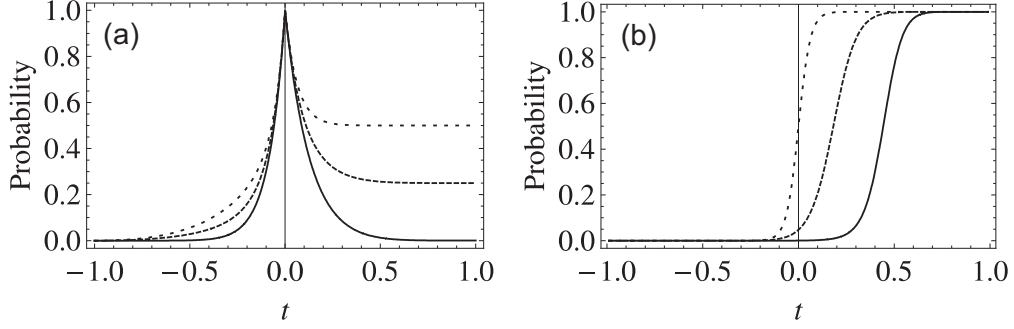


Figure 3.4: (a) Maximum probabilities of obtaining five-qubit FES states, under the assumption that the initial states are $|\Phi(\pi/100)\rangle$ (solid line), $|\Phi(\pi/4)\rangle$ (dashed line) and $|\Phi(\pi/2)\rangle$ (dotted line). (b) Maximum probability of obtaining a final state in the vicinity of the separable state $|\psi_{50}\rangle$ when the initial states are arbitrary points on the curves generated from $|\Phi(\pi/2)\rangle$ (dotted line), $|\Phi(\pi/10)\rangle$ (dashed line) and $|\Phi(\pi/100)\rangle$ (solid line).

state in the close neighborhood of one of the separable states when the initial state is $|\Theta(\theta)\rangle = (\sin \theta/\sqrt{2})(|\psi_{40}\rangle + |\psi_{04}\rangle) + \cos \theta|\psi_{22}\rangle$ with $0 < \theta < \pi/2$. Considering the plots, one can conclude that the closer the entangled four-qubit FES states to the entangled state $|\psi_{22}\rangle$, the more robust they become in the sense that the optimum probability of converting them to the states lying in the vicinity of $|\psi_{04}\rangle$ and $|\psi_{40}\rangle$ vanishes.

For five qubits, the number of curves, which corresponds to the number of different FES SLOCC classes, are also infinite and again only three of them are considered. While all three initial states tend to the separable state $|\psi_{50}\rangle$ as $t \rightarrow 1$, they approach to the entangled state $|\psi_{14}\rangle$ as $t \rightarrow -1$. Fig. 3.4(a) illustrates the probability of success of optimal FES transformations, assuming that the initial states are $|\Phi(\pi/100)\rangle$ (solid line), $|\Phi(\pi/4)\rangle$ (dashed line) and $|\Phi(\pi/2)\rangle$ (dotted line). The asymmetry in the plot is due to the fact that $|\psi_{14}\rangle$ is an entangled state while $|\psi_{50}\rangle$ is a separable state. Fig. 3.4(b) shows the maximum probability of obtaining a final state in the close neighborhood of the separable state $|\psi_{50}\rangle$ when the initial states are arbitrary points on the three curves generated from $|\Phi(\pi/2)\rangle$ (dotted line), $|\Phi(\pi/10)\rangle$ (dashed line) and $|\Phi(\pi/100)\rangle$ (solid line). Consequently, five-qubit entangled states, which are in the vicinity of the curve connecting $|\psi_{32}\rangle$ and $|\psi_{14}\rangle$, are more robust than other entangled states.

Although our calculations have been limited to the three, four and five-qubit cases, the generalization of the present work to include n -qubit FES states is straightforward, since a systematic method has been presented for classifying these states under SLOCC [69]. An obvious open question is the optimal local conversion probabilities of FES states under FES ILOs when classical communication is allowed between the parties, i.e., when use of more than one successful branches is permitted.

Chapter 4

DECOHERENCE

The present chapter is intended to deal with the emergence of classicality in quantum systems. We will start by providing an introduction to the fundamentals of the decoherence program. We will present a simple model which demonstrates the occurrence of environment-induced decoherence for a single qubit. We will then conclude the chapter by presenting our results on the spontaneous breaking of exchange symmetry in quantum states that are evolving under different types of decoherence models [78, 79]. For in-depth overviews on the appearance of classicality in quantum theory, interested reader may refer to [7, 80–83], where various different aspects of the subject are analyzed.

4.1 Basics of the decoherence program

The theory of decoherence aims to provide an explanation to the emergence of classicality in quantum systems. It is based on the idea that every physical system is in interaction with its environment which typically consists of a large number of uncontrollable degrees of freedom, and this interaction leads to entanglement between the two counterparts. Although Zeh emphasized that macroscopic quantum systems are impossible to isolate from their surroundings in 1970 [84, 85], the relation between the interaction of a quantum system with its environment and the transition from quantum to classical was not fully revealed until the seminal papers of Zurek in early 1980s [86, 87]. This might be due to the fact that the fundamental problems of classical physics can always be solved considering isolated systems alone. The decoherence program deals with the two consequences of openness of quantum systems: environment-induced decoherence and environment-induced superselection, also known by the nickname einselection. Whereas decoherence is usually defined as the disappearance of interference between different states of the system, einselection is the decoherence-imposed selection of the preferred set of pointer states that are stable in spite of the interaction with environment. Thus, decoherence and einselection can be considered as two complimentary aspects of the same phenomenon.

In order to demonstrate the situation mathematically, let us assume that the principal system of interest S is represented by the state vectors $|s_n\rangle$, and the system of environment E is described by the state vectors $|e_n\rangle$ which are not orthogonal in general. We also suppose that the system is interacting with its environment via an interaction of the form

$$H_{int} = \sum_n |s_n\rangle\langle s_n| \otimes A_n, \quad (4.1)$$

where A_n are arbitrary operators acting only on the Hilbert space of the environment. This type of an interaction Hamiltonian induces a (non-collapse) measurement-like process on the system in the sense that while an eigenstate $|s_n\rangle$ of the observable measured by this interaction remains unchanged, the environment obtains information about the state of the principal system:

$$|s_n\rangle|e_0\rangle \rightarrow \exp(-iH_{int}t/\hbar)|s_n\rangle|e_0\rangle = |s_n\rangle|e_n(t)\rangle, \quad (4.2)$$

where $|e_0\rangle$ is the initial state of the environment and the resulting states of the environment $|e_n(t)\rangle$ are called pointer positions. Provided that the initial state of the system is given by the superposition $\sum_n c_n|s_n\rangle$, the linearity of quantum mechanics automatically yields

$$\left(\sum_n c_n|s_n\rangle \right) |e_0\rangle \rightarrow \sum_n c_n|s_n\rangle|e_n(t)\rangle, \quad (4.3)$$

which is an entangled state of the composite system SE containing a superposition of all possible measurement results. The phase relations c_n which have been initially representing a coherent superposition of the system states, are now transferred into the combined state of the system and environment. In other words, the initial coherence of the system state has become delocalized and redistributed over the degrees of freedom of the composite state of the system and its surroundings SE . The density matrix of the combined state can be easily obtained as

$$\rho^{SE}(t) = \sum_{nm} c_n(t)c_m^*(t)|s_n\rangle|e_n(t)\rangle\langle s_m|\langle e_m(t)|. \quad (4.4)$$

By tracing over the environmental degrees of freedom, we can straightforwardly calculate the local density matrix of the principal system S ,

$$\rho^S(t) = \sum_{nm} c_n(t)c_m^*(t)|s_n\rangle\langle s_m|\langle e_n(t)|e_m(t)\rangle. \quad (4.5)$$

Despite the fact that interaction between the systems S and E is unitary (and thus the process is in principle reversible), decoherence can always be assumed to be an irreversible process in practice since the environment has a large number of uncontrollable degrees of

freedom. Indeed, it has been revealed by many physical simulations that the large number of degrees of freedom make the environmental states rapidly approach orthogonality $\langle e_n(t)|e_m(t)\rangle \rightarrow \delta_{mn}$. Consequently, the reduced density matrix of the principal system S becomes diagonal in a selected basis,

$$\rho^S \rightarrow \sum_n |c_n|^2 |s_n\rangle\langle s_n|. \quad (4.6)$$

The basis in which the resulting reduced density matrix becomes diagonal is entirely determined by the form of the interaction between the system and its environment. We observe that the off-diagonal elements corresponding to the interference terms are locally destroyed in this basis, i.e., the coherence present in the composite system has become unobservable locally at the level of the principle system S . This simple example demonstrates the local suppression of interference as a result of the decoherence process induced by the interaction with the environment. We note that although the reduced density matrix (4.6) looks like a classical ensemble representing an ignorance-interpretable mixture, we should not conclude that the principal system is actually in one of the states $|s_n\rangle$ since all of these components remain fully present in the state of the global system SE .

4.1.1 Dynamics of quantum measurements

The first formal description of the measurement process was due to von Neumann [18] who has considered the measurement devices as quantum objects in sharp contrast with the postulate of the Copenhagen school that the measurement apparatuses are classical and should not to be treated using the laws of quantum theory. The von Neumann measurement scheme is called ideal as the measurement interaction does not alter the state of the principal system. Such measurements that leave the state of the system unchanged are known as quantum non-demolition measurements [88] and are very difficult to experimentally implement in real world conditions. In fact, what von Neumann defined as a measurement process is already described by (4.3) provided we replace the system of the environment E with the system of the measurement apparatus A . In particular, a von Neumann type measurement scheme can be represented as

$$\left(\sum_n c_n |s_n\rangle \right) |a_0\rangle \rightarrow \sum_n c_n |s_n\rangle |a_n\rangle, \quad (4.7)$$

where $|a_0\rangle$ is the initial state of the measurement apparatus A and $|a_n\rangle$ are the states of the apparatus corresponding to macroscopically distinguishable pointer positions. We notice that, similarly to the previously discussed case of the system and environment, the

superposition initially present only in the principal system is now transferred to the level of the apparatus in the sense that the final state is a superposition of both the system and the apparatus. We also note that this measurement scheme is usually referred to as pre-measurement since at this stage it is not possible to conclude that the measurement has actually been completed. Actually, it is clear that, without the help of an additional physical mechanism, we are not able to explain why we observe the pointer in a certain position instead of in a superposition of all pointer positions [80]. Another important issue with the von Neumann measurement scheme is that the expansion of the final composite system is not in general unique. Indeed, it is a direct consequence of the Schmidt decomposition theorem that the final premeasurement state of the system and the apparatus

$$|\psi\rangle = \sum_n c_n |s_n\rangle |a_n\rangle, \quad (4.8)$$

is unique only if all coefficients c_n are distinct. If not, it is possible to express the same state using different basis states as

$$|\psi\rangle = \sum_n c'_n |s'_n\rangle |a'_n\rangle. \quad (4.9)$$

This immediately tells us that the basis in which the state $|\psi\rangle$ is expressed, defines the measured observable. Moreover, this basis ambiguity implies that the apparatus might simultaneously measure certain non-commuting observables of the system, which is in obvious contradiction with the laws of quantum mechanics [80, 82]. The problem of basis ambiguity can be remedied by extending the von Neumann measurement scheme via the introduction of an environmental system as a third element in addition to the principal system and the measurement apparatus. In this case, by the same mechanism, we have

$$\left(\sum_n c_n |s_n\rangle \right) |a_0\rangle |e_0\rangle \rightarrow \left(\sum_n c_n |s_n\rangle |a_n\rangle \right) |e_0\rangle \rightarrow \sum_n c_n |s_n\rangle |a_n\rangle |e_n\rangle, \quad (4.10)$$

where $|e_0\rangle$ and $|a_0\rangle$ are the initial states of the environment and the apparatus, respectively. As a consequence, the basis ambiguity is now removed by existence of the tri-decompositional uniqueness theorem which states that if a composite quantum state can be decomposed as the final state in (4.10), then the uniqueness of the decomposition is guaranteed [89]. Furthermore, assuming $\langle e_n(t) | e_m(t) \rangle \rightarrow \delta_{mn}$, we also obtain

$$\rho^{SA} \rightarrow \sum_n |c_n|^2 |s_n\rangle \langle s_n| \otimes |a_n\rangle \langle a_n|, \quad (4.11)$$

which only preserves the classical correlations between the system and apparatus states, as expected from a measurement process. Once again, we see that the considered mea-

surement type interaction dynamically defines the pointer states of the apparatus $|a_n\rangle$. However, for an arbitrary interaction Hamiltonian, identifying the basis in which the diagonalization takes place is not an easy task. According to Zurek [7], the preferred pointer basis of the apparatus must be the one in which the correlations between the principal system and the apparatus $|s_n\rangle|a_n\rangle$ are least effected by the interaction between the apparatus and the environment. Despite the fact that the reference to the object that does not interact with the environment is usually omitted for the sake of simplicity, preservation of the system-apparatus correlations is the criterion that actually defines the preferred pointer basis. While there exists a simple sufficient criterion (known as the commutativity criterion) to detect the preferred pointer basis states for some simple toy models, more general methods have been proposed to identify the pointer basis in more realistic situations [7, 90]. Lastly, we emphasize that although the decoherence program provides significant insights about the process of measurement in quantum theory and removes the preferred basis problem, it still does not completely solve what is referred to as the measurement problem in the literature. The main reason for this is that the partial trace operation, which is required to obtain the reduced density matrix of the system, is inherently connected with the probabilistic interpretation of the state vectors [80].

4.1.2 A simple model of one-qubit decoherence

Let us now consider a simple model for a two-state system (a spin-1/2 object) to demonstrate how the states of the environment become approximately mutually orthogonal and therefore environment-induced decoherence takes place. This model has been introduced by Zurek in one of his seminal papers on the subject [87]. Despite its simplicity, it effectively captures the essence of the emergence of classicality in quantum systems. Consider a central two-level system S having quantum states $\{|\uparrow\rangle, |\downarrow\rangle\}$ that interacts with an environment E represented by a bath of N other two-level spins $\{|\uparrow\rangle_k, |\downarrow\rangle_k\}$ with $k = 1, 2, \dots, N$. If we assume that the dynamical evolution of the system is dominated by the interaction between the system S and the environment E , then the self-Hamiltonians of S and E and the self-interaction Hamiltonian of the environment can taken to be zero. In this case, the interaction Hamiltonian describing the coupling of the central system to the environmental spins is of the form

$$H_{SE} = \frac{1}{2}(|\uparrow\rangle\langle\uparrow| - |\downarrow\rangle\langle\downarrow|) \otimes \sum_k g_k (|\uparrow\rangle\langle\uparrow| - |\downarrow\rangle\langle\downarrow|)_k \otimes_{k' \neq k} I_{k'}, \quad (4.12)$$

where $I_k = (|\uparrow\rangle\langle\uparrow| + |\downarrow\rangle\langle\downarrow|)_k$ is the identity operator for the k 'th environmental spin and the g_k are coupling constants. Supposing the initial state of the composite system of

central spin and environmental spins is given by

$$|\psi(0)\rangle = (a|\uparrow\rangle + b|\downarrow\rangle) \otimes_{k=1}^N (\alpha_k|\uparrow\rangle_k + \beta_k|\downarrow\rangle_k), \quad (4.13)$$

the interaction Hamiltonian determines the time evolution of the initial state:

$$|\psi(t)\rangle = a|\uparrow\rangle|E_{\uparrow}(t)\rangle + b|\downarrow\rangle|E_{\downarrow}(t)\rangle, \quad (4.14)$$

where the two environmental quantum states $|E_{\uparrow}(t)\rangle$ and $|E_{\downarrow}(t)\rangle$ read

$$|E_{\uparrow}(t)\rangle = |E_{\downarrow}(-t)\rangle = \otimes_{k=1}^N (\alpha_k e^{ig_k t/2} |\uparrow\rangle_k + \beta_k e^{-ig_k t/2} |\downarrow\rangle_k). \quad (4.15)$$

The reduced density matrix of the central two-level system S is obtained as

$$\rho_S = |a|^2 |\uparrow\rangle\langle\uparrow| + ab^* r(t) |\uparrow\rangle\langle\downarrow| + a^* b r^*(t) |\downarrow\rangle\langle\uparrow| + |b|^2 |\downarrow\rangle\langle\downarrow|. \quad (4.16)$$

The coefficient $r(t)$ determines the weight of the off-diagonal terms and is given by

$$r(t) = \langle E_{\uparrow}(t) | E_{\downarrow}(t) \rangle = \prod_{k=1}^N (|\alpha_k|^2 e^{ig_k t} + |\beta_k|^2 e^{-ig_k t}). \quad (4.17)$$

This kind of a system-environment model is called a pure dephasing model since the diagonal elements (populations) of the reduced density matrix of the central spin is not effected by the interaction, i.e., the decoherence process does not alter the energy of the system. We notice that the interference terms are untouched and fully present at $t = 0$. However, under the realistic assumption of random distribution of initial environmental states and coupling constants for large spin baths consisting of many spins, the off-diagonal elements at large times become considerably small:

$$|r(t)|^2 \simeq 2^{-N} \prod_{k=1}^N [1 + (|\alpha|^2 - |\beta|^2)^2]. \quad (4.18)$$

In fact, under some quite general assumptions, it has been shown that $r(t)$ shows a Gaussian time dependence of the form $r(t) \sim e^{iAt} e^{-B^2 t^2/2}$ with A and B being real constants [7]. Furthermore, by considering various different more detailed models, it has been verified that the decoherence takes place in extremely short time scales. In particular, for mesoscopic systems such as dust particles, even the cosmic microwave background radiation is sufficient to induce an almost immediate decoherence. Lastly, note that $r(t)$ is constructed from periodic functions and thus will eventually return to its initial value. Although this reappearance of coherence might occur in a relatively short time under idealistic conditions, for realistic environments this time can be as long as the age of the universe, proving the irreversibility of the decoherence process for all practical purposes.

4.2 Decoherence induced symmetry breaking

In this section, we focus on a different aspect of decoherence process of entangled states. Certain two-qubit entangled states have the property that they remain unchanged under the exchange of two qubits. We will concentrate on a decoherence model which also has an exchange symmetry, i.e., having a Hamiltonian invariant upon swapping the first and second qubits. Our goal is to understand how the exchange symmetry properties of symmetric pure states alter as the quantum system evolves in time under a symmetric Hamiltonian. More specifically, we will investigate the exchange symmetry properties of three of the four Bell states. Bell states are defined as maximally entangled quantum states of two-qubit systems and given as

$$|B_1\rangle = \frac{1}{\sqrt{2}}(|00\rangle + |11\rangle), \quad (4.19)$$

$$|B_2\rangle = \frac{1}{\sqrt{2}}(|00\rangle - |11\rangle), \quad (4.20)$$

$$|B_3\rangle = \frac{1}{\sqrt{2}}(|01\rangle + |10\rangle), \quad (4.21)$$

$$|B_4\rangle = \frac{1}{\sqrt{2}}(|01\rangle - |10\rangle). \quad (4.22)$$

We will only consider the first three of these states which are symmetric under exchange operation. However, our discussion can be extended to include anti-symmetric states like $|B_4\rangle$. The first three Bell states are among the symmetric pure two-qubit states which can be represented in the most general case by the density matrix

$$\rho_{sym} = \begin{pmatrix} |a|^2 & ac^* & ac^* & ab^* \\ ca^* & |c|^2 & |c|^2 & cb^* \\ ca^* & |c|^2 & |c|^2 & cb^* \\ ba^* & bc^* & bc^* & |b|^2 \end{pmatrix}, \quad (4.23)$$

where the unit trace condition of density matrices implies that $|a|^2 + 2|c|^2 + |b|^2 = 1$.

4.2.1 Classical dephasing noise

We assume that the two qubits are interacting with separate baths locally and the initial two-qubit system is not entangled with the local baths. The model Hamiltonian we consider was first introduced and studied by Yu and Eberly [91] and can be thought as the representative of the class of interactions generating a pure dephasing process defined as

$$H(t) = -\frac{1}{2}\mu[n_A(t)(\sigma_z \otimes I) + n_B(t)(I \otimes \sigma_z)], \quad (4.24)$$

where we take $\hbar = 1$ and σ_z is the usual Pauli spin operator in the z-direction. Here μ is the gyromagnetic ratio and $n_A(t)$ and $n_B(t)$ are two stochastic noise fields that lead to statistically independent Markov processes satisfying

$$\langle n_i(t) \rangle = 0, \quad (4.25)$$

$$\langle n_i(t)n_i(t') \rangle = \frac{\Gamma_i}{\mu^2} \delta(t - t'), \quad (4.26)$$

where $\langle \dots \rangle$ stands for ensemble average and $\Gamma_i (i = A, B)$ are the damping rates associated with the stochastic fields $n_A(t)$ and $n_B(t)$. The time evolution of the system's density matrix can be straightforwardly obtained as

$$\rho(t) = \langle U(t)\rho(0)U^\dagger(t) \rangle, \quad (4.27)$$

where ensemble averages are evaluated over the two noise fields $n_A(t)$ and $n_B(t)$ and the time evolution operator $U(t)$ is given by

$$U(t) = \exp\left[-i \int_0^t dt' H(t')\right]. \quad (4.28)$$

The resulting density matrix in the product basis $\{|00\rangle, |01\rangle, |10\rangle, |11\rangle\}$ can be written as

$$\rho(t) = \begin{pmatrix} \rho_{11} & \rho_{12}\gamma_B & \rho_{13}\gamma_A & \rho_{14}\gamma_A\gamma_B \\ \rho_{21}\gamma_B & \rho_{22} & \rho_{23}\gamma_A\gamma_B & \rho_{24}\gamma_A \\ \rho_{31}\gamma_A & \rho_{32}\gamma_A\gamma_B & \rho_{33} & \rho_{34}\gamma_B \\ \rho_{41}\gamma_A\gamma_B & \rho_{42}\gamma_A & \rho_{43}\gamma_B & \rho_{44} \end{pmatrix}, \quad (4.29)$$

where ρ_{ij} stands for the elements of the initial density matrix and γ_A and γ_B are given by

$$\gamma_A(t) = e^{-t\Gamma_A/2}, \quad \gamma_B(t) = e^{-t\Gamma_B/2}. \quad (4.30)$$

For our purposes, we want the local baths to be identical in the sense that they have the same dephasing rate. Therefore, we let $\Gamma_A = \Gamma_B = \Gamma$. The resulting density matrix of the system in the same basis with the consideration of identical baths is now given by

$$\rho(t) = \begin{pmatrix} \rho_{11} & \rho_{12}\gamma & \rho_{13}\gamma & \rho_{14}\gamma^2 \\ \rho_{21}\gamma & \rho_{22} & \rho_{23}\gamma^2 & \rho_{24}\gamma \\ \rho_{31}\gamma & \rho_{32}\gamma^2 & \rho_{33} & \rho_{34}\gamma \\ \rho_{41}\gamma^2 & \rho_{42}\gamma & \rho_{43}\gamma & \rho_{44} \end{pmatrix}. \quad (4.31)$$

In order to examine the symmetry properties, we express the dynamical evolution of $\rho(t)$ in terms of quantum operations. The decoherence process of the considered quantum system can be regarded as a completely positive linear map $\Phi(\rho)$, that takes an initial

state $\rho(0)$ and maps it to some final state $\rho(t)$. The effect of the map is then given by

$$\rho(t) = \Phi(\rho(0)) = \sum_{\mu=1}^N K_{\mu}(t)\rho(0)K_{\mu}^{\dagger}(t), \quad (4.32)$$

where K_{μ} are the Kraus operators which satisfy the unit trace condition

$$\sum_{\mu=1}^N K_{\mu}^{\dagger}(t)K_{\mu}(t) = I. \quad (4.33)$$

In our investigation, it turns out that the effect of the mapping $\Phi(\rho)$ on the two-qubit system can be expressed by a set of four Kraus operators as

$$K_1 = \text{diag}[-\omega(t), 0, 0, \omega(t)]/\sqrt{2}, \quad (4.34)$$

$$K_2 = \text{diag}[0, -\omega(t), \omega(t), 0]/\sqrt{2}, \quad (4.35)$$

$$K_3 = \text{diag}[\alpha(t), -\alpha(t), -\alpha(t), \alpha(t)]/2, \quad (4.36)$$

$$K_4 = \text{diag}[\beta(t), \beta(t), \beta(t), \beta(t)]/2, \quad (4.37)$$

where the time dependent parameters $\omega(t)$, $\alpha(t)$ and $\beta(t)$ are given by

$$\omega(t) = \sqrt{1 - \gamma(t)^2}, \quad \alpha(t) = \gamma(t) - 1, \quad \beta(t) = \gamma(t) + 1. \quad (4.38)$$

Knowing that this representation is not unique, we recall that the collective action of the set of four Kraus operators $\{K_1, K_2, K_3, K_4\}$ is equivalent to the collective action of another set $\{E_1, E_2, E_3, E_4\}$ if and only if there exists complex numbers u_{ij} such that $E_i = \sum_j u_{ij}K_j$ where u_{ij} are the elements of a 4×4 unitary matrix. Consequently, the mapping described by the Kraus operators $\{K_1, K_2, K_3, K_4\}$ is equivalent to the mappings described by the following four operators

$$E_{\mu} = \text{diag}\left[-\frac{\omega u_{\mu 1}}{\sqrt{2}} + \frac{\alpha u_{\mu 3}}{2} + \frac{\beta u_{\mu 4}}{2}, -\frac{\omega u_{\mu 2}}{\sqrt{2}} - \frac{\alpha u_{\mu 3}}{2} + \frac{\beta u_{\mu 4}}{2}, \right. \quad (4.39)$$

$$\left. \frac{\omega u_{\mu 2}}{\sqrt{2}} - \frac{\alpha u_{\mu 3}}{2} + \frac{\beta u_{\mu 4}}{2}, \frac{\omega u_{\mu 1}}{\sqrt{2}} + \frac{\alpha u_{\mu 3}}{2} + \frac{\beta u_{\mu 4}}{2}\right]. \quad (4.40)$$

4.2.2 Exchange symmetry of the Bell states

Having calculated all possible Kraus operator sets, we are in a position to evaluate the possible final states for the symmetric initial Bell states. The density matrices of possible final states for $|B_1\rangle$ and $|B_2\rangle$ are obtained as

$$\rho_{\mu}^{B_1}(t) = \frac{E_{\mu}(t)\rho^{B_1}(0)E_{\mu}^{\dagger}(t)}{\text{Tr}(E_{\mu}(t)\rho^{B_1}(0)E_{\mu}^{\dagger}(t))}, \quad \rho_{\mu}^{B_2}(t) = \frac{E_{\mu}(t)\rho^{B_2}(0)E_{\mu}^{\dagger}(t)}{\text{Tr}(E_{\mu}(t)\rho^{B_2}(0)E_{\mu}^{\dagger}(t))}, \quad (4.41)$$

where $\mu = 1, 2, 3, 4$ and $\rho^{B_i}(0) = |B_i\rangle\langle B_i|$ for $i = 1, 2$. The explicit forms of the density matrices $\rho_\mu^{B_1}(t)$ and $\rho_\mu^{B_2}(t)$ are given by

$$\rho_\mu^{B_1}(t) = \frac{1}{|e|^2 + |f|^2} \begin{pmatrix} |e|^2 & 0 & 0 & ef^* \\ 0 & 0 & 0 & 0 \\ 0 & 0 & 0 & 0 \\ e^*f & 0 & 0 & |f|^2 \end{pmatrix}, \quad (4.42)$$

$$\rho_\mu^{B_2}(t) = \frac{1}{|e|^2 + |f|^2} \begin{pmatrix} |e|^2 & 0 & 0 & -ef^* \\ 0 & 0 & 0 & 0 \\ 0 & 0 & 0 & 0 \\ -e^*f & 0 & 0 & |f|^2 \end{pmatrix}, \quad (4.43)$$

with

$$e = \left(\frac{-\omega u_{\mu 1}}{\sqrt{2}} + \frac{\alpha u_{\mu 3}}{2} + \frac{\beta u_{\mu 4}}{2} \right), \quad f = \left(\frac{\omega u_{\mu 1}}{\sqrt{2}} + \frac{\alpha u_{\mu 3}}{2} + \frac{\beta u_{\mu 4}}{2} \right). \quad (4.44)$$

Obviously, the symmetry condition given by (4.23) brings no restriction on these density matrices. Thus, it is guaranteed that the Bell states $|B_1\rangle$ and $|B_2\rangle$ always preserve their exchange symmetry as they evolve in time under the considered dephasing channel. On the other hand, the density matrices of the possible final states for $|B_3\rangle$ are written as

$$\rho_\mu^{B_3}(t) = \frac{E_\mu(t)\rho^{B_3}(0)E_\mu^\dagger(t)}{\text{Tr}(E_\mu(t)\rho^{B_3}(0)E_\mu^\dagger(t))}, \quad (4.45)$$

where $\mu = 1, 2, 3, 4$ and $\rho^{B_3}(0) = |B_3\rangle\langle B_3|$. The explicit form $\rho_\mu^{B_3}(t)$ then reads as

$$\rho_\mu^{B_3}(t) = \frac{1}{|r|^2 + |s|^2} \begin{pmatrix} 0 & 0 & 0 & 0 \\ 0 & |r|^2 & rs^* & 0 \\ 0 & r^*s & |s|^2 & 0 \\ 0 & 0 & 0 & 0 \end{pmatrix}, \quad (4.46)$$

with

$$r = \left(\frac{-\omega u_{\mu 2}}{\sqrt{2}} - \frac{\alpha u_{\mu 3}}{2} + \frac{\beta u_{\mu 4}}{2} \right), \quad s = \left(\frac{\omega u_{\mu 2}}{\sqrt{2}} - \frac{\alpha u_{\mu 3}}{2} + \frac{\beta u_{\mu 4}}{2} \right). \quad (4.47)$$

As can be seen from the form of the density matrix of the most general two-qubit symmetric pure state in (4.23), for possible final states to be symmetric we need all non-zero elements of the matrix (4.46) to be equal to each other, that is, $r = s$. This condition can only be satisfied in case of $u_{\mu 2} = 0$. We can immediately conclude that it is impossible for all of the possible final states to be symmetric since any 4×4 unitary matrix

has to satisfy the condition that $|u_{12}|^2 + |u_{22}|^2 + |u_{32}|^2 + |u_{42}|^2 = 1$. Thus, $|B_3\rangle$ cannot evolve in time under our model Hamiltonian in a way that preserves its qubit exchange symmetry with unit probability. In other words, the exchange symmetry of this two-qubit state has to be broken with some non-zero probability. Considering the symmetry of the initial state and the Hamiltonian, this is a very interesting result. A natural question is the maximum probability of finding a symmetric possible final state as the system evolves in time. In order to answer this question, we need to consider three different cases, namely, the cases of having one, two or three symmetric possible final states. If we assume only one of the possible final states to be symmetric, say the outcome of E_1 ($u_{12} = 0$), then the probability of getting a symmetric output state is

$$P_{sym}(t \rightarrow \infty) = \frac{1}{4}|u_{13} + u_{14}|^2. \quad (4.48)$$

If we assume two of the possible final states to be symmetric, that is $u_{12} = 0$, $u_{22} = 0$, then the probability of having a symmetric output is

$$P_{sym}(t \rightarrow \infty) = \frac{1}{4}|u_{13} + u_{14}|^2 + \frac{1}{4}|u_{23} + u_{24}|^2. \quad (4.49)$$

Finally, if three of the possible final states are symmetric, that is, $u_{12} = 0$, $u_{22} = 0$, $u_{32} = 0$, then the probability of having a symmetric output is

$$P_{sym}(t \rightarrow \infty) = \frac{1}{4}|u_{13} + u_{14}|^2 + \frac{1}{4}|u_{23} + u_{24}|^2 + \frac{1}{4}|u_{33} + u_{34}|^2. \quad (4.50)$$

In all cases, the maximum probability of getting a symmetric state turns out to be 0.5.

4.2.3 Quantum mechanical dephasing

When it comes to modeling the baths as large spin environments, one of the simplest decoherence models, introduced in [87], is that of two central spins interacting with N independent spins through the Hamiltonian [92],

$$H = c_{1z} \sum_{k=1}^{N_1} \hbar\omega_{1k} \sigma_{1kz} + c_{2z} \sum_{k=1}^{N_2} \hbar\omega_{2k} \sigma_{2kz}. \quad (4.51)$$

This model is a direct two-spin generalization of the one discussed in Section 4.1.2, and describes two central spins, with z -component operators c_{1z} and c_{2z} , coupled to bath spins represented by σ_{nkz} , where $n = 1, 2$ labels the baths and $k = 1, 2, 3, \dots, N_n$ labels the individual spins. All spins are assumed to be $1/2$ and c_{1z}, c_{2z} and σ_{nkz} denote the corresponding Pauli matrices. Assuming that the central spins are not entangled with none of the spin the baths at $t = 0$, the initial state will be in product form

$|\Psi(0)\rangle = |\Psi_c(0)\rangle|\Psi_{\sigma_1}(0)\rangle|\Psi_{\sigma_2}(0)\rangle$ whose components can be expressed as

$$|\Psi_c(0)\rangle = (a_{\uparrow\uparrow}|\uparrow\uparrow\rangle + a_{\uparrow\downarrow}|\uparrow\downarrow\rangle + a_{\downarrow\uparrow}|\downarrow\uparrow\rangle + a_{\downarrow\downarrow}|\downarrow\downarrow\rangle), \quad (4.52)$$

$$|\Psi_{\sigma_n}(0)\rangle = \bigotimes_{k=1}^{N_n} (\alpha_{nk}|\uparrow_{nk}\rangle + \beta_{nk}|\downarrow_{nk}\rangle). \quad (4.53)$$

Here $|\uparrow_{nk}\rangle$ and $|\downarrow_{nk}\rangle$ are the eigenstates of σ_{nkz} with eigenvalues +1 and -1, respectively, and $|\alpha_{nk}|^2 + |\beta_{nk}|^2 = 1$. The reduced density matrix of two central spins at later times will be given by tracing out the bath degrees of freedom from the total density matrix of the system, $\rho(t)$, as $\rho_c(t) = Tr_{\sigma}\rho(t)$ where subscript σ means that trace is evaluated by summing over all possible nk states and $\rho(t) = |\Psi(t)\rangle\langle\Psi(t)|$. The resulting reduced density matrix in product basis $\{|\uparrow\uparrow\rangle, |\uparrow\downarrow\rangle, |\downarrow\uparrow\rangle, |\downarrow\downarrow\rangle\}$ is found to be

$$\rho_c = \begin{pmatrix} |a_{\uparrow\uparrow}|^2 & a_{\uparrow\uparrow}a_{\uparrow\downarrow}^*r_2 & a_{\uparrow\uparrow}a_{\downarrow\uparrow}^*r_1 & a_{\uparrow\uparrow}a_{\downarrow\downarrow}^*r_1r_2 \\ a_{\uparrow\uparrow}^*a_{\uparrow\downarrow}r_2^* & |a_{\uparrow\downarrow}|^2 & a_{\uparrow\downarrow}a_{\downarrow\uparrow}^*r_1r_2^* & a_{\uparrow\downarrow}a_{\downarrow\downarrow}^*r_1 \\ a_{\uparrow\uparrow}^*a_{\downarrow\uparrow}r_1^* & a_{\uparrow\downarrow}^*a_{\downarrow\uparrow}r_1^*r_2 & |a_{\downarrow\uparrow}|^2 & a_{\downarrow\uparrow}a_{\downarrow\downarrow}^*r_2 \\ a_{\uparrow\uparrow}^*a_{\downarrow\downarrow}r_1^*r_2^* & a_{\uparrow\downarrow}^*a_{\downarrow\downarrow}r_1^* & a_{\downarrow\uparrow}^*a_{\downarrow\downarrow}r_2^* & |a_{\downarrow\downarrow}|^2 \end{pmatrix}, \quad (4.54)$$

where the decoherence factors $r_1(t)$ and $r_2(t)$ are given by

$$r_n(t) = \prod_{k=1}^{N_n} (|\alpha_{nk}|^2 e^{-i2\omega_{nk}t} + |\beta_{nk}|^2 e^{i2\omega_{nk}t}). \quad (4.55)$$

In general both expansion coefficients α_{nk} , β_{nk} and interaction strengths ω_{nk} are random. For our purposes, we will assume that the baths are identical, which means we let expansion coefficients and interaction strengths of the two baths be equal to each other as $\alpha_{1k} = \alpha_{2k} = \alpha_k$, $\beta_{1k} = \beta_{2k} = \beta_k$ and $\omega_{1k} = \omega_{2k} = \omega_k$. This assumption implies that the decoherence factors of two baths are equal so that $r_1(t) = r_2(t) = r(t)$. Thus, the reduced density matrix of two central spins is simplified to

$$\rho_c = \begin{pmatrix} |a_{\uparrow\uparrow}|^2 & a_{\uparrow\uparrow}a_{\uparrow\downarrow}^*r & a_{\uparrow\uparrow}a_{\downarrow\uparrow}^*r & a_{\uparrow\uparrow}a_{\downarrow\downarrow}^*r^2 \\ a_{\uparrow\uparrow}^*a_{\uparrow\downarrow}r^* & |a_{\uparrow\downarrow}|^2 & a_{\uparrow\downarrow}a_{\downarrow\uparrow}^*|r|^2 & a_{\uparrow\downarrow}a_{\downarrow\downarrow}^*r \\ a_{\uparrow\uparrow}^*a_{\downarrow\uparrow}r^* & a_{\uparrow\downarrow}^*a_{\downarrow\uparrow}r^*|r|^2 & |a_{\downarrow\uparrow}|^2 & a_{\downarrow\uparrow}a_{\downarrow\downarrow}^*r \\ a_{\uparrow\uparrow}^*a_{\downarrow\downarrow}(r^*)^2 & a_{\uparrow\downarrow}^*a_{\downarrow\downarrow}r^* & a_{\downarrow\uparrow}^*a_{\downarrow\downarrow}r^* & |a_{\downarrow\downarrow}|^2 \end{pmatrix}, \quad (4.56)$$

where

$$r(t) = \prod_{k=1}^N (|\alpha_k|^2 e^{-i2\omega_k t} + |\beta_k|^2 e^{i2\omega_k t}). \quad (4.57)$$

We immediately observe that the form of ρ_c under the assumption of identical baths is very similar to the form of the output density matrix we obtained for classical noise Hamilto-

nian. In particular, when the initial expansion coefficients α_k and β_k are equal to each other, we will have exactly the same form of the mapping obtained for classical dephasing case. Hence, decay of $r(t)$ to zero at later times and the form of the possible Kraus operators in this case guarantee that the qubit exchange symmetry properties of symmetric Bell states $|B_1\rangle$, $|B_2\rangle$ and $|B_3\rangle$ interacting with two local large spin environments will be the same as their behavior under local stochastic noise fields.

Since we interpret decay of $r(t)$ as a signature of decoherence, we identify decoherence as the main source of spontaneous breaking of qubit exchange symmetry. Accordingly, we conclude that the spontaneous breaking of exchange symmetry for some possible final states is a characteristic feature of decoherence processes, independent of the particular features of the considered models.

4.2.4 Experimental demonstration of symmetry breaking

The phenomenon of decoherence-induced spontaneous symmetry breaking has been recently experimentally investigated by Huang et al. [79] using a conceptually different method from the one described here in the previous sections. Instead of following a selective quantum operations approach as we have done by examining the possible final states of the system [78], they have reconstructed the density matrix of the whole ensemble during the time-evolution by performing quantum state tomography on the system of two independent spin-1/2 objects (polarization degrees of freedom of photons in this case). Defining a simple expression for quantifying the exchange symmetry property of the considered Bell states, the performed experiment has analyzed the exchange symmetries of symmetric Bell states in an exchange symmetric pure dephasing process with a two-photon system generated from spontaneous parametric down-conversion.

Results of the experiment have confirmed that, under such an exchange-symmetric local-noise Hamiltonian, while the exchange symmetry is always preserved for symmetric Bell states $|B_1\rangle$ and $|B_2\rangle$, when it comes to the third symmetric Bell state $|B_3\rangle$, the exchange symmetry property breaks and survives only with a maximum probability of 0.5 at the asymptotic limit. Additionally, they have also explored the symmetry of the antisymmetric Bell state $|B_4\rangle$ and have found that the exchange symmetry property in this case increases and achieves a maximum value of 0.5 at the asymptotic limit. For the details of the experimental process and the setup, interested reader may refer to [79].

Chapter 5

BEYOND ENTANGLEMENT

In this chapter we will first give a short review of some of the recently introduced measures of quantum and total correlations. We will then present our results related to the dynamics of classical and quantum correlation measures for hybrid qubit-qutrit states that are under the action of local and global pure dephasing environments [93]. Thermal total and quantum correlations of the one-dimensional anisotropic spin-1/2 XY model will also be analyzed to discuss their relevance to quantum phase transitions occurring in this system [94]. Quantification of the non-classicality in quantum states beyond entanglement and the dynamics of possible quantifiers in open quantum systems have been a major focus of research in recent literature. Even though the field is still continuously growing, interested reader may refer to [95–97] for the latest progress on the subject.

5.1 Measures of quantum correlations

Besides its foundational importance for the quantum theory, entanglement has also been widely considered as the sole resource of quantum computation, quantum cryptography and quantum information processing protocols for a long time [3]. However, recent investigations have demonstrated that entanglement is not the only kind of useful correlation present in quantum states. For instance, Knill and Laflamme has introduced the concept of the deterministic quantum computation with one qubit, which does not require any entanglement [98]. Moreover, it has also been demonstrated both theoretically and experimentally that some separable states might perform better than their classical counterparts for certain tasks [99–107]. Various different correlation measures have been proposed to detect the non-classical correlations that cannot be captured by entanglement [5, 108–115]. Among them, quantum discord [108, 109], defined as the difference between quantum versions of two classically equivalent expressions for mutual information, has attracted considerable attention [95, 116–132]. In the next two subsections, we give the definitions of the quantum discord and its geometrized version, and discuss their properties.

5.1.1 Quantum discord

The total amount of quantum and classical correlations in a quantum state can be obtained without difficulty by evaluating the quantum mutual information which is defined as

$$I(\rho^{AB}) = S(\rho^A) + S(\rho^B) - S(\rho^{AB}), \quad (5.1)$$

where ρ^{AB} and ρ^k ($k = A, B$) are the density matrix of the total system and reduced density matrix of subsystems, respectively, and $S(\rho) = -\text{Tr}(\rho \log_2 \rho)$ is the von-Neumann entropy. On the other hand, a measure of classical correlations contained in a quantum state is provided by [108, 109]

$$C(\rho^{AB}) = S(\rho^B) - \min_{\{\Pi_k^A\}} \sum_k p_k S(\rho_k^B), \quad (5.2)$$

where $\{\Pi_k^A\}$ defines a set of orthonormal projectors (a von-Neumann measurement), performed on subsystem A and $\rho_k^B = \text{Tr}_A((\Pi_k^A \otimes I^B)\rho^{AB})/p_k$ is the remaining state of subsystem B after obtaining the outcome k with the probability $p_k = \text{Tr}((\Pi_k^A \otimes I^B)\rho^{AB})$. In our later discussions, we intend to evaluate $C(\rho^{AB})$ assuming that the measurement is performed on the qubit part of a quantum system. A von-Neumann measurement $\{\Pi_1^A, \Pi_2^A\}$ can be represented by

$$\Pi_1^A = \frac{1}{2} \left(I_2^A + \sum_{j=1}^3 n_j \sigma_j^A \right), \quad (5.3)$$

$$\Pi_2^A = \frac{1}{2} \left(I_2^A - \sum_{j=1}^3 n_j \sigma_j^A \right), \quad (5.4)$$

where σ_j ($j = 1, 2, 3$) are the Pauli spin operators and $n = (\sin \theta \cos \phi, \sin \theta \sin \phi, \cos \theta)^T$ is a unit vector on the Bloch sphere with $\theta \in [0, \pi)$ and $\phi \in [0, 2\pi)$. Quantum discord [108], which measures the amount of quantum correlations, is then defined as the difference between total and classical correlations

$$D(\rho^{AB}) = I(\rho^{AB}) - C(\rho^{AB}). \quad (5.5)$$

Notice that that quantum discord is not a symmetric quantity in general, which means that its value depends on whether the measurement is performed on subsystem A or the subsystem B . Furthermore, it is not necessarily zero for all mixed separable states as it claims to contain more general non-classical correlations than entanglement measures. For pure states, quantum discord becomes a measure of entanglement being reduced to entanglement entropy. In fact, in order to evaluate classical correlation and thus quantum

discord, it is in general desirable to perform the optimization procedure over all possible POVMs instead of the set of all possible orthogonal measurements [109]. All the same, most of the studies in literature have only considered the orthogonal measurements since, even for this simpler case, there are no available general analytical expression for discord and analytical results have been obtained only in few restricted cases of qubit-qubit and qubit-qudit systems [133–141]. It has also been recently shown that orthogonal measurements are almost sufficient for calculating the quantum discord of two qubits, and they are always optimal for the case of rank-2 states [142]. We lastly note that, for the relatively simple mixed states used in our later investigations, we intend to obtain the quantum discord via numerical optimization of the von Neumann measurements, which includes a minimization process over two independent real parameters θ and ϕ .

5.1.2 Geometric quantum discord

In order to overcome the difficulties experienced with the analytical calculation of quantum discord, Dakić et al. have proposed an alternative geometrized version called geometric measure of quantum discord [110]. The so-called geometric discord aims to measure the nearest distance between a given state and the set of zero-discord states. It can be mathematically defined as

$$D^g(\rho^{AB}) = 2 \min_{\chi} \|\rho^{AB} - \chi\|^2, \quad (5.6)$$

where the minimum is over the set of zero-discord states and the geometric quantity $\|X - Y\|^2 = \text{Tr}(X - Y)^2$ denotes the square of the Hilbert-Schmidt norm. A state χ on $\mathcal{H}_A \otimes \mathcal{H}_B$ has vanishing discord if and only if it is a classical-quantum state, that is

$$\chi = \sum_{k=1}^m p_k |k\rangle\langle k| \otimes \rho_k \quad (5.7)$$

where $\{p_k\}$ is a probability distribution, $\{|k\rangle\}$ is an arbitrary orthonormal basis for \mathcal{H}_A and ρ_k is a set of arbitrary density operators on \mathcal{H}_B . Recently, an exact analytical formula has been obtained for the geometric discord of an arbitrary bipartite state of $2 \times n$ dimensions [143–146]. The density operators acting on a bipartite system $\mathcal{H}_A \otimes \mathcal{H}_B$ with $\dim \mathcal{H}_A = 2$ and $\dim \mathcal{H}_B = n$ can be represented as

$$\begin{aligned} \rho^{AB} &= \frac{1}{\sqrt{2n}} \frac{I^A}{\sqrt{2}} \otimes \frac{I^B}{\sqrt{n}} + \sum_{i=1}^3 x_i X_i \otimes \frac{I^B}{\sqrt{n}} \\ &+ \frac{I^A}{\sqrt{2}} \otimes \sum_{j=1}^{n^2-1} y_j Y_j + \sum_{i=1}^3 \sum_{j=1}^{n^2-1} t_{ij} X_i \otimes Y_j, \end{aligned} \quad (5.8)$$

where the matrices $\{X_i : i = 0, 1, 2, 3\}$ and $\{Y_j : j = 0, 1, \dots, n^2 - 1\}$, satisfying $\text{Tr}(X_k X_l) = \text{Tr}(Y_k Y_l) = \delta_{kl}$, are the traceless Hermitian generators of $SU(2)$ and $SU(n)$, respectively. The components of the local Bloch vectors $\vec{x} = \{x_i\}$, $\vec{y} = \{y_j\}$ and the correlation matrix $T = t_{ij}$ can be obtained as

$$\begin{aligned} x_i &= \text{Tr}\rho^{ab}(X_i \otimes I^b)/\sqrt{2}, \\ y_j &= \text{Tr}\rho^{ab}(I^a \otimes Y_j)/\sqrt{m}, \\ t_{ij} &= \text{Tr}\rho^{ab}(X_i \otimes Y_j). \end{aligned} \quad (5.9)$$

Then, the exact formula for the geometric discord of qubit-qudit states is expressed as

$$D^g(\rho^{AB}) = 2 \left(\|\vec{x}\|^2 + \|T\|^2 - k_{max} \right) \quad (5.10)$$

where $\vec{x} = (x_1, x_2, x_3)^T$ and k_{max} is the greatest eigenvalue of the matrix $(\vec{x}\vec{x}^T + TT^T)$. Although geometric discord enjoys a closed analytical formula, unlike the original quantum discord, for a relatively general class of states, it has been claimed that it might not be a good measure for the quantumness of correlations, as it can increase even under trivial local reversible operations of the party whose nonclassicality is not tested [147].

In addition, Girolami and Adesso have recently obtained an interesting analytical formula for the geometric discord of an arbitrary two-qubit state [148]

$$D_G(\rho^{AB}) = 2(\text{Tr}S - \max\{c_i\}), \quad (5.11)$$

where $S = \vec{x}\vec{x}^t + TT^t$ and

$$c_i = \frac{\text{Tr}S}{3} + \frac{\sqrt{6\text{Tr}S^2 - 2(\text{Tr}S)^2}}{3} \cos\left(\frac{\theta + \alpha_i}{3}\right), \quad (5.12)$$

with $\theta = \arccos\{(2\text{Tr}S^3 - 9\text{Tr}S\text{Tr}S^2 + 9\text{Tr}S^3)\sqrt{2/(3\text{Tr}S^2 - (\text{Tr}S)^2)^3}\}$ and $\{\alpha_i\} = \{0, 2\pi, 4\pi\}$. Observing that $\cos\left(\frac{\theta + \alpha_i}{3}\right)$ reaches its maximum for $\alpha_i = 0$ and choosing θ to be zero, they have obtained a very tight lower bound to the geometric discord:

$$Q(\rho^{AB}) = \frac{2}{3}(2\text{Tr}S - \sqrt{6\text{Tr}S^2 - 2(\text{Tr}S)^2}). \quad (5.13)$$

This quantity can be regarded as a meaningful measure of quantum correlations on its own and it has the desirable feature that it requires no optimization procedure. It is known as the observable measure of quantum correlations (OMQC) in literature since, besides being easier to manage than the original geometric discord, it can be measured by performing only seven local projections on up to four copies of the state. Therefore, $Q(\rho)$ is also very experimentally friendly since one does not need to perform a full tomography of the state.

5.2 Measures of total correlations

While gaining a complete understanding of the quantumness of states is of crucial importance for many reasons, it is still desirable to quantify more general correlations from as many different aspects as possible to reveal their meaning. Although quantum mutual information given in (5.1) has been widely used as the original measure of total correlations, it is not the only available quantifier of such correlations present in literature [149, 150]. In the following two subsections, we introduce two recently proposed quantities that encapsulate both classical and quantum correlations from different perspectives.

5.2.1 Measurement-induced non-locality

Measurement-induced non-locality (MIN) captures more general kind of correlations than the quantum non-locality connected with the violation of Bell inequalities [149]. It might be regarded as a kind of (geometric) measure of total correlations or non-locality contained in a quantum state and can be defined as

$$N(\rho^{AB}) = 2 \max_{\Pi^A} \|\rho^{AB} - \Pi^A(\rho^{AB})\|^2, \quad (5.14)$$

where the maximum is taken over the von Neumann measurements $\Pi^A = \{\Pi_k^A\}$ that do not change ρ^A locally, meaning $\sum_k \Pi_k^A \rho^A \Pi_k^A = \rho^A$, and $\|\cdot\|^2$ denotes the square of the Hilbert-Schmidt norm. MIN aims to capture the non-local effect of the measurements on the state ρ^{AB} by requiring that the measurements do not disturb the local state ρ^A . Although a closed formula for the most general case of bipartite quantum systems is not known, provided that we have a two-qubit system, MIN can be analytically evaluated as

$$N(\rho^{AB}) = \begin{cases} 2(\text{Tr}TT^T - \frac{1}{\|\vec{x}\|^2} \vec{x}^t T T^T \vec{x}) & \text{if } \vec{x} \neq 0, \\ 2(\text{Tr}TT^T - \lambda_3) & \text{if } \vec{x} = 0, \end{cases} \quad (5.15)$$

where λ_3 is the minimum eigenvalue of the 3×3 dimensional matrix TT^T and the definitions of the vector \vec{x} and the matrix T are given in (5.9).

5.2.2 Wigner-Yanase information based measure

In a recent work, Luo has proposed a new measure of total correlations [150] by making use of the notion of Wigner-Yanase skew information

$$I(\rho, X) = -\frac{1}{2} \text{Tr}[\sqrt{\rho}, X]^2, \quad (5.16)$$

which has been first introduced by Wigner and Yanase [151]. Here X is an observable (an Hermitian operator) and $[\cdot, \cdot]$ denotes commutator. For pure states, $I(\rho, X)$ reduces to the variance $V(\rho, X) = \text{Tr}\rho X^2 - (\text{Tr}\rho X)^2$. Since the skew information $I(\rho, X)$ depends both on the state ρ and the observable X , Luo introduced an average quantity in order to get an intrinsic expression [152]

$$Q(\rho) = \sum_i I(\rho, X_i), \quad (5.17)$$

where $\{X_i\}$ is a family of observables which constitutes an orthonormal basis. Global information content of a bipartite quantum system ρ^{AB} with respect to the local observables of the subsystem A can be defined by

$$Q_A(\rho^{AB}) = \sum_i I(\rho^{AB}, X_i \otimes I^B), \quad (5.18)$$

which does not depend on the choice of the orthonormal basis $\{X_i\}$. Then, the difference between the information content of ρ^{AB} and $\rho^A \otimes \rho^B$ with respect to the local observables of the subsystem A can be adopted as a correlation measure for ρ^{AB} ,

$$\begin{aligned} F(\rho^{AB}) &= \frac{2}{3}(Q_A(\rho^{AB}) - Q_A(\rho^A \otimes \rho^B)) \\ &= \frac{2}{3}(Q_A(\rho^{AB}) - Q_A(\rho^A)). \end{aligned} \quad (5.19)$$

Despite the evaluation of most of the measures requires a potentially complex optimization procedure, Wigner-Yanase skew information based measure of total correlations (WYSIM) $F(\rho^{ab})$ has the advantage that it can be calculated straightforwardly.

5.3 Correlations of qubit-qutrit states under dephasing

As we have already discussed in the previous chapter, realistic physical systems are always in contact with their environments. This unavoidable system-environment interaction lies at the heart of the phenomenon of the environment-induced decoherence [7]. Before starting to investigate the dephasing dynamics of quantum correlation measures for some specific qubit-qutrit systems, we briefly mention some of the important dynamical properties of such measures in open quantum systems [95, 96]. One of the most striking consequences of decoherence on the dynamics of entanglement is the experimentally confirmed [153] phenomenon of the total loss of entanglement between the parts of a composite system in finite time, which is termed as entanglement sudden death (ESD) [154–160]. On the other hand, both Markovian and non-Markovian dynamics of more

general quantum and classical correlations have been investigated extensively under various decoherence models [95, 96, 161–188]. Under the conditions where entanglement exhibits a sudden death, quantum discord has been shown to disappear instantaneously in non-Markovian environments [161–163] and has been observed to resist sudden death in Markovian environments [164]. Another remarkable result first demonstrated in [165], is the existence of a sharp transition between classical and quantum loss of correlations, which has also been experimentally confirmed [53]. This sudden transition implies that there exists a finite time interval, in which only classical correlation is lost and quantum discord is unaffected by noisy environment. Moreover, it has also been demonstrated that quantum discord might get forever frozen at a positive value depending on the initial state when both qubits locally interact with non-Markovian purely dephasing environments [187]. Consequently, it has been suggested that quantum discord may be more robust than entanglement, and quantum computation models based on quantum discord correlations might be more relevant than those based on entanglement.

We now turn our attention to the analysis of quantum and classical correlations for certain qubit-qutrit systems that are interacting with classical pure dephasing environments. We consider a composite system of uncoupled spin-1/2 and spin-1 objects, both of which are under the effect of stochastic environmental fluctuations. The model Hamiltonian we use is a direct generalization of (4.24), and can be thought as the representative of the class of interactions generating a pure dephasing process

$$H(t) = -\frac{1}{2}\mu[n_A(t)\sigma_z^A + n_B(t)c_z^B + n_{AB}(t)(\sigma_z^A + c_z^B)], \quad (5.20)$$

where we take $\hbar = 1$. While σ_z is the usual Pauli spin operator in z-direction, c_z corresponds to z-component of the three level spin $c_z = \text{diag}[1, 0, -1]$. Here μ is the gyromagnetic ratio. $n_i(t)$ ($i = A, B, AB$) are stochastic noise fields that lead to statistically independent Markov processes satisfying

$$\langle n_i(t) \rangle = 0, \quad (5.21)$$

$$\langle n_i(t)n_i(t') \rangle = \frac{\Gamma_i}{\mu^2}\delta(t-t'), \quad (5.22)$$

where $\langle \dots \rangle$ stands for ensemble average, and Γ_i is the damping rate associated with the stochastic field $n_i(t)$. The time evolution of the density matrix of the system is given by

$$\rho(t) = \langle U(t)\rho(0)U^\dagger(t) \rangle, \quad (5.23)$$

where ensemble averages are evaluated over the three noise fields and the time evolution operator $U(t)$ can be straightforwardly obtained as $U(t) = \exp[-i \int_0^t dt' H(t')]$. We

assume that all the damping parameters are the same ($\Gamma_A = \Gamma_B = \Gamma_{AB} = \Gamma$) for the sake of simplicity. First, we focus our attention to the case of multilocal dephasing, i.e., $n_{AB}(t) = 0$. In this setting, qubit and qutrit are only interacting with their own environments locally. The resulting time-evolved density matrix in the product basis $\{|ij\rangle : i = 0, 1, j = 0, 1, 2\}$ can be written as

$$\rho(t) = \begin{pmatrix} \rho_{11} & \rho_{12}\gamma & \rho_{13}\gamma^4 & \rho_{14}\gamma^4 & \rho_{15}\gamma^5 & \rho_{16}\gamma^8 \\ \rho_{21}\gamma & \rho_{22} & \rho_{23}\gamma & \rho_{24}\gamma^5 & \rho_{25}\gamma^4 & \rho_{26}\gamma^5 \\ \rho_{31}\gamma^4 & \rho_{32}\gamma & \rho_{33} & \rho_{34}\gamma^8 & \rho_{35}\gamma^5 & \rho_{36}\gamma^4 \\ \rho_{41}\gamma^4 & \rho_{42}\gamma^5 & \rho_{43}\gamma^8 & \rho_{44} & \rho_{45}\gamma & \rho_{46}\gamma^4 \\ \rho_{51}\gamma^5 & \rho_{52}\gamma^4 & \rho_{53}\gamma^5 & \rho_{54}\gamma & \rho_{55} & \rho_{56}\gamma \\ \rho_{61}\gamma^8 & \rho_{62}\gamma^5 & \rho_{63}\gamma^4 & \rho_{64}\gamma^4 & \rho_{65}\gamma & \rho_{66} \end{pmatrix}, \quad (5.24)$$

where ρ_{ij} stands for the elements of the initial density matrix $\rho(0)$ and $\gamma(t) = e^{-t\Gamma/8}$. Second, we consider a global dephasing scenario where the spins are interacting with a shared environment collectively and local baths are absent, i.e., $n_A(t) = n_B(t) = 0$. In this case, dynamics of the initial density matrix can be expressed in the same basis as

$$\rho(t) = \begin{pmatrix} \rho_{11} & \rho_{12}\gamma & \rho_{13}\gamma^4 & \rho_{14}\gamma^4 & \rho_{15}\gamma^9 & \rho_{16}\gamma^{16} \\ \rho_{21}\gamma & \rho_{22} & \rho_{23}\gamma & \rho_{24}\gamma & \rho_{25}\gamma^4 & \rho_{26}\gamma^9 \\ \rho_{31}\gamma^4 & \rho_{32}\gamma & \rho_{33} & \rho_{34} & \rho_{35}\gamma & \rho_{36}\gamma^4 \\ \rho_{41}\gamma^4 & \rho_{42}\gamma & \rho_{43} & \rho_{44} & \rho_{45}\gamma & \rho_{46}\gamma^4 \\ \rho_{51}\gamma^9 & \rho_{52}\gamma^4 & \rho_{53}\gamma & \rho_{54}\gamma & \rho_{55} & \rho_{56}\gamma \\ \rho_{61}\gamma^{16} & \rho_{62}\gamma^9 & \rho_{63}\gamma^4 & \rho_{64}\gamma^4 & \rho_{65}\gamma & \rho_{66} \end{pmatrix}. \quad (5.25)$$

We notice that some elements of the initial density matrix $\rho(0)$ are not affected by decoherence in the global dephasing setting. This special region, which does not feel the noisy environment, is an indicator of the existence of decoherence-free subspaces.

In the next two subsections, we investigate the correlation dynamics for two different families of hybrid qubit-qutrit states: entangled $\rho_e(p)$ and separable $\rho_s(r)$ defined by

$$\begin{aligned} \rho_e(p) &= \frac{p}{2}(|00\rangle\langle 00| + |01\rangle\langle 01| + |00\rangle\langle 12| + |11\rangle\langle 11| + |12\rangle\langle 12| \\ &\quad + |12\rangle\langle 00|) + \frac{1-2p}{2}(|02\rangle\langle 02| + |02\rangle\langle 10| + |10\rangle\langle 02| + |10\rangle\langle 10|) \end{aligned} \quad (5.26)$$

$$\begin{aligned} \rho_s(r) &= \frac{r}{2}(|00\rangle\langle 00| + |01\rangle\langle 01| + |00\rangle\langle 12| + |11\rangle\langle 11| + |12\rangle\langle 12| \\ &\quad + |12\rangle\langle 00| + |02\rangle\langle 10| + |10\rangle\langle 02|) + \frac{1-2r}{2}(|02\rangle\langle 02| + |10\rangle\langle 10|) \end{aligned} \quad (5.27)$$

where the parameters p and r satisfy that $0 \leq p \leq 1/2$ and $0 \leq r \leq 1/3$. Note that the family of entangled states given by $\rho_e(p)$ reduces to a separable state for $p = 1/3$.

5.3.1 Correlations under multilocal dephasing

We first discuss the time evolution of correlations under multilocal classical dephasing noise. The separable family $\rho_s(r)$ naturally contains no entanglement since it has PPT for all possible values of r . Negativity of the entangled family $\rho_e(p)$ is given as

$$N_e(p, \tilde{\gamma}) = \frac{1}{2}[|p(1 + 2\tilde{\gamma}) - \tilde{\gamma}| + |p(2 + \tilde{\gamma}) - 1| - (p - 1)(\tilde{\gamma} - 1)], \quad (5.28)$$

where $\tilde{\gamma}(t) = e^{-t\Gamma}$. On the other hand, both of the families have non-vanishing geometric discord in general, which can be calculated as

$$D_e^g(p, \tilde{\gamma}) = \frac{1}{4}[1 + 2\tilde{\gamma}^2 - 2p(3 + 4\tilde{\gamma}^2) + p^2(9 + 10\tilde{\gamma}^2) - \max\{(1 - 3p)^2, (1 - 3p)^2\tilde{\gamma}^2, (1 - p)^2\tilde{\gamma}^2\}], \quad (5.29)$$

$$D_s^g(r, \tilde{\gamma}) = \frac{1}{4}[1 - 6r + r^2(9 + 4\tilde{\gamma}^2) - \max\{(1 - 3r)^2, 4r^2\tilde{\gamma}^2\}]. \quad (5.30)$$

Dynamics of the entangled family: We start our investigation by considering $\rho_e(0)$ and $\rho_e(1/2)$. Correlation dynamics of these two states are completely different from the other members of the family. For $\rho_e(1/2)$, Fig. 5.1(a) displays that while classical correlation is not affected by external noise, all three quantum correlations decay in a monotonic fashion. In this case, negativity seems to be more robust than quantum and geometric discords. On the other hand, $\rho_e(0)$ is a maximally entangled state and its general behavior is almost the same as $\rho_e(1/2)$ except all of its correlations are one initially. Dynamics of the correlations for the remaining members of the family are far more interesting. For all of the states corresponding to the regime $1/2 > p > 0$ (excluding $p = 1/3$), entanglement disappears in a finite time suffering ESD. More important, we observe the sudden transition from classical to quantum decoherence [52], i.e, there exists a critical instant t_c at which the quantum state stops losing classical correlation and starts losing quantum discord. Geometric discord fails to keep up with quantum discord in the classical decoherence region, but its decay still suddenly hastens at the critical time t_c . Fig. 5.1(b) shows an example of this behavior for $p = 0.25$. It is possible to prolong the time interval in which quantum discord remains constant but there exists a trade-off between the initial magnitude of the quantum discord and its survival time. Fig. 5.1(c) illustrates the case for $p = 0.2$. Although sudden changes of all correlation measures occur at the same time instant for all the initial states considered in our study, this is not a general feature of all quantum states. Examples of states have been presented in [188] for which evolutions of quantum and geometric discords are completely independent of each other, and are not affected by the discontinuities in each others dynamics.

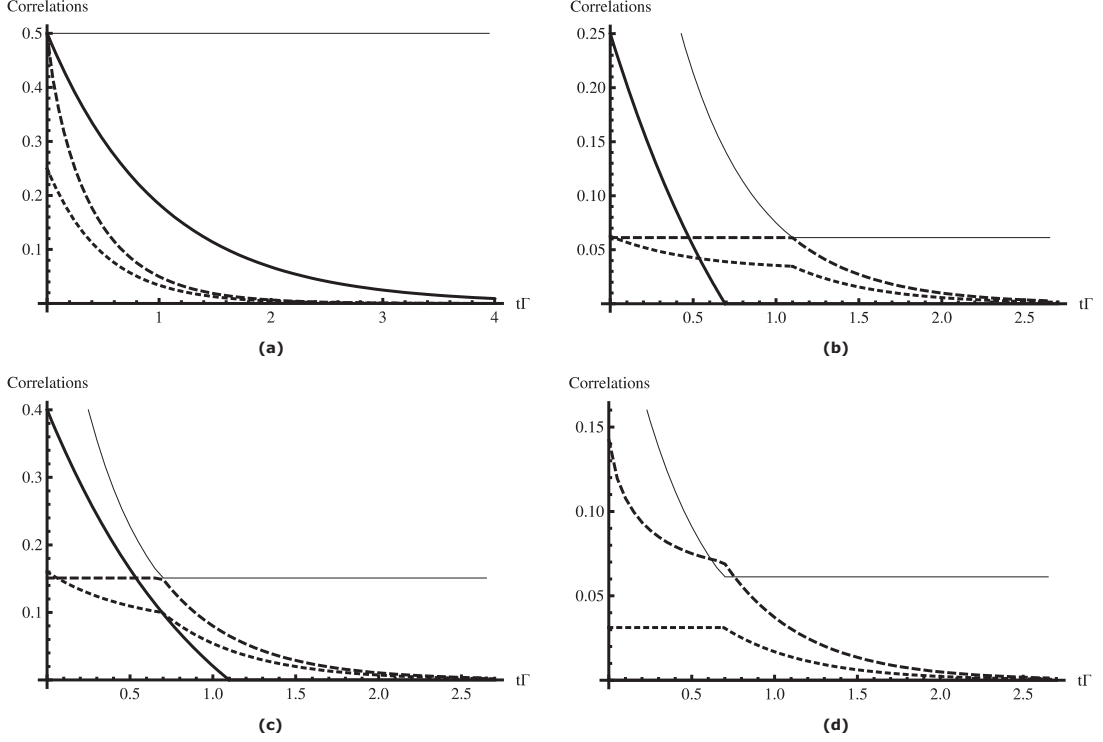


Figure 5.1: Dynamics of negativity N (thick solid line), geometric discord D^g (dotted line), numerically evaluated quantum discord D (dashed line) and classical correlation C (thin solid line) as a function of the dimensionless parameter $t\Gamma$ under the effect of multilocal classical dephasing noise. The initial states are $\rho_e(p)$ with (a) $p = 0.5$ (b) $p = 0.25$ (c) $p = 0.2$ and $\rho_s(r)$ for (d) $r = 0.25$.

Dynamics of the separable family: The two end points of this family, namely, $\rho_s(0)$ and $\rho_s(1/3)$, are not particularly interesting since they do not contain any quantum correlations. For the initial states corresponding to the interval $1/5 \geq r > 0$, classical correlation does not feel the noise fields, whereas quantum and geometric discords decay monotonically. However, the regime $1/3 > r > 1/5$ is definitely more interesting. In this case, though quantum discord is not constant and decays together with the classical correlation, we notice that geometric discord is unaffected by environment for a finite time interval. In other words, there exists an instant of time \tilde{t}_c until which the system has frozen geometric discord. An example is presented in Fig. 5.1(d), where $r = 0.25$ and the critical time $\tilde{t}_c = \ln 2/\Gamma$. Note that the state keeps losing quantum discord throughout the dynamics but as soon as \tilde{t}_c is reached, the decay rate of quantum discord hastens.

5.3.2 Correlations under global dephasing

We now discuss the time evolution of correlations under global classical dephasing noise.

Negativity of the entangled family $\rho_e(p)$ reads as

$$N_e(p, \tilde{\gamma}) = \frac{1}{2} [|3p - 1| + |p(2 + \tilde{\gamma}^2) - 1| - p(1 - \tilde{\gamma}^2)]. \quad (5.31)$$

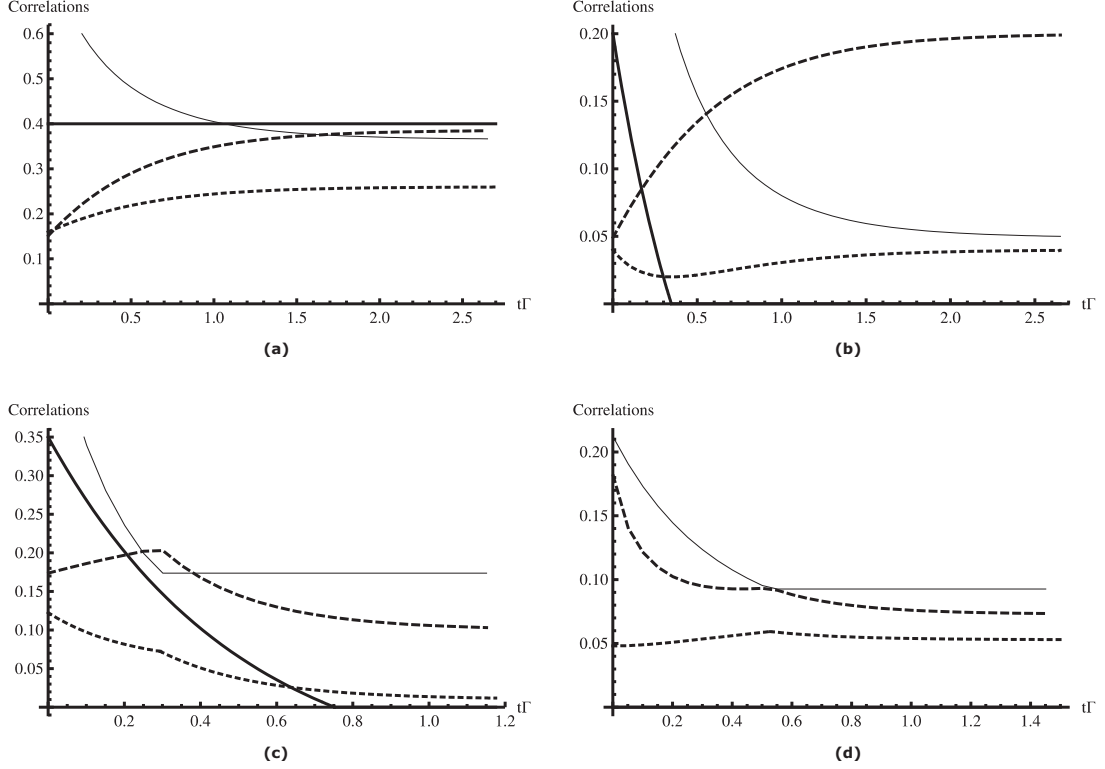


Figure 5.2: Dynamics of negativity N (thick solid line), geometric discord D^g (dotted line), numerically evaluated quantum discord D (dashed line) and classical correlation C (thin solid line) as a function of the dimensionless parameter $t\Gamma$ under the effect of global classical dephasing noise. The initial states are $\rho_e(p)$ with (a) $p = 0.2$ (b) $p = 0.4$ (c) $p = 0.45$ and $\rho_s(r)$ for (d) $r = 0.23$.

Geometric discord for the two families can also be obtained as

$$D_e^g(p, \tilde{\gamma}) = \frac{1}{4} [3 - 14p + p^2(17 + 2\tilde{\gamma}^4) - \max\{(1 - 3p)^2, (p(\tilde{\gamma}^2 - 2) + 1)^2, (p(\tilde{\gamma}^2 + 2) - 1)^2\}], \quad (5.32)$$

$$D_s^g(r, \tilde{\gamma}) = \frac{1}{4} [1 - 6r + r^2(11 + 2\tilde{\gamma}^4) - \max\{(1 - 3r)^2, r^2(1 - \tilde{\gamma}^2)^2, r^2(1 + \tilde{\gamma}^2)^2\}]. \quad (5.33)$$

$$r^2(1 - \tilde{\gamma}^2)^2, r^2(1 + \tilde{\gamma}^2)^2\}. \quad (5.34)$$

Dynamics of the entangled family: The correlation dynamics of the entangled family under global noise is a lot richer than its dynamics under multilocal noise. While all of the correlations hold unchanged for the maximally entangled state $\rho_e(0)$, correlation dynamics of the state $\rho_e(1/2)$ is no different than what's described in Fig. 5.1(a) except for the fact that correlations decay faster. In the regime $1/3 \geq p > 0$, quantum and geometric discords are both uniformly amplified and become stable after a certain point. Negativity is conserved since this regime consist of decoherence-free states. Fig. 5.2(a) displays an example of this case for $p = 0.2$. Classical correlation, which can be greater or smaller than quantum discord, decreases monotonically and gets stable as well. For the regime $2/5 \geq p > 1/3$, behaviors of classical correlation and quantum discord are unchanged.

On the other hand, geometric discord acquires a minimum without a sudden change. Although all other correlations survive the effects of the environment, negativity disappears in a finite time suffering sudden death. Fig. 5.2(b) illustrates the situation for $p = 0.4$. It is noteworthy that geometric discord can decrease as quantum discord increases. Next, we examine the interval $1/2 > p > 2/5$. Whereas the states keep experiencing ESD, all other correlations show sudden changes in their evolutions at the same instant. Fig. 5.2(c) gives an example this behavior for $p = 0.45$. Note that geometric discord and classical correlation diminish as quantum discord gets amplified until a critical time is reached. After that instant, both quantum and geometric discords start to weaken until they reach a stable value, but classical correlation is not affected by noise at all.

Dynamics of the separable family: Starting with $\rho_s(1/3)$, we immediately see that smooth amplification of both quantum and geometric discords is possible in this setting. In the regime $1/5 \geq r > 0$, classical correlation is unaffected by noise but quantum and geometric discords decay in a monotonic way until they eventually become stable. In the interval $1/4 > r > 1/5$, all correlations start to evolve in a different fashion but they all become discontinuous simultaneously at a certain critical instant. After that instant, classical correlation becomes constant as other measures starts to decrease until they finally get stable. Fig. 5.2(d) illustrates this behavior for $r = 0.23$.

To sum up, in the above two subsections, we have analyzed the dynamics of negativity, quantum discord, geometric discord and classical correlation for two different one-parameter families of qubit-qutrit states, assuming that the states are in a classical dephasing environment. We have noticed that dynamics of correlations are strongly dependent on the initial conditions even for such simple one-parameter families of states. In the multilocal dephasing case, we have demonstrated the phenomenon of sudden transition from classical to quantum decoherence for hybrid qubit-qutrit systems extending the results of [165]. In fact, this transition might be a generic feature existing in all bipartite quantum systems but a definitive demonstration would require an analytic expression for quantum discord in arbitrary dimensions. Furthermore, for a class of separable states, we have observed an analogue of this phenomenon for geometric discord. Under global noise, dynamics of correlations are quite diverse. We have shown that although quantum and geometric discords can evolve initially completely independent of each other for a certain time period, they tend to be eventually in accord. Smooth amplification of quantum and geometric discords is also possible in this case. On the other hand, we have confirmed that entanglement as quantified by negativity can suffer sudden death for qubit-qutrit states both in global and multilocal dephasing settings. Our findings clearly indicate that different measures of quantum correlations are conceptually different.

5.3.3 Time invariant quantum discord

In this subsection, we evaluate the dynamics of certain hybrid qubit-qutrit states under the assumption that only the qutrit is interacting with a Markovian dephasing environment and the qubit is protected. The operator-sum representation of the considered qutrit dephasing channel can be described by a set of Kraus operators [159, 160]

$$M_1 = \text{diag}(1, \gamma(t), \gamma(t)), \quad (5.35)$$

$$M_2 = \text{diag}(0, \omega(t), 0), \quad (5.36)$$

$$M_3 = \text{diag}(0, 0, \omega(t)), \quad (5.37)$$

where $\gamma(t) = e^{-\Gamma t/2}$ and $\omega(t) = \sqrt{1 - \gamma^2(t)}$ with Γ denoting the decay rate. We note that this dephasing channel is not the same as the one we have considered in our previous discussion. In particular, this specific quantum channel is chosen so that the rate of dephasing between the ground state and each of the two excited states are the same. Having defined the decoherence channel for a single qutrit, we can obtain the time evolution of an arbitrary initial qubit-qutrit system $\rho(0)$ under local dephasing of the qutrit as

$$\rho(t) = \sum_{i=1}^3 (I_2 \otimes M_i) \rho(0) (I_2 \otimes M_i)^\dagger, \quad (5.38)$$

where I_2 denotes the 2×2 identity matrix acting on the qubit part of the composite system. The resulting time-evolved density matrix in the product basis $\{|ij\rangle : i = 0, 1, j = 0, 1, 2\}$ can be then written as

$$\rho(t) = \begin{pmatrix} \rho_{11} & \rho_{12}\gamma & \rho_{13}\gamma & \rho_{14} & \rho_{15}\gamma & \rho_{16}\gamma \\ \rho_{21}\gamma & \rho_{22} & \rho_{23}\gamma^2 & \rho_{24}\gamma & \rho_{25} & \rho_{26}\gamma^2 \\ \rho_{31}\gamma & \rho_{32}\gamma^2 & \rho_{33} & \rho_{34}\gamma & \rho_{35}\gamma^2 & \rho_{36} \\ \rho_{41} & \rho_{42}\gamma & \rho_{43}\gamma & \rho_{44} & \rho_{45}\gamma & \rho_{46}\gamma \\ \rho_{51}\gamma & \rho_{52} & \rho_{53}\gamma^2 & \rho_{54}\gamma & \rho_{55} & \rho_{56}\gamma^2 \\ \rho_{61}\gamma & \rho_{62}\gamma^2 & \rho_{63} & \rho_{64}\gamma & \rho_{65}\gamma^2 & \rho_{66} \end{pmatrix}. \quad (5.39)$$

We choose to analyze the time evolution of quantum correlations for a one-parameter family of entangled qubit-qutrit mixed states

$$\begin{aligned} \rho = & \frac{p}{2}(|00\rangle\langle 00| + |01\rangle\langle 01| + |12\rangle\langle 12| + |11\rangle\langle 11| + |01\rangle\langle 11| + |11\rangle\langle 01| + |00\rangle\langle 12| \\ & + |12\rangle\langle 00|) + \frac{1-2p}{2}(|02\rangle\langle 02| + |02\rangle\langle 10| + |10\rangle\langle 02| + |10\rangle\langle 10|), \end{aligned} \quad (5.40)$$

where $p \in [0, 0.5]$ and ρ turns out to be separable only for $p = 1/3$. In Fig. 5.3(a), we present our results on the dynamics of negativity and quantum discord as a function of the

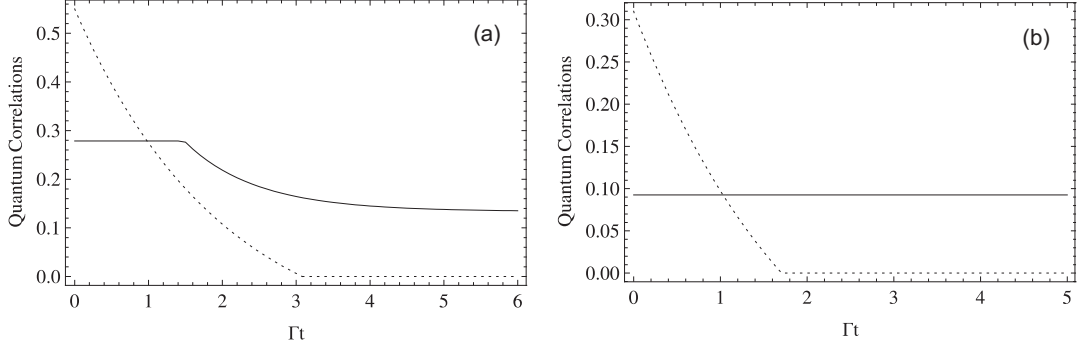


Figure 5.3: Dynamics of negativity (dotted line) and quantum discord (solid line) as a function of the dimensionless parameter Γt for $p = 0.15$ (a) and $p = 0.23$ (b).

dimensionless parameter Γt for $p = 0.15$. We notice that although the coherence in the qubit-qutrit system is only partially lost, entanglement as quantified by negativity suffers a sudden death and disappears after a certain finite time. On the other hand, quantum discord remains frozen for a while but then when a critical instance is reached, it decays to a finite non-zero value. The survival of quantum discord at the asymptotic limit ($t \rightarrow \infty$) is not unexpected since the quantum state is still partially coherent and almost all quantum states have non-classical correlations [117]. Regardless, Fig. 5.3(b) displays a curious behavior of the correlations for $p = 0.23$. In this case, we observe that even if the negativity evaporates quickly due to sudden death, the partial coherence left in the qubit-qutrit system enables quantum discord to remain invariant during the whole time evolution. It is important to emphasize that this is a rather surprising feature of non-classical correlations that are more general than entanglement.

5.4 Thermal correlations in the anisotropic XY chain

This section is devoted to the analysis of thermal quantum and total correlations in the one-dimensional spin-1/2 XY model in transverse magnetic field. Before starting our investigation, we briefly review certain concepts that are relevant to our purposes. Quantum phase transitions (QPTs) are sudden changes occurring in the ground states of many-body systems when one or more of the physical parameters of the system are continuously varied at absolute zero temperature [189]. These radical changes, which strongly affect the macroscopic properties of the system, are manifestations of quantum fluctuations. Despite the fact that reaching absolute zero temperature is practically impossible, QPTs might still be observed at sufficiently low temperatures, where thermal fluctuations are not significant enough to excite the system from its ground state. In recent years, the methods of quantum information theory have been widely applied to quantum critical systems. In particular, entanglement and quantum discord have been shown to identify the critical

points (CPs) of QPTs with success in several different critical spin chains, both at zero [95, 96, 190–200] and finite temperature [201–203]. It has also been noted that unlike pairwise entanglement, which is typically short ranged, quantum discord does not vanish even for distant spin pairs [197]. Another interesting aspect of quantum spin chains in transverse magnetic field is the occurrence of a non-trivial factorized ground state [204]. In order to gain a complete understanding of these factorized states, the effects of spontaneous symmetry breaking (SSB) should be considered [205–207]. In fact, concurrence is known to signal the factorization point of the anisotropic XY chain corresponding to a product ground state [207]. Moreover, it has been demonstrated that quantum discord is also able to detect such points, provided that either SSB is taken into account or quantum discord is calculated for several different distances of the spins [208, 209].

Let us start our analysis by introducing the Hamiltonian of the one-dimensional spin-1/2 XY model in transverse magnetic field:

$$H_{XY} = -\frac{\lambda}{2} \sum_{j=1}^N [(1 + \gamma)\sigma_j^x \sigma_{j+1}^x + (1 - \gamma)\sigma_j^y \sigma_{j+1}^y] - \sum_{j=1}^N \sigma_j^z \quad (5.41)$$

where N is the number of spins, σ_j^α ($\alpha = x, y, z$) is the usual Pauli operators for a spin-1/2 at j th site, γ ($0 \leq \gamma \leq 1$) is the anisotropy parameter and λ is the strength of the inverse external field. For $\gamma = 0$ the above Hamiltonian corresponds to the XX model. When $\gamma \geq 0$ it is in the Ising universality class, and reduces to the Ising Hamiltonian in a transverse field for $\gamma = 1$. We are interested in the region where the XY model exhibits two phases, a ferromagnetic and a paramagnetic phase, which are separated by a second-order QPT at the CP $\lambda_c = 1$. In the thermodynamic limit, the XY model can be solved exactly via a Jordan-Wigner map followed by a Bogoluibov transformation. Reduced density matrix of two spins i and j depends only on the distance between them, $r = |i - j|$, due to the translational invariance of the system. The Hamiltonian is also invariant under parity transformation, meaning it exhibits Z_2 symmetry. Taking these properties into account, and neglecting the effects of spontaneous symmetry breaking (which are studied in Ref. [205–209]), the two-spin reduced density matrix of the system at thermal equilibrium is given by [190]

$$\rho_{0,r} = \frac{1}{4} [I_{0,r} + \langle \sigma^z \rangle (\sigma_0^z + \sigma_r^z)] + \frac{1}{4} \sum_{\alpha=x,y,z} \langle \sigma_0^\alpha \sigma_r^\alpha \rangle \sigma_0^\alpha \sigma_r^\alpha, \quad (5.42)$$

where $I_{0,r}$ is the four-dimensional identity matrix. The transverse magnetization of the system is given by [210]

$$\langle \sigma^z \rangle = - \int_0^\pi \frac{(1 + \lambda \cos \phi) \tanh(\beta \omega_\phi)}{2\pi \omega_\phi} d\phi, \quad (5.43)$$

where $\omega_\phi = \sqrt{(\gamma\lambda \sin \phi)^2 + (1 + \lambda \cos \phi)^2}/2$, $\beta = 1/k_b T$ with k_b being the Boltzmann constant and T is the absolute temperature. Two-point correlation functions are defined as [211]

$$\langle \sigma_0^x \sigma_r^x \rangle = \begin{vmatrix} G_{-1} & G_{-2} & \cdots & G_{-r} \\ G_0 & G_{-1} & \cdots & G_{-r+1} \\ \vdots & \vdots & \ddots & \vdots \\ G_{r-2} & G_{r-3} & \cdots & G_{-1} \end{vmatrix}, \quad \langle \sigma_0^y \sigma_r^y \rangle = \begin{vmatrix} G_1 & G_0 & \cdots & G_{-r+2} \\ G_2 & G_1 & \cdots & G_{-r+3} \\ \vdots & \vdots & \ddots & \vdots \\ G_r & G_{r-1} & \cdots & G_1 \end{vmatrix}, \quad (5.44)$$

$$\langle \sigma_0^z \sigma_r^z \rangle = \langle \sigma^z \rangle^2 - G_r G_{-r}, \quad (5.45)$$

where

$$G_r = \int_0^\pi \frac{\tanh(\beta\omega_\phi) \cos(r\phi)(1 + \lambda \cos \phi)}{2\pi\omega_\phi} d\phi - \gamma\lambda \int_0^\pi \frac{\tanh(\beta\omega_\phi) \sin(r\phi) \sin(\phi)}{2\pi\omega_\phi} d\phi. \quad (5.46)$$

In Fig. 5.4, we present our results regarding the thermal total correlations quantified by MIN and WYSIM for first nearest neighbors as a function of λ for $kT = 0, 0.1, 0.5$ and $\gamma = 0.001, 0.5, 1$. We note that although MIN and WYSIM behave in a similar fashion for $\gamma = 1$, they show qualitatively different behaviors in the case of $\gamma = 0.001$. Namely, WYSIM experiences a more dramatic increase about the CP $\lambda = 1$ than MIN, and reaches to a constant value more quickly. Furthermore, it is also important to observe that as temperature increases, both of the correlation measures cease to exhibit a non-trivial behavior in the vicinity of the CP.

It has been shown that QPTs can be characterized by carefully examining the two-spin reduced density matrix and its derivatives with respect to the tuning parameter driving the transition [191, 192]. Since correlation measures are directly determined from the reduced density matrix, they provide information about the CPs and the order of QPTs. The CP for a second-order QPT at zero temperature is signalled by a divergence or discontinuity in the first derivative of the correlation measures. If the first derivative is discontinuous, then the divergence of the second derivative pinpoints the CP [191–193]. In Fig. 5.5, we plot the derivatives of MIN and WYSIM as a function of λ for $kT = 0, 0.1, 0.5$ and $\gamma = 0.001, 0.5, 1$. We observe that both of the measures are capable of spotlighting the CP at $kT = 0$ for all values of γ . It is worth to note that with increasing temperature, the divergent behaviors of the correlation measures at CP disappears and the peaks of the derivatives start to shift sideways. Therefore, the correlation measures lose their significance in determining the CP of the transition.

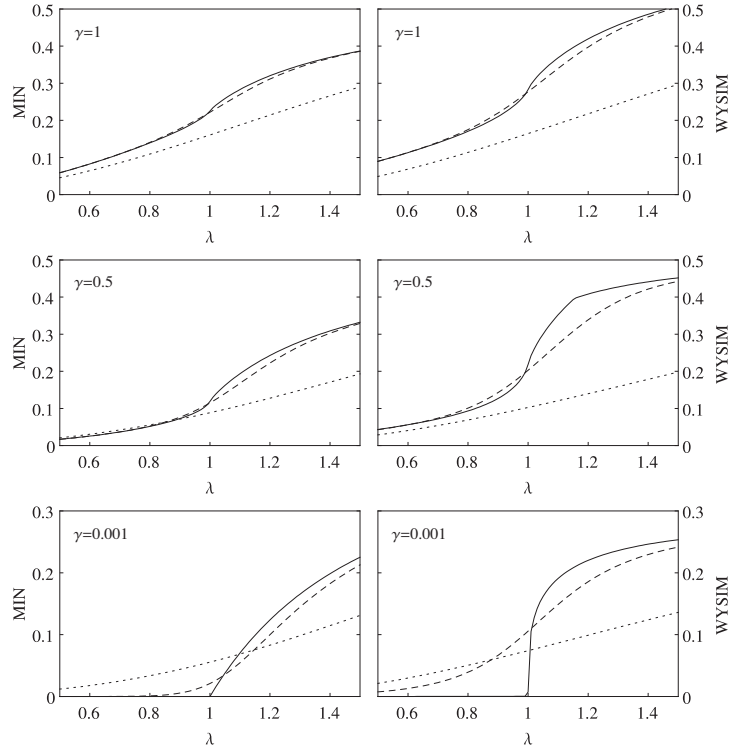


Figure 5.4: The thermal total correlations quantified by MIN and WYSIM as a function of λ for $\gamma = 0.001, 0.5, 1$ at $kT = 0$ (solid line), $kT = 0.1$ (dashed line) and $kT = 0.5$ (dotted line). The graphs are for first nearest neighbors.

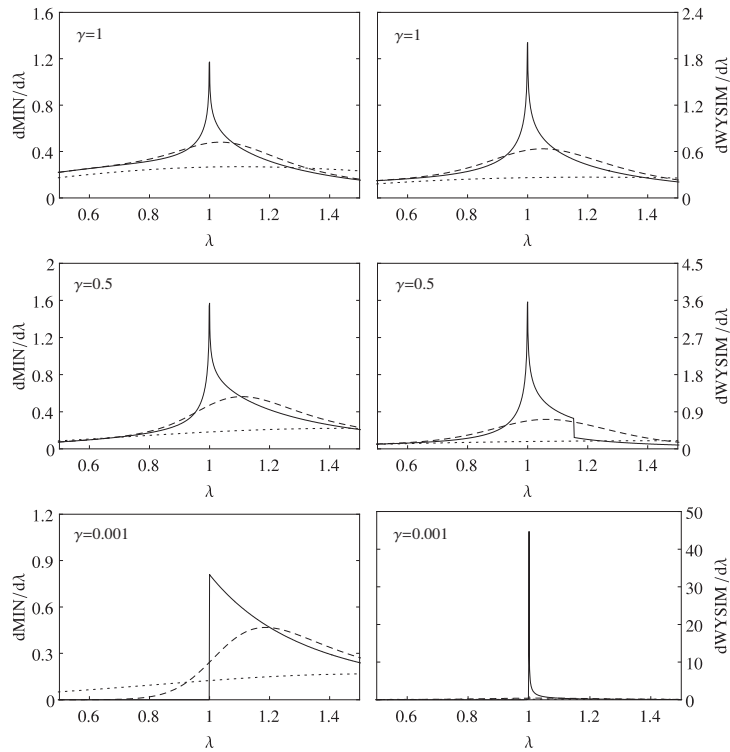


Figure 5.5: The first derivatives of MIN and WYSIM as a function of λ for $\gamma = 0.001, 0.5, 1$ at $kT = 0$ (solid line), $kT = 0.1$ (dashed line) and $kT = 0.5$ (dotted line). The graphs are for first nearest neighbors.

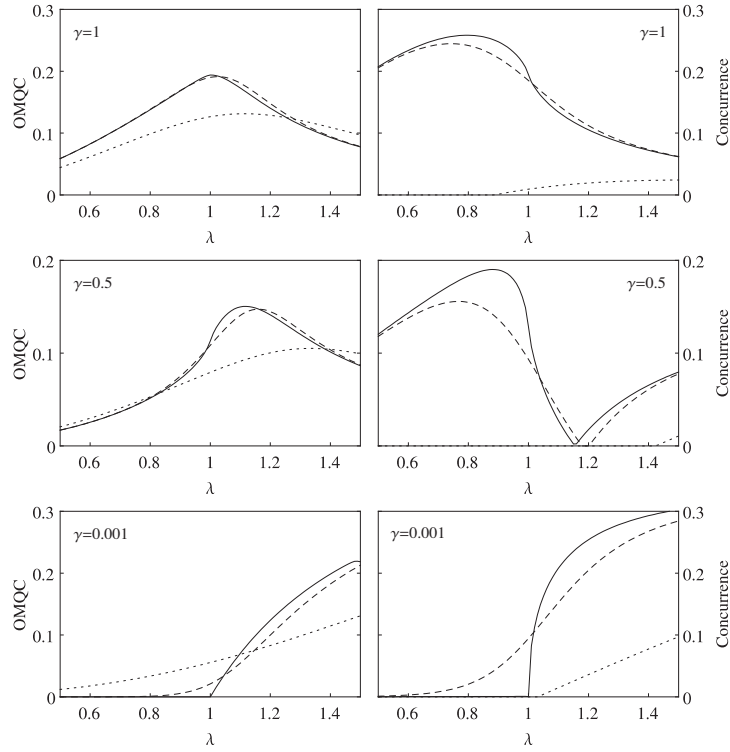


Figure 5.6: The thermal quantum correlations quantified by OMQC and concurrence as a function of λ for $\gamma = 0.001, 0.5, 1$ at $kT = 0$ (solid line), $kT = 0.1$ (dashed line) and $kT = 0.5$ (dotted line). The graphs are for first nearest neighbors.

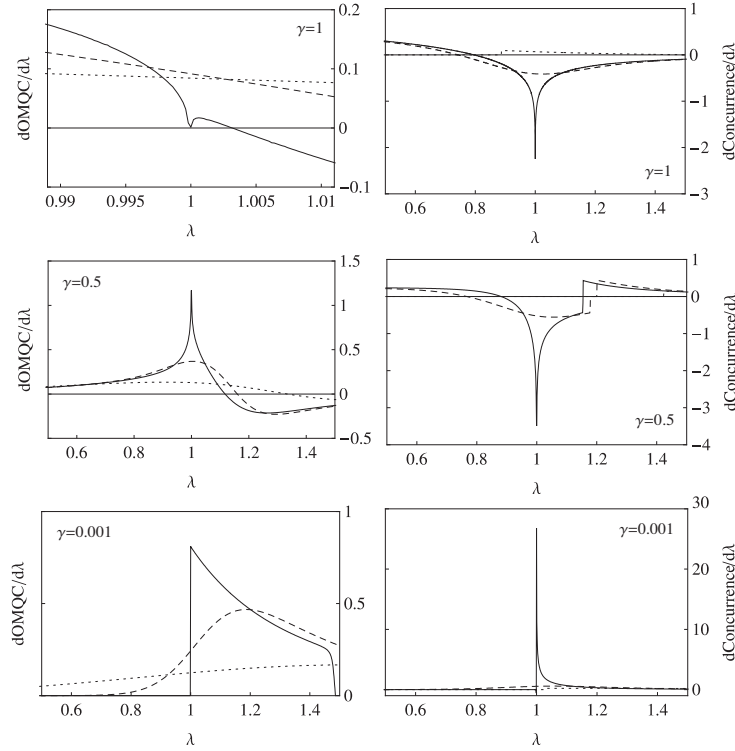


Figure 5.7: The first derivatives of OMQC and concurrence as a function of λ for $\gamma = 0.001, 0.5, 1$ at $kT = 0$ (solid line), $kT = 0.1$ (dashed line) and $kT = 0.5$ (dotted line). The graphs are for first nearest neighbors.

We now turn our attention to the analysis of thermal quantum correlations quantified by OMQC and concurrence. In Fig. 5.6 and Fig. 5.7, we plot these measures and their derivatives with respect to the driving parameter λ for first nearest neighbors as a function of λ for $kT = 0, 0.1, 0.5$. While concurrence suffers a drastic decrease as temperature increases, OMQC still captures significant amount of correlation, making it more robust against thermal effects. It can also be seen that at $kT = 0$ the CP can be detected by analyzing the non-analyticities in the first derivatives of the measures.

Next, we discuss the question of whether the studied correlation measures can signal the emergence of non-trivial product ground state in the XY spin chain. Despite the fact that the ground state of the model is entangled in general, for some special values of γ and λ , the ground state becomes completely factorized. In particular, except the trivial factorization points $\lambda = 0$ and $\lambda \rightarrow \infty$, there also exists a non-trivial factorization line corresponding to $\gamma^2 + \lambda^{-2} = 1$. Accordingly, as can be seen from the behavior of concurrence in Fig. 5.6 for $\gamma = 0.5$, entanglement vanishes at $\lambda \simeq 1.15$, which spotlights the occurrence of a product ground state. It is shown in Fig. 5.5 that, unlike OMQC and MIN, WYSIM can signal this factorization point through a non-analytical behavior in its derivative. For quantum discord to identify this point when the distance between the spins is fixed, the effects of SSB must be taken into account [208, 209]. Therefore, it is important to recognize that the calculation of WYSIM between the spins at a fixed distance enables us to detect the product ground state even in the absence of SSB.

5.4.1 Estimation of the critical points

Having discussed the behaviors of the thermal total and quantum correlations, we explore the ability of these measures to correctly estimate the CP of the QPT at finite temperature. Despite the disappearance of the singular behavior of MIN, WYSIM, OMQC and concurrence with increasing temperature, it might still be possible to estimate the CP at finite temperature [202]. For sufficiently low temperatures, divergent behaviors of the first derivatives of correlation measures at $T = 0$ will be replaced by a local maximum or minimum about the CP. Therefore, in order to estimate the CP, we search for this extremum point. On the other hand, a discontinuous first derivative at $T = 0$ requires us to look for an extremum point in the second derivative for $T > 0$. In Fig. 5.8, we present the results of our analysis regarding the estimation of CP as a function of kT for first and second nearest neighbors when $\gamma = 0.001, 0.5, 1$. Before starting to compare the ability of MIN, WYSIM, OMQC and concurrence to indicate the CP, we notice that the success rates of these measures strongly depends on the anisotropy parameter of the Hamiltonian. In the

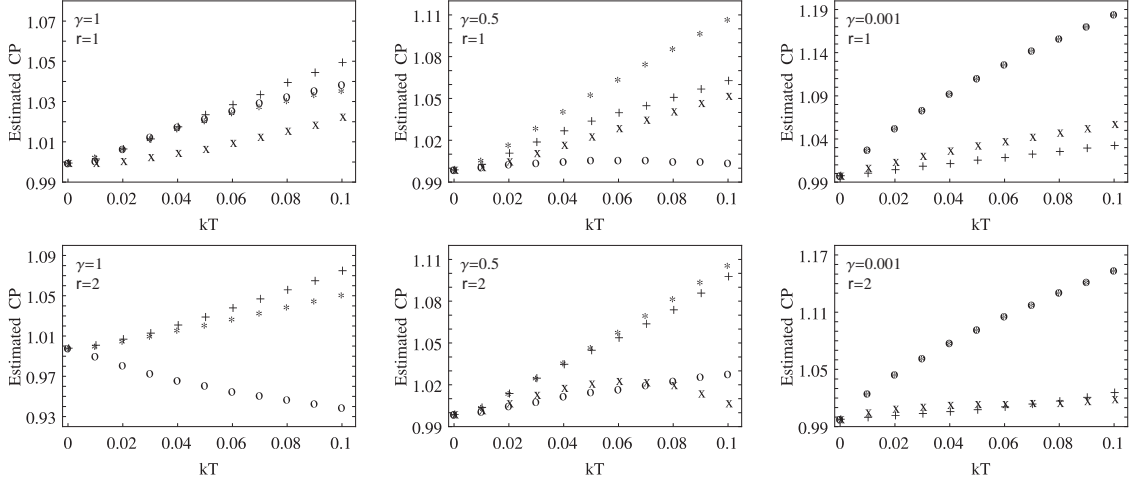


Figure 5.8: The estimated values of the CP as a function of kT for three different values of the anisotropy parameter $\gamma = 0.001, 0.5, 1$. The CPs are estimated by OMQC (denoted by o), WYSIM (denoted by +), MIN (denoted by *) and concurrence (denoted by x). Concurrence is not included for $\gamma = 1$ and $r = 2$, since it vanishes at even very low temperatures.

case of first nearest neighbors, at $\gamma = 1$, all of the correlation measures are able to predict the CP reliably, with concurrence being the most effective among them. When $\gamma = 0.5$ MIN turns out to be the worst CP estimator. While WYSIM and concurrence points out the CP relatively well as compared to MIN, OMQC clearly outperforms all others and estimates the CP in an exceptionally accurate way. For $\gamma = 0.001$, MIN and OMQC become identical, and they predict the location of the CP significantly worse than WYSIM and concurrence. For second nearest neighbors, even though we do not present the graphs of correlation measures and their derivatives, the CP has been inspected by performing the same analysis as in the first nearest neighbor case. The CPs estimated by WYSIM, OMQC and MIN for $\gamma = 1$ deviate from the true CP by the same amount but they are still acceptable. In the case of $\gamma = 0.5$, both concurrence and OMQC estimate the CP very well in contrast to WYSIM and MIN. Finally, when $\gamma = 0.001$, while WYSIM and concurrence spotlight the CP remarkably well, OMQC and MIN perform very poorly. It is also worth to notice that concurrence performs even better than the first nearest neighbors case for $\gamma = 0.5$ and $\gamma = 0.001$. Furthermore, the ability of entanglement of formation and quantum discord to estimate the CP of the XY spin chain at finite temperature has been recently studied by Werlang et al. [202]. The performance of the the considered measures as compared to quantum discord and entanglement of formation depends on the anisotropy parameter and also on the distance between the spin pairs. For instance, in the first nearest neighbors case at $\gamma = 0.5$, only OMQC performs as well as quantum discord and entanglement of formation. On the other hand, for the second nearest neighbors at $\gamma = 0.001$, while WYSIM and concurrence turn out to be better CP estimators than discord and entanglement of formation, MIN and OMQC do not perform as well.

5.4.2 Long-range behavior of the correlations

We now examine the long-range behavior of the thermal correlations. Fig. 5.9 demonstrates our results related to the dependence of MIN, WYSIM and OMQC on the distance between the spin pairs at finite temperature, for $\lambda = 0.75, 0.95, 1.05, 1.5$ and $\gamma = 0.001, 1$. In case of $\gamma = 0.001$, neither of the correlation measures remain significant when the distance between the spin pairs is increased. We can also see that the decay of the correlations hastens when the temperature rises. For $\gamma = 1$, even though MIN, WYSIM and OMQC approach to a finite value in the ordered phase for sufficiently low temperatures, thermal effects wipe out the correlations between distant spin pairs after a certain temperature.

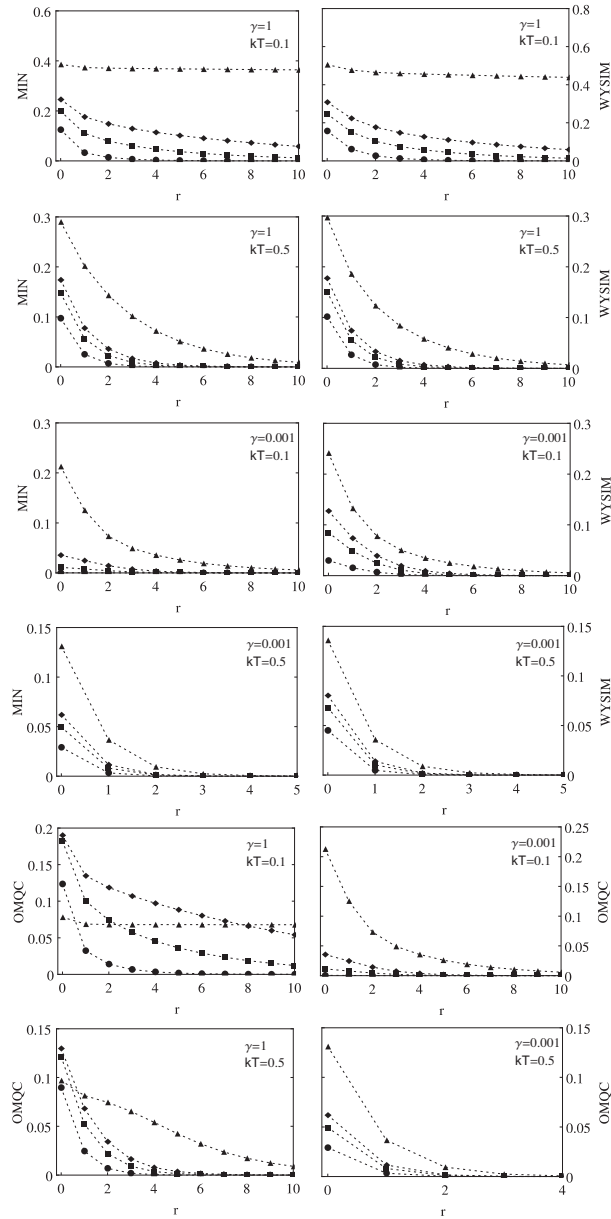


Figure 5.9: Long-range behavior of the thermal total and quantum correlations for $\gamma = 0.001$ and $\gamma = 1$ at $kT = 0.1, 0.5$. The circles, squares, diamonds and triangles correspond to $\lambda = 0.75, \lambda = 0.95, \lambda = 1.05$ and $\lambda = 1.5$, respectively.

Chapter 6

CONCLUSION

In this thesis, we have investigated a collection of subjects in quantum information theory, including the symmetry properties of quantum states under decoherence, the optimal local transformations of multipartite FES states, the dynamics of various correlation measures in dephasing environments and the thermal correlations in the XY spin chain. The main results of the thesis are constructed from four publications [21, 78, 93, 94], and presented here in three chapters, namely the chapters three to five.

In the third chapter, we have studied the local one-shot entanglement transformations of FES states. We have determined the structure of optimal transformations that relate multiqubit FES states with the maximum possible probability of success. We have also demonstrated that certain entangled states are more robust than others, that is, the optimum probability of converting these robust states to the states lying in the close neighborhood of separable ones vanishes under local FES operations.

In the fourth chapter, we have examined the exchange symmetry of Bell states when two qubits interact with local baths having identical parameters. We have considered a pure dephasing model which is also invariant under swapping the qubits. We have found that as the system evolves in time, one of the symmetric Bell states fails to preserve the exchange symmetry. This phenomenon, known as the decoherence induced spontaneous symmetry breaking, has been demonstrated experimentally.

In the fifth chapter, we have first explored the dynamics of classical and quantum correlations for qubit-qutrit systems in independent and global dephasing environments. In these cases, we have demonstrated several interesting phenomena such as the frozen quantum discord and frozen geometric discord. Then, we have investigated the thermal quantum and total correlations in the anisotropic XY spin chain in transverse field. We have shown that the ability of correlation measures to estimate the critical point of the phase transition at finite temperature strongly depends on the anisotropy parameter of the model. We have also identified a correlation measure which detects the factorized ground state. Finally, we have studied the effect of temperature on long-range correlations.

Bibliography

- [1] E. Schrödinger, “Discussion of probability relations between separated systems,” *Mathematical Proceedings of the Cambridge Philosophical Society*, vol. 31, no. 04, pp. 555–563, 1935.
- [2] A. Einstein, B. Podolsky, and N. Rosen, “Can quantum-mechanical description of physical reality be considered complete?,” *Physical Review*, vol. 47, pp. 777–780, 1935.
- [3] R. Horodecki, P. Horodecki, M. Horodecki, and K. Horodecki, “Quantum entanglement,” *Reviews of Modern Physics*, vol. 81, pp. 865–942, 2009.
- [4] M. Nielsen and I. Chuang, *Quantum computation and quantum information*. Cambridge University Press, 2000.
- [5] K. Modi, T. Paterek, W. Son, V. Vedral, and M. Williamson, “Unified view of quantum and classical correlations,” *Physical Review Letters*, vol. 104, p. 080501, 2010.
- [6] L. Amico, R. Fazio, A. Osterloh, and V. Vedral, “Entanglement in many-body systems,” *Reviews of Modern Physics*, vol. 80, pp. 517–576, 2008.
- [7] W. H. Zurek, “Decoherence, einselection, and the quantum origins of the classical,” *Reviews of Modern Physics*, vol. 75, pp. 715–775, 2003.
- [8] G. Benenti, G. Casati, and G. Strini, *Principles of quantum computation and information: basic concepts*. World Scientific, 2004.
- [9] G. Benenti, G. Casati, and G. Strini, *Principles of quantum computation and information: basic tools and special topics*. World Scientific, 2007.
- [10] L. Diósi, *A short course in quantum information theory: an approach from theoretical physics*. Springer, 2007.
- [11] D. Griffiths, *Introduction to quantum mechanics*. Pearson Prentice Hall, 2005.
- [12] R. Shankar, *Principles of quantum mechanics*. Springer, 1994.

- [13] J. Sakurai and J. Napolitano, *Modern quantum mechanics*. Addison-Wesley, 2010.
- [14] E. Merzbacher, *Quantum mechanics*. John Wiley and Sons, 3rd ed., 1998.
- [15] K. Gottfried and T. Yan, *Quantum mechanics: fundamentals*. Springer, 2003.
- [16] A. Peres, *Quantum theory: concepts and methods*. Springer, 1995.
- [17] W. K. Wootters and W. H. Zurek, “A single quantum cannot be cloned,” *Nature*, vol. 299, no. 5886, pp. 802–803, 1982.
- [18] J. von Neumann, *Mathematical Foundations of Quantum Mechanics*. Princeton Landmarks in Mathematics and Physics, Princeton University Press, 1955.
- [19] M.-D. Choi, “Completely positive linear maps on complex matrices,” *Linear Algebra and its Applications*, vol. 10, no. 3, pp. 285–290, 1975.
- [20] K. Kraus, *States, effects, and operations: fundamental notions of quantum theory*. Springer-Verlag, 1983.
- [21] G. Karpat and Z. Gedik, “Optimal local transformations of flip and exchange symmetric entangled states,” *Physics Letters A*, vol. 376, no. 2, pp. 75–79, 2011.
- [22] R. F. Werner, “Quantum states with Einstein-Podolsky-Rosen correlations admitting a hidden-variable model,” *Physical Review A*, vol. 40, pp. 4277–4281, 1989.
- [23] A. Peres, “Separability criterion for density matrices,” *Physical Review Letters*, vol. 77, pp. 1413–1415, 1996.
- [24] M. Horodecki, P. Horodecki, and R. Horodecki, “Separability of mixed states: necessary and sufficient conditions,” *Physics Letters A*, vol. 223, no. 1–2, pp. 1–8, 1996.
- [25] S. Hill and W. K. Wootters, “Entanglement of a pair of quantum bits,” *Physical Review Letters*, vol. 78, pp. 5022–5025, 1997.
- [26] W. K. Wootters, “Entanglement of formation of an arbitrary state of two qubits,” *Physical Review Letters*, vol. 80, pp. 2245–2248, 1998.
- [27] G. Vidal and R. F. Werner, “Computable measure of entanglement,” *Physical Review A*, vol. 65, p. 032314, 2002.

- [28] C. H. Bennett, G. Brassard, S. Popescu, B. Schumacher, J. A. Smolin, and W. K. Wootters, “Purification of noisy entanglement and faithful teleportation via noisy channels,” *Physical Review Letters*, vol. 76, pp. 722–725, 1996.
- [29] C. H. Bennett, H. J. Bernstein, S. Popescu, and B. Schumacher, “Concentrating partial entanglement by local operations,” *Physical Review A*, vol. 53, pp. 2046–2052, 1996.
- [30] C. H. Bennett, D. P. DiVincenzo, J. A. Smolin, and W. K. Wootters, “Mixed-state entanglement and quantum error correction,” *Physical Review A*, vol. 54, pp. 3824–3851, 1996.
- [31] C. H. Bennett, S. Popescu, D. Rohrlich, J. A. Smolin, and A. V. Thapliyal, “Exact and asymptotic measures of multipartite pure-state entanglement,” *Physical Review A*, vol. 63, p. 012307, 2000.
- [32] C. H. Bennett, G. Brassard, C. Crépeau, R. Jozsa, A. Peres, and W. K. Wootters, “Teleporting an unknown quantum state via dual classical and Einstein-Podolsky-Rosen channels,” *Physical Review Letters*, vol. 70, pp. 1895–1899, 1993.
- [33] C. H. Bennett, D. P. DiVincenzo, C. A. Fuchs, T. Mor, E. Rains, P. W. Shor, J. A. Smolin, and W. K. Wootters, “Quantum nonlocality without entanglement,” *Physical Review A*, vol. 59, pp. 1070–1091, 1999.
- [34] V. Gheorghiu and R. B. Griffiths, “Separable operations on pure states,” *Physical Review A*, vol. 78, p. 020304, 2008.
- [35] R. Duan, Y. Feng, Y. Xin, and M. Ying, “Distinguishability of quantum states by separable operations,” *IEEE Transactions on Information Theory*, vol. 55, no. 3, pp. 1320–1330, 2009.
- [36] E. Chitambar and R. Duan, “Nonlocal entanglement transformations achievable by separable operations,” *Physical Review Letters*, vol. 103, p. 110502, 2009.
- [37] E. Chitambar, W. Cui, and H.-K. Lo, “Increasing entanglement monotones by separable operations,” *Physical Review Letters*, vol. 108, p. 240504, 2012.
- [38] E. Chitambar, W. Cui, and H.-K. Lo, “Entanglement monotones for W-type states,” *Physical Review A*, vol. 85, p. 062316, 2012.
- [39] G. Vidal, “Entanglement monotones,” *Journal of Modern Optics*, vol. 47, no. 2–3, pp. 355–376, 2000.

- [40] V. Vedral, M. B. Plenio, M. A. Rippin, and P. L. Knight, “Quantifying entanglement,” *Physical Review Letters*, vol. 78, pp. 2275–2279, 1997.
- [41] V. Vedral and M. B. Plenio, “Entanglement measures and purification procedures,” *Physical Review A*, vol. 57, pp. 1619–1633, 1998.
- [42] M. B. Plenio, “Logarithmic negativity: a full entanglement monotone that is not convex,” *Physical Review Letters*, vol. 95, p. 090503, 2005.
- [43] M. Horodecki, “Entanglement measures,” *Quantum Information and Computation*, vol. 1, pp. 3–26, 2001.
- [44] M. B. Plenio and S. Virmani, “An introduction to entanglement measures,” *Quantum Information and Computation*, vol. 7, pp. 1–51, 2007.
- [45] C. Shannon, “A mathematical theory of communication,” *The Bell System Technical Journal*, vol. 27, pp. 379–423, 623–656, 1948.
- [46] S. Popescu and D. Rohrlich, “Thermodynamics and the measure of entanglement,” *Physical Review A*, vol. 56, pp. R3319–R3321, 1997.
- [47] B. Kraus, “Local unitary equivalence of multipartite pure states,” *Physical Review Letters*, vol. 104, p. 020504, 2010.
- [48] B. Kraus, “Local unitary equivalence and entanglement of multipartite pure states,” *Physical Review A*, vol. 82, p. 032121, 2010.
- [49] B. Liu, J.-L. Li, X. Li, and C.-F. Qiao, “Local unitary classification of arbitrary dimensional multipartite pure states,” *Physical Review Letters*, vol. 108, p. 050501, 2012.
- [50] M. A. Nielsen, “Conditions for a class of entanglement transformations,” *Physical Review Letters*, vol. 83, pp. 436–439, 1999.
- [51] W. Dür, G. Vidal, and J. I. Cirac, “Three qubits can be entangled in two inequivalent ways,” *Physical Review A*, vol. 62, p. 062314, 2000.
- [52] H.-K. Lo and S. Popescu, “Concentrating entanglement by local actions: beyond mean values,” *Physical Review A*, vol. 63, p. 022301, 2001.
- [53] V. Coffman, J. Kundu, and W. K. Wootters, “Distributed entanglement,” *Physical Review A*, vol. 61, p. 052306, 2000.

- [54] Y. Cao and A. M. Wang, “Discussion of the entanglement classification of a 4-qubit pure state,” *The European Physical Journal D - Atomic, Molecular, Optical and Plasma Physics*, vol. 44, pp. 159–166, 2007.
- [55] L. Lamata, J. León, D. Salgado, and E. Solano, “Inductive entanglement classification of four qubits under stochastic local operations and classical communication,” *Physical Review A*, vol. 75, p. 022318, 2007.
- [56] H. H. Dafa Li, Xiangrong Li and X. Li, “SLOCC classification for nine families of four-qubits,” *Quantum Information and Computation*, vol. 7, pp. 778–800, 2009.
- [57] D. Li, X. Li, H. Huang, and X. Li, “Classification of four-qubit states by means of a stochastic local operation and the classical communication invariant and semi-invariants,” *Physical Review A*, vol. 76, p. 052311, 2007.
- [58] O. Viehmann, C. Eltschka, and J. Siewert, “Polynomial invariants for discrimination and classification of four-qubit entanglement,” *Physical Review A*, vol. 83, p. 052330, 2011.
- [59] F. Verstraete, J. Dehaene, B. De Moor, and H. Verschelde, “Four qubits can be entangled in nine different ways,” *Physical Review A*, vol. 65, p. 052112, 2002.
- [60] L. Borsten, D. Dahanayake, M. J. Duff, A. Marrani, and W. Rubens, “Four-qubit entanglement classification from string theory,” *Physical Review Letters*, vol. 105, p. 100507, 2010.
- [61] O. Chterental and D. Z. Djoković, *Linear Algebra Research Advances*. Nova Science Publishers, 2007.
- [62] A. Miyake and F. Verstraete, “Multipartite entanglement in $2 \times 2 \times n$ quantum systems,” *Physical Review A*, vol. 69, p. 012101, 2004.
- [63] X. Li and D. Li, “Stochastic local operations and classical communication equations and classification of even n qubits,” *Journal of Physics A: Mathematical and Theoretical*, vol. 44, no. 15, p. 155304, 2011.
- [64] X. Li and D. Li, “Rank-based SLOCC classification for odd n qubits,” *Quantum Information and Computation*, vol. 7, pp. 695–705, 2009.
- [65] D. Li, X. Li, H. Huang, and X. Li, “Stochastic local operations and classical communication properties of the n -qubit symmetric Dicke states,” *Europhysics Letters*, vol. 87, no. 2, p. 20006, 2009.

- [66] T. Bastin, S. Krins, P. Mathonet, M. Godefroid, L. Lamata, and E. Solano, “Operational families of entanglement classes for symmetric n -qubit states,” *Physical Review Letters*, vol. 103, p. 070503, 2009.
- [67] P. Mathonet, S. Krins, M. Godefroid, L. Lamata, E. Solano, and T. Bastin, “Entanglement equivalence of n -qubit symmetric states,” *Physical Review A*, vol. 81, p. 052315, 2010.
- [68] X. Li and D. Li, “Classification of general n -qubit states under stochastic local operations and classical communication in terms of the rank of coefficient matrix,” *Physical Review Letters*, vol. 108, p. 180502, 2012.
- [69] Z. Gedik, “Stability of flip and exchange symmetric entangled state classes under invertible local operations,” *Optics Communications*, vol. 284, no. 2, pp. 681–684, 2011.
- [70] B. He and J. A. Bergou, “Entanglement transformation with no classical communication,” *Physical Review A*, vol. 78, p. 062328, 2008.
- [71] G. Vidal, “Entanglement of pure states for a single copy,” *Physical Review Letters*, vol. 83, pp. 1046–1049, 1999.
- [72] A. Yildiz, “Optimal distillation of three-qubit W states,” *Physical Review A*, vol. 82, p. 012317, 2010.
- [73] L.-M. Liang and C.-Z. Li, “Distillation of a m -GHZ state from an arbitrary pure states of m qubits under one successful branch protocol,” *Physics Letters A*, vol. 308, no. 5, pp. 343–348, 2003.
- [74] W. Cui, W. Helwig, and H.-K. Lo, “Bounds on probability of transformations between multipartite pure states,” *Physical Review A*, vol. 81, p. 012111, 2010.
- [75] W. Cui, E. Chitambar, and H.-K. Lo, “Optimal entanglement transformations among n -qubit W -class states,” *Physical Review A*, vol. 82, p. 062314, 2010.
- [76] S. Kintaş and S. Turgut, “Transformations of W -type entangled states,” *Journal of Mathematical Physics*, vol. 51, no. 9, p. 092202, 2010.
- [77] H.-K. Lo and S. Popescu, “Classical communication cost of entanglement manipulation: Is entanglement an interconvertible resource?,” *Physical Review A*, vol. 83, pp. 1459–1462, 1999.

- [78] G. Karpat and Z. Gedik, “Decoherence induced spontaneous symmetry breaking,” *Optics Communications*, vol. 282, no. 22, pp. 4460 – 4463, 2009.
- [79] Y.-F. Huang, L. Peng, L. Li, B.-H. Liu, C.-F. Li, and G.-C. Guo, “Experimental demonstration of decoherence-induced spontaneous symmetry breaking,” *Physical Review A*, vol. 83, p. 052105, 2011.
- [80] M. Schlosshauer, “Decoherence, the measurement problem, and interpretations of quantum mechanics,” *Reviews of Modern Physics*, vol. 76, pp. 1267–1305, 2005.
- [81] E. Joos, H. Zeh, C. Kiefer, D. Giulini, J. Kupsch, and I. Stamatescu, *Decoherence and the Appearance of a Classical World in Quantum Theory*. Physics and astronomy online library, Springer, 2003.
- [82] M. Schlosshauer, *Decoherence: and the Quantum-To-Classical Transition*. The Frontiers Collection, Springer, 2008.
- [83] P. Blanchard, D. Giulini, E. Joos, C. Kiefer, and I. Stamatescu, *Decoherence: Theoretical, Experimental, and Conceptual Problems: Proceedings of a Workshop Held at Bielefeld, Germany, 10-14 November 1998*. Lecture Notes in Physics, Springer, 2010.
- [84] H. Zeh, “On the interpretation of measurement in quantum theory,” *Foundations of Physics*, vol. 1, pp. 69–76, 1970.
- [85] H. Zeh, “Toward a quantum theory of observation,” *Foundations of Physics*, vol. 3, pp. 109–116, 1973.
- [86] W. H. Zurek, “Pointer basis of quantum apparatus: Into what mixture does the wave packet collapse?,” *Physical Review D*, vol. 24, pp. 1516–1525, 1981.
- [87] W. H. Zurek, “Environment-induced superselection rules,” *Physical Review D*, vol. 26, pp. 1862–1880, 1982.
- [88] V. B. Braginsky and F. Y. Khalili, “Quantum nondemolition measurements: the route from toys to tools,” *Reviews of Modern Physics*, vol. 68, pp. 1–11, 1996.
- [89] A. Elby and J. Bub, “Triorthogonal uniqueness theorem and its relevance to the interpretation of quantum mechanics,” *Physical Review A*, vol. 49, pp. 4213–4216, 1994.

- [90] W. H. Zurek, S. Habib, and J. P. Paz, “Coherent states via decoherence,” *Physical Review Letters*, vol. 70, pp. 1187–1190, 1993.
- [91] T. Yu and J. H. Eberly, “Qubit disentanglement and decoherence via dephasing,” *Physical Review B*, vol. 68, p. 165322, 2003.
- [92] Z. Gedik, “Spin bath decoherence of quantum entanglement,” *Solid State Communications*, vol. 138, no. 2, pp. 82 – 85, 2006.
- [93] G. Karpat and Z. Gedik, “Correlation dynamics of qubit-qutrit systems in a classical dephasing environment,” *Physics Letters A*, vol. 375, no. 47, pp. 4166 – 4171, 2011.
- [94] B. Çakmak, G. Karpat, and Z. Gedik, “Critical point estimation and long-range behavior in the one-dimensional XY model using thermal quantum and total correlations,” *Physics Letters A*, vol. 376, no. 45, pp. 2982 – 2988, 2012.
- [95] K. Modi, A. Brodutch, H. Cable, T. Paterek, and V. Vedral, “The classical-quantum boundary for correlations: discord and related measures,” *Reviews of Modern Physics*, vol. 84, pp. 1655–1707, 2012.
- [96] J. S. Xu and C. F. Li, “Quantum discord under system-environment coupling: the two-qubit case,” *International Journal of Modern Physics B*, vol. 27, no. 01n03, p. 1345054, 2013.
- [97] L. C. Céleri, J. Maziero, and R. M. Serra, “Theoretical and experimental aspects of quantum discord and related measures,” *International Journal of Quantum Information*, vol. 9, pp. 1837–1873, 2011.
- [98] E. Knill and R. Laflamme, “Power of one bit of quantum information,” *Physical Review Letters*, vol. 81, pp. 5672–5675, 1998.
- [99] S. L. Braunstein, C. M. Caves, R. Jozsa, N. Linden, S. Popescu, and R. Schack, “Separability of very noisy mixed states and implications for nmr quantum computing,” *Physical Review Letters*, vol. 83, pp. 1054–1057, 1999.
- [100] D. A. Meyer, “Sophisticated quantum search without entanglement,” *Physical Review Letters*, vol. 85, pp. 2014–2017, 2000.
- [101] A. Datta, S. T. Flammia, and C. M. Caves, “Entanglement and the power of one qubit,” *Physical Review A*, vol. 72, p. 042316, 2005.

- [102] A. Datta and G. Vidal, “Role of entanglement and correlations in mixed-state quantum computation,” *Physical Review A*, vol. 75, p. 042310, 2007.
- [103] A. Datta, A. Shaji, and C. M. Caves, “Quantum discord and the power of one qubit,” *Physical Review Letters*, vol. 100, p. 050502, 2008.
- [104] B. P. Lanyon, M. Barbieri, M. P. Almeida, and A. G. White, “Experimental quantum computing without entanglement,” *Physical Review Letters*, vol. 101, p. 200501, 2008.
- [105] B. Li, S.-M. Fei, Z.-X. Wang, and H. Fan, “Assisted state discrimination without entanglement,” *Physical Review A*, vol. 85, p. 022328, 2012.
- [106] K. Modi, H. Cable, M. Williamson, and V. Vedral, “Quantum correlations in mixed-state metrology,” *Physical Review X*, vol. 1, p. 021022, 2011.
- [107] L. Roa, J. C. Retamal, and M. Alid-Vaccarezza, “Dissonance is required for assisted optimal state discrimination,” *Physical Review Letters*, vol. 107, p. 080401, 2011.
- [108] H. Ollivier and W. H. Zurek, “Quantum discord: a measure of the quantumness of correlations,” *Physical Review Letters*, vol. 88, p. 017901, 2001.
- [109] L. Henderson and V. Vedral, “Classical, quantum and total correlations,” *Journal of Physics A: Mathematical and General*, vol. 34, no. 35, p. 6899, 2001.
- [110] B. Dakić, V. Vedral, and C. Brukner, “Necessary and sufficient condition for nonzero quantum discord,” *Physical Review Letters*, vol. 105, p. 190502, 2010.
- [111] J. Oppenheim, M. Horodecki, P. Horodecki, and R. Horodecki, “Thermodynamical approach to quantifying quantum correlations,” *Physical Review Letters*, vol. 89, p. 180402, 2002.
- [112] B. Groisman, S. Popescu, and A. Winter, “Quantum, classical, and total amount of correlations in a quantum state,” *Physical Review A*, vol. 72, p. 032317, 2005.
- [113] S. Luo, “Using measurement-induced disturbance to characterize correlations as classical or quantum,” *Physical Review A*, vol. 77, p. 022301, 2008.
- [114] T. Zhou, J. Cui, and G. L. Long, “Measure of nonclassical correlation in coherence-vector representation,” *Physical Review A*, vol. 84, p. 062105, 2011.

- [115] A. Brodutch and K. Modi, “Criteria for measures of quantum correlations,” *Quantum Information and Computation*, vol. 12, pp. 0721–0742, 2009.
- [116] W. H. Zurek, “Quantum discord and Maxwell’s demons,” *Physical Review A*, vol. 67, p. 012320, 2003.
- [117] A. Ferraro, L. Aolita, D. Cavalcanti, and F. M. Cucchietti, “Almost all quantum states have nonclassical correlations,” *Physical Review A*, vol. 81, p. 052318, 2010.
- [118] A. Shabani and D. A. Lidar, “Vanishing quantum discord is necessary and sufficient for completely positive maps,” *Physical Review Letters*, vol. 102, p. 100402, 2009.
- [119] D. Cavalcanti, L. Aolita, S. Boixo, K. Modi, M. Piani, and A. Winter, “Operational interpretations of quantum discord,” *Physical Review A*, vol. 83, p. 032324, 2011.
- [120] V. Madhok and A. Datta, “Interpreting quantum discord through quantum state merging,” *Physical Review A*, vol. 83, p. 032323, 2011.
- [121] F. Galve, G. L. Giorgi, and R. Zambrini, “Maximally discordant mixed states of two qubits,” *Physical Review A*, vol. 83, p. 012102, 2011.
- [122] M. Piani, P. Horodecki, and R. Horodecki, “No-local-broadcasting theorem for multipartite quantum correlations,” *Physical Review Letters*, vol. 100, p. 090502, 2008.
- [123] M. Piani, S. Gharibian, G. Adesso, J. Calsamiglia, P. Horodecki, and A. Winter, “All nonclassical correlations can be activated into distillable entanglement,” *Physical Review Letters*, vol. 106, p. 220403, 2011.
- [124] A. Streltsov, H. Kampermann, and D. Bruß, “Linking quantum discord to entanglement in a measurement,” *Physical Review Letters*, vol. 106, p. 160401, 2011.
- [125] G. Adesso and A. Datta, “Quantum versus classical correlations in Gaussian states,” *Physical Review Letters*, vol. 105, p. 030501, 2010.
- [126] F. F. Fanchini, M. F. Cornelio, M. C. de Oliveira, and A. O. Caldeira, “Conservation law for distributed entanglement of formation and quantum discord,” *Physical Review A*, vol. 84, p. 012313, 2011.
- [127] M. F. Cornelio, M. C. de Oliveira, and F. F. Fanchini, “Entanglement irreversibility from quantum discord and quantum deficit,” *Physical Review Letters*, vol. 107, p. 020502, 2011.

- [128] T. K. Chuan, J. Maillard, K. Modi, T. Paterek, M. Paternostro, and M. Piani, “Quantum discord bounds the amount of distributed entanglement,” *Physical Review Letters*, vol. 109, p. 070501, 2012.
- [129] C. A. Rodríguez-Rosario, K. Modi, A.-M. Kuah, A. Shaji, and E. C. G. Sudarshan, “Completely positive maps and classical correlations,” *Journal of Physics A: Mathematical and Theoretical*, vol. 41, no. 20, p. 205301, 2008.
- [130] F. F. Fanchini, L. K. Castelano, M. F. Cornelio, and M. C. de Oliveira, “Locally inaccessible information as a fundamental ingredient to quantum information,” *New Journal of Physics*, vol. 14, no. 1, p. 013027, 2012.
- [131] A. Streltsov, H. Kampermann, and D. Bruß, “Behavior of quantum correlations under local noise,” *Physical Review Letters*, vol. 107, p. 170502, 2011.
- [132] F. Ciccarello and V. Giovannetti, “Creating quantum correlations through local nonunitary memoryless channels,” *Physical Review A*, vol. 85, p. 010102, 2012.
- [133] S. Luo, “Quantum discord for two-qubit systems,” *Physical Review A*, vol. 77, p. 042303, 2008.
- [134] M. Ali, A. R. P. Rau, and G. Alber, “Quantum discord for two-qubit X states,” *Physical Review A*, vol. 81, p. 042105, 2010.
- [135] X.-M. Lu, J. Ma, Z. Xi, and X. Wang, “Optimal measurements to access classical correlations of two-qubit states,” *Physical Review A*, vol. 83, p. 012327, 2011.
- [136] P. Giorda and M. G. A. Paris, “Gaussian quantum discord,” *Physical Review Letters*, vol. 105, p. 020503, 2010.
- [137] M. Shi, C. Sun, F. Jiang, X. Yan, and J. Du, “Optimal measurement for quantum discord of two-qubit states,” *Physical Review A*, vol. 85, p. 064104, 2012.
- [138] Q. Chen, C. Zhang, S. Yu, X. X. Yi, and C. H. Oh, “Quantum discord of two-qubit X states,” *Physical Review A*, vol. 84, p. 042313, 2011.
- [139] L.-X. Cen, X.-Q. Li, J. Shao, and Y. Yan, “Quantifying quantum discord and entanglement of formation via unified purifications,” *Physical Review A*, vol. 83, p. 054101, 2011.
- [140] M. Shi, W. Yang, F. Jiang, and J. Du, “Quantum discord of two-qubit rank-2 states,” *Journal of Physics A: Mathematical and Theoretical*, vol. 44, no. 41, p. 415304, 2011.

- [141] M. Ali, “Quantum discord for a two-parameter class of states in $2 \times d$ quantum systems,” *Journal of Physics A: Mathematical and Theoretical*, vol. 43, no. 49, p. 495303, 2010.
- [142] F. Galve, G. L. Giorgi, and R. Zambrini, “Orthogonal measurements are almost sufficient for quantum discord of two qubits,” *Europhysics Letters*, vol. 96, no. 4, p. 40005, 2011.
- [143] S. Vinjanampathy and A. R. P. Rau, “Quantum discord for qubit-qudit systems,” *Journal of Physics A: Mathematical and Theoretical*, vol. 45, no. 9, p. 095303, 2012.
- [144] S. Luo and S. Fu, “Geometric measure of quantum discord,” *Physical Review A*, vol. 82, p. 034302, 2010.
- [145] A. S. M. Hassan, B. Lari, and P. S. Joag, “Tight lower bound to the geometric measure of quantum discord,” *Physical Review A*, vol. 85, p. 024302, 2012.
- [146] S. Rana and P. Parashar, “Tight lower bound on geometric discord of bipartite states,” *Physical Review A*, vol. 85, p. 024102, 2012.
- [147] M. Piani, “Problem with geometric discord,” *Physical Review A*, vol. 86, p. 034101, 2012.
- [148] D. Girolami and G. Adesso, “Observable measure of bipartite quantum correlations,” *Physical Review A*, vol. 108, p. 150403, 2012.
- [149] S. Luo and S. Fu, “Measurement-induced nonlocality,” *Physical Review Letters*, vol. 106, p. 120401, 2011.
- [150] S. Luo, S. Fu, and C. H. Oh, “Quantifying correlations via the Wigner-Yanase skew information,” *Physical Review A*, vol. 85, p. 032117, 2012.
- [151] E. P. Wigner and M. M. Yanase, “Information contents of distributions,” *Proceedings of the National Academy of Sciences of the United States of America*, vol. 49, pp. 910–918, 1963.
- [152] S. Luo, “Quantum uncertainty of mixed states based on skew information,” *Physical Review A*, vol. 73, p. 022324, 2006.
- [153] M. P. Almeida, F. de Melo, M. Hor-Meyll, A. Salles, S. P. Walborn, P. H. S. Ribeiro, and L. Davidovich, “Environment-induced sudden death of entanglement,” *Science*, vol. 316, no. 5824, pp. 579–582, 2007.

- [154] T. Yu and J. H. Eberly, “Finite-time disentanglement via spontaneous emission,” *Physical Review Letters*, vol. 93, p. 140404, 2004.
- [155] T. Yu and J. H. Eberly, “Quantum open system theory: bipartite aspects,” *Physical Review Letters*, vol. 97, p. 140403, 2006.
- [156] T. Yu and J. Eberly, “Sudden death of entanglement: classical noise effects,” *Optics Communications*, vol. 264, no. 2, pp. 393 – 397, 2006.
- [157] T. Yu and J. H. Eberly, “Sudden death of entanglement,” *Science*, vol. 323, no. 5914, pp. 598–601, 2009.
- [158] A. Al-Qasimi and D. F. V. James, “Sudden death of entanglement at finite temperature,” *Physical Review A*, vol. 77, p. 012117, 2008.
- [159] K. Ann and G. Jaeger, “Local-dephasing-induced entanglement sudden death in two-component finite-dimensional systems,” *Physical Review A*, vol. 76, p. 044101, 2007.
- [160] K. Ann and G. Jaeger, “Entanglement sudden death in qubit-qutrit systems,” *Physics Letters A*, vol. 372, no. 5, pp. 579 – 583, 2008.
- [161] F. F. Fanchini, T. Werlang, C. A. Brasil, L. G. E. Arruda, and A. O. Caldeira, “Non-Markovian dynamics of quantum discord,” *Phys. Rev. A*, vol. 81, p. 052107, 2010.
- [162] B. Wang, Z.-Y. Xu, Z.-Q. Chen, and M. Feng, “Non-Markovian effect on the quantum discord,” *Phys. Rev. A*, vol. 81, p. 014101, 2010.
- [163] F. Altintas, “Geometric measure of quantum discord in non-Markovian environments,” *Optics Communications*, vol. 283, no. 24, pp. 5264 – 5268, 2010.
- [164] T. Werlang, S. Souza, F. F. Fanchini, and C. J. Villas Boas, “Robustness of quantum discord to sudden death,” *Physical Review A*, vol. 80, p. 024103, 2009.
- [165] L. Mazzola, J. Piilo, and S. Maniscalco, “Sudden transition between classical and quantum decoherence,” *Physical Review Letters*, vol. 104, p. 200401, 2010.
- [166] A. K. Pal and I. Bose, “Quantum discord in the ground and thermal states of spin clusters,” *Journal of Physics B: Atomic, Molecular and Optical Physics*, vol. 44, no. 4, p. 045101, 2011.

- [167] D. O. Soares-Pinto, L. C. Céleri, R. Auccaise, F. F. Fanchini, E. R. deAzevedo, J. Maziero, T. J. Bonagamba, and R. M. Serra, “Nonclassical correlation in NMR quadrupolar systems,” *Physical Review A*, vol. 81, p. 062118, 2010.
- [168] F. Altintas and R. Eryigit, “Dynamics of entanglement and Bell non-locality for two stochastic qubits with dipole-dipole interaction,” *Journal of Physics A: Mathematical and Theoretical*, vol. 43, no. 41, p. 415306, 2010.
- [169] F. Altintas and R. Eryigit, “Quantum correlations in non-Markovian environments,” *Physics Letters A*, vol. 374, no. 42, pp. 4283 – 4296, 2010.
- [170] F. Altintas and R. Eryigit, “Quantum correlations between identical and unidentical atoms in a dissipative environment,” *Journal of Physics B: Atomic, Molecular and Optical Physics*, vol. 44, no. 12, p. 125501, 2011.
- [171] X. S. Ma, G. X. Zhao, J. Y. Zhang, and A. M. Wang, “Dynamics of quantum discord under decoherence from a spin environment,” *Optics Communications*, vol. 284, no. 1, pp. 555 – 560, 2011.
- [172] Y. Li, B. Luo, and H. Guo, “Entanglement and quantum discord dynamics of two atoms under practical feedback control,” *Physical Review A*, vol. 84, p. 012316, 2011.
- [173] F. Francica, F. Plastina, and S. Maniscalco, “Quantum Zeno and anti-Zeno effects on quantum and classical correlations,” *Physical Review A*, vol. 82, p. 052118, Nov 2010.
- [174] F. F. Fanchini, L. K. Castelano, and A. O. Caldeira, “Entanglement versus quantum discord in two coupled double quantum dots,” *New Journal of Physics*, vol. 12, no. 7, p. 073009, 2010.
- [175] J. Maziero, L. C. Céleri, R. M. Serra, and V. Vedral, “Classical and quantum correlations under decoherence,” *Physical Review A*, vol. 80, p. 044102, 2009.
- [176] J.-B. Yuan, L.-M. Kuang, and J.-Q. Liao, “Amplification of quantum discord between two uncoupled qubits in a common environment by phase decoherence,” *Journal of Physics B: Atomic, Molecular and Optical Physics*, vol. 43, no. 16, p. 165503, 2010.
- [177] Z. Y. Xu, W. L. Yang, X. Xiao, and M. Feng, “Comparison of different measures for quantum discord under non-Markovian noise,” *Journal of Physics A: Mathematical and Theoretical*, vol. 44, no. 39, p. 395304, 2011.

- [178] J.-Q. Li and J.-Q. Liang, “Quantum and classical correlations in a classical dephasing environment,” *Physics Letters A*, vol. 375, no. 13, pp. 1496 – 1503, 2011.
- [179] J.-S. Xu, C.-F. Li, C.-J. Zhang, X.-Y. Xu, Y.-S. Zhang, and G.-C. Guo, “Experimental investigation of the non-Markovian dynamics of classical and quantum correlations,” *Physical Review A*, vol. 82, p. 042328, 2010.
- [180] J.-S. Xu, C.-F. Li, C.-J. Zhang, X.-Y. Xu, Y.-S. Zhang, and G.-C. Guo, “Experimental investigation of classical and quantum correlations under decoherence,” *Nature Communications*, vol. 1, no. 7, 2010.
- [181] L. C. Céleri, A. G. S. Landulfo, R. M. Serra, and G. E. A. Matsas, “Sudden change in quantum and classical correlations and the Unruh effect,” *Physical Review A*, vol. 81, p. 062130, 2010.
- [182] Q.-L. He, J.-B. Xu, D.-X. Yao, and Y.-Q. Zhang, “Sudden transition between classical and quantum decoherence in dissipative cavity qed and stationary quantum discord,” *Physical Review A*, vol. 84, p. 022312, 2011.
- [183] R. Vasile, P. Giorda, S. Olivares, M. G. A. Paris, and S. Maniscalco, “Nonclassical correlations in non-Markovian continuous-variable systems,” *Physical Review A*, vol. 82, p. 012313, 2010.
- [184] L. Mazzola, J. Piilo, and S. Maniscalco, “Frozen discord in non-markovian dephasing channels,” *International Journal of Quantum Information*, vol. 09, no. 03, pp. 981–991, 2011.
- [185] R. Lo Franco, B. Bellomo, E. Andersson, and G. Compagno, “Revival of quantum correlations without system-environment back-action,” *Physical Review A*, vol. 85, p. 032318, 2012.
- [186] B. Bellomo, R. Lo Franco, and G. Compagno, “Dynamics of geometric and entropic quantifiers of correlations in open quantum systems,” *Physical Review A*, vol. 86, p. 012312, 2012.
- [187] P. Haikka, T. H. Johnson, and S. Maniscalco, “Non-markovianity of local dephasing channels and time-invariant discord,” *Physical Review A*, vol. 87, p. 010103, 2013.
- [188] X.-M. Lu, Z. Xi, Z. Sun, and X. Wang, “Geometric measure of quantum discord under decoherence,” *Quantum Information and Computation*, vol. 10, pp. 0994–1003, 2010.

- [189] S. Sachdev, *Quantum Phase Transitions*. Cambridge University Press, 2001.
- [190] T. J. Osborne and M. A. Nielsen, “Entanglement in a simple quantum phase transition,” *Physical Review A*, vol. 66, p. 032110, 2002.
- [191] R. Dillenschneider, “Quantum discord and quantum phase transition in spin chains,” *Physical Review B*, vol. 78, p. 224413, 2008.
- [192] L.-A. Wu, M. S. Sarandy, and D. A. Lidar, “Quantum phase transitions and bipartite entanglement,” *Physical Review Letters*, vol. 93, p. 250404, 2004.
- [193] M. S. Sarandy, “Classical correlation and quantum discord in critical systems,” *Physical Review A*, vol. 80, p. 022108, 2009.
- [194] J. Batle and M. Casas, “Nonlocality and entanglement in the XY model,” *Physical Review A*, vol. 82, p. 062101, 2010.
- [195] J. Maziero, H. C. Guzman, L. C. Céleri, M. S. Sarandy, and R. M. Serra, “Quantum and classical thermal correlations in the XY spin- $\frac{1}{2}$ chain,” *Physical Review A*, vol. 82, p. 012106, 2010.
- [196] B.-Q. Liu, B. Shao, J.-G. Li, J. Zou, and L.-A. Wu, “Quantum and classical correlations in the one-dimensional XY model with Dzyaloshinskii-Moriya interaction,” *Physical Review A*, vol. 83, p. 052112, 2011.
- [197] J. Maziero, L. C. Céleri, R. Serra, and M. Sarandy, “Long-range quantum discord in critical spin systems,” *Physics Letters A*, vol. 376, no. 18, pp. 1540–1544, 2012.
- [198] L. Justino and T. R. de Oliveira, “Bell inequalities and entanglement at quantum phase transitions in the XXZ model,” *Physical Review A*, vol. 85, p. 052128, 2012.
- [199] W. Cheng, C. Shan, Y. Sheng, L. Gong, S. Zhao, and B. Zheng, “Geometric discord approach to quantum phase transition in the anisotropy XY spin model,” *Physica E: Low-dimensional Systems and Nanostructures*, vol. 44, no. 7–8, pp. 1320–1323, 2012.
- [200] C. C. Rulli and M. S. Sarandy, “Global quantum discord in multipartite systems,” *Physical Review A*, vol. 84, p. 042109, 2011.
- [201] T. Werlang, C. Trippe, G. A. P. Ribeiro, and G. Rigolin, “Quantum correlations in spin chains at finite temperatures and quantum phase transitions,” *Physical Review Letters*, vol. 105, p. 095702, 2010.

- [202] T. Werlang, G. A. P. Ribeiro, and G. Rigolin, “Spotlighting quantum critical points via quantum correlations at finite temperatures,” *Physical Review A*, vol. 83, p. 062334, 2011.
- [203] Y.-C. Li and H.-Q. Lin, “Thermal quantum and classical correlations and entanglement in the XY spin model with three-spin interaction,” *Physical Review A*, vol. 83, p. 052323, 2011.
- [204] J. Kurmann, H. Thomas, and G. Müller, “Antiferromagnetic long-range order in the anisotropic quantum spin chain,” *Physica A: Statistical Mechanics and its Applications*, vol. 112, no. 1–2, pp. 235 – 255, 1982.
- [205] T. R. de Oliveira, G. Rigolin, M. C. de Oliveira, and E. Miranda, “Symmetry-breaking effects upon bipartite and multipartite entanglement in the XY model,” *Physical Review A*, vol. 77, p. 032325, 2008.
- [206] O. F. Syljuåsen, “Entanglement and spontaneous symmetry breaking in quantum spin models,” *Physical Review A*, vol. 68, p. 060301, 2003.
- [207] A. Osterloh, G. Palacios, and S. Montangero, “Enhancement of pairwise entanglement via Z_2 symmetry breaking,” *Physical Review Letters*, vol. 97, p. 257201, 2006.
- [208] B. Tomasello, D. Rossini, A. Hamma, and L. Amico, “Ground-state factorization and correlations with broken symmetry,” *Europhysics Letters*, vol. 96, no. 2, p. 27002, 2011.
- [209] A. Saguia, C. C. Rulli, T. R. de Oliveira, and M. S. Sarandy, “Witnessing nonclassical multipartite states,” *Physical Review A*, vol. 84, p. 042123, 2011.
- [210] E. Barouch, B. M. McCoy, and M. Dresden, “Statistical mechanics of the XY model I,” *Physical Review A*, vol. 2, pp. 1075–1092, 1970.
- [211] E. Barouch and B. M. McCoy, “Statistical mechanics of the XY model II. Spin-correlation functions,” *Physical Review A*, vol. 3, pp. 786–804, 1971.